

# 6

## The Frequency-Response Design Method



### A Perspective on the Frequency-Response Design Method

The design of feedback control systems in industry is probably accomplished using frequency-response methods more often than any other. Frequency-response design is popular primarily because it provides good designs in the face of uncertainty in the plant model. For example, for systems with poorly known or changing high-frequency resonances, we can temper their feedback compensation to alleviate the effects of those uncertainties. Currently, this tempering is carried out more easily using frequency-response design than with any other method.

Another advantage of using frequency response is the ease with which experimental information can be used for design purposes. Raw measurements of the output amplitude and phase of a plant undergoing a sinusoidal input excitation are sufficient to design a suitable feedback control. No intermediate processing of the data (such as finding poles and zeros or determining system matrices) is required to arrive at the system model. The wide availability of computers has rendered this advantage less important now than it was years ago; however, for relatively simple systems, frequency response is often still the most cost-effective design method. The method is most effective for systems that are stable in open loop.

<sup>1</sup> Photo courtesy of Cirrus Design Corporation.

Yet another advantage is that it is the easiest method to use for designing compensation. A simple rule can be used to provide reasonable designs with a minimum of trial and error.

Although the underlying theory is somewhat challenging and requires a rather broad knowledge of complex variables, the methodology of frequency-response design is easy, and the insights gained by learning the theory are well worth the struggle.

## Chapter Overview

The chapter opens with a discussion of how to obtain the frequency response of a system by analyzing its poles and zeros. An important extension of this discussion is how to use Bode plots to graphically display the frequency response. In Sections 6.2 and 6.3 we discuss stability briefly, and then in more depth the use of the Nyquist stability criterion. In Sections 6.4 through 6.6 we introduce the notion of stability margins, discuss Bode's gain–phase relationship, and study the closed-loop frequency response of dynamic systems. The gain–phase relationship suggests a very simple rule for compensation design: Shape the frequency response magnitude so that it crosses magnitude 1 with a slope of  $-1$ . As with our treatment of the root-locus method, we describe how adding dynamic compensation can adjust the frequency response (Section 6.7) and improve system stability and/or error characteristics. We also show how to implement compensation digitally in an example.

Several alternate methods of displaying frequency-response data have been developed over the years; we present two of them—the Nichols chart and the inverse Nyquist plot—in optional Section 6.8. In optional Section 6.9 we discuss issues of sensitivity that relate to the frequency response, including optional material on sensitivity functions and stability robustness. The final section on analyzing time delays in the system represents additional, somewhat advanced material that may also be considered optional.

## 6.1 Frequency Response

The basic concepts of frequency response were discussed in Section 3.1.2. In this section we will review those ideas and extend the concepts for use in control system design.

### Frequency response

A linear system's response to sinusoidal inputs—called the system's **frequency response**—can be obtained from knowledge of its pole and zero locations.

To review the ideas, we consider a system described by

$$\frac{Y(s)}{U(s)} = G(s),$$

where the input  $u(t)$  is a sine wave with an amplitude  $A$ :

$$u(t) = A \sin(\omega_o t) 1(t).$$

This sine wave has a Laplace transform

$$U(s) = \frac{A\omega_o}{s^2 + \omega_o^2}.$$

With zero initial conditions, the Laplace transform of the output is

$$Y(s) = G(s) \frac{A\omega_o}{s^2 + \omega_o^2}. \quad (6.1)$$

### Partial fraction expansion

A partial-fraction expansion of Eq. (6.1) [assuming that the poles of  $G(s)$  are distinct] will result in an equation of the form

$$Y(s) = \frac{\alpha_1}{s - p_1} + \frac{\alpha_2}{s - p_2} + \cdots + \frac{\alpha_n}{s - p_n} + \frac{\alpha_o}{s + j\omega_o} + \frac{\alpha_o^*}{s - j\omega_o}, \quad (6.2)$$

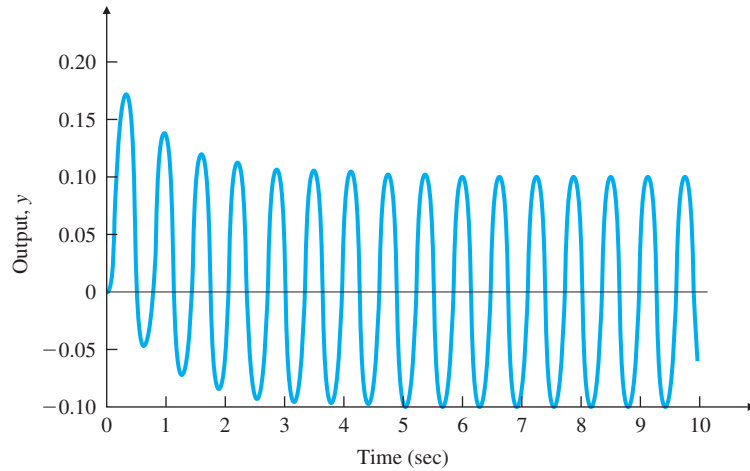
where  $p_1, p_2, \dots, p_n$  are the poles of  $G(s)$ ,  $\alpha_o$  would be found by performing the partial-fraction expansion, and  $\alpha_o^*$  is the complex conjugate of  $\alpha_o$ . The time response that corresponds to  $Y(s)$  is

$$y(t) = \alpha_1 e^{p_1 t} + \alpha_2 e^{p_2 t} \cdots + \alpha_n e^{p_n t} + 2|\alpha_o| \sin(\omega_o t + \phi), \quad t \geq 0, \quad (6.3)$$

where

$$\phi = \tan^{-1} \left[ \frac{\text{Im}(\alpha_o)}{\text{Re}(\alpha_o)} \right].$$

**Figure 6.1**  
Response of  
 $G(s) = 1/(s + 1)$  to  
 $\sin 10t$



If all the poles of the system represent stable behavior (the real parts of  $p_1, p_2, \dots, p_n < 0$ ), the natural unforced response will die out eventually, and therefore the steady-state response of the system will be due solely to the sinusoidal term in Eq. (6.3), which is caused by the sinusoidal excitation. Example 3.3 determined the response of the system  $G(s) = 1/(s + 1)$  to the input  $u = \sin 10t$  and showed that response in Fig. 3.2, which is repeated here as Fig. 6.1. It shows that  $e^{-t}$ , the natural part of the response associated with  $G(s)$ , disappears after several time constants, and the pure sinusoidal response is essentially all that remains. Example 3.4 showed that the remaining sinusoidal term in Eq. (6.3) can be expressed as

$$y(t) = AM \sin(\omega_o t + \phi), \quad (6.4)$$

where

$$M = |G(j\omega_o)| = |G(s)|_{s=j\omega_o} = \sqrt{\{\text{Re}[G(j\omega_o)]\}^2 + \{\text{Im}[G(j\omega_o)]\}^2}, \quad (6.5)$$

$$\phi = \tan^{-1} \left[ \frac{\text{Im}[G(j\omega_o)]}{\text{Re}[G(j\omega_o)]} \right] = \angle G(j\omega_o). \quad (6.6)$$

In polar form,

$$G(j\omega_o) = M e^{j\phi}. \quad (6.7)$$

Equation (6.4) shows that a stable system with transfer function  $G(s)$  excited by a sinusoid with unit amplitude and frequency  $\omega_o$  will, after the response has reached steady-state, exhibit a sinusoidal output with a magnitude  $M(\omega_o)$  and a phase  $\phi(\omega_o)$  at the frequency  $\omega_o$ . The facts that the output  $y$  is a sinusoid with the *same* frequency as the input  $u$  and that the magnitude ratio  $M$  and phase  $\phi$  of the output are independent of the amplitude  $A$  of the input are a

Frequency response plot

consequence of  $G(s)$  being a linear constant system. If the system being excited were a nonlinear or time-varying system, the output might contain frequencies other than the input frequency, and the output–input ratio might be dependent on the input magnitude.

#### Magnitude and phase

More generally, the **magnitude**  $M$  is given by  $|G(j\omega)|$ , and the **phase**  $\phi$  is given by  $\angle[G(j\omega)]$ ; that is, the magnitude and angle of the complex quantity  $G(s)$  are evaluated with  $s$  taking on values along the imaginary axis ( $s = j\omega$ ). The frequency response of a system consists of these functions of frequency that tell us how a system will respond to a sinusoidal input of any frequency. We are interested in analyzing the frequency response not only because it will help us understand how a system responds to a sinusoidal input, but also because evaluating  $G(s)$  with  $s$  taking on values along the  $j\omega$  axis will prove to be very useful in determining the stability of a closed-loop system. As we saw in Chapter 3, the  $j\omega$  axis is the boundary between stability and instability; we will see in Section 6.4 that evaluating  $G(j\omega)$  provides information that allows us to determine closed-loop stability from the open-loop  $G(s)$ .

#### EXAMPLE 6.1

#### *Frequency-Response Characteristics of a Capacitor*

Consider the capacitor described by the equation

$$i = C \frac{dv}{dt},$$

where  $v$  is the input and  $i$  is the output. Determine the sinusoidal steady-state response of the capacitor.

**Solution.** The transfer function of this circuit is

$$\frac{I(s)}{V(s)} = G(s) = Cs,$$

so

$$G(j\omega) = Cj\omega.$$

Computing the magnitude and phase, we find that

$$M = |Cj\omega| = C\omega \quad \text{and} \quad \phi = \angle(Cj\omega) = 90^\circ.$$

For a unit-amplitude sinusoidal input  $v$ , the output  $i$  will be a sinusoid with magnitude  $C\omega$ , and the phase of the output will lead the input by  $90^\circ$ . Note that for this example the magnitude is proportional to the input frequency while the phase is independent of frequency.

## EXAMPLE 6.2

*Frequency-Response Characteristics of a Lead Compensator*

Recall from Chapter 5 [Eq. (5.88)] the transfer function of the lead compensation, which is equivalent to

$$D(s) = K \frac{Ts + 1}{\alpha Ts + 1}, \quad \alpha < 1. \quad (6.8)$$

- (a) Analytically determine its frequency-response characteristics and discuss what you would expect from the result.
- (b) Use MATLAB to plot  $D(j\omega)$  with  $K = 1$ ,  $T = 1$ , and  $\alpha = 0.1$  for  $0.1 \leq \omega \leq 100$ , and verify the features predicted from the analysis in (a).

**Solution.**

- (a) **Analytical evaluation:** Substituting  $s = j\omega$  into Eq. (6.8), we get

$$D(j\omega) = K \frac{Tj\omega + 1}{\alpha Tj\omega + 1}.$$

From Eqs. (6.5) and (6.6) the amplitude is

$$M = |D| = |K| \frac{\sqrt{1 + (\omega T)^2}}{\sqrt{1 + (\alpha \omega T)^2}},$$

and the phase is given by

$$\begin{aligned} \phi &= \angle(1 + j\omega T) - \angle(1 + j\alpha\omega T) \\ &= \tan^{-1}(\omega T) - \tan^{-1}(\alpha\omega T). \end{aligned}$$

At very low frequencies the amplitude is just  $|K|$ , and at very high frequencies it is  $|K/\alpha|$ . Therefore, the amplitude increases as a function of frequency. The phase is zero at very low frequencies and goes back to zero at very high frequencies. At intermediate frequencies, evaluation of the  $\tan^{-1}(\cdot)$  functions would reveal that  $\phi$  becomes positive. These are the general characteristics of lead compensation.

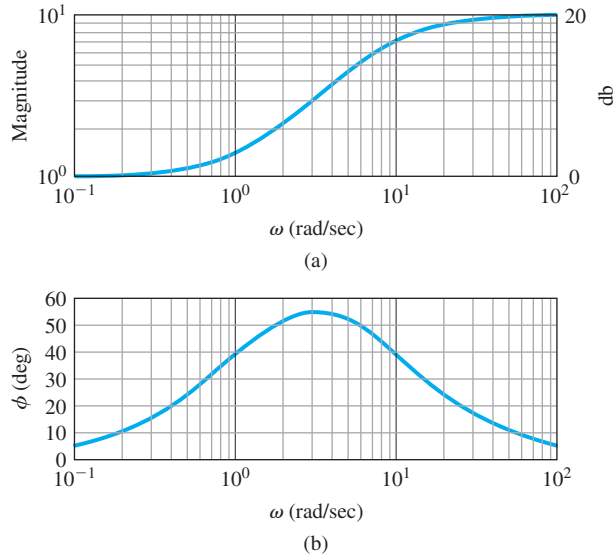
- (b) **Computer evaluation:** A MATLAB script for frequency-response evaluation was shown for Example 3.4. A similar script for the lead compensation is

```
num = [1 1];
den = [0.1 1];
sysD = tf(num,den);
[mag,phase,w] = bode(sysD);    % computes magnitude, phase, and frequen-
                                % cies over range of interest

loglog(w,mag)
semilogx(w,phase)
```

produces the frequency response magnitude and phase plots shown in Fig. 6.2.

**Figure 6.2**  
 (a) Magnitude and (b) phase  
 for the lead compensation  
 in Example 6.2



The analysis indicated that the low-frequency magnitude should be  $K (= 1)$  and the high-frequency magnitude should be  $K/\alpha (= 10)$ , which are both verified by the magnitude plot. The phase plot also verifies that the value approaches zero at high and low frequencies and that the intermediate values are positive.

In the cases for which we do not have a good model of the system and wish to determine the frequency-response magnitude and phase experimentally, we can excite the system with a sinusoid varying in frequency. The magnitude  $M(\omega)$  is obtained by measuring the ratio of the output sinusoid to input sinusoid in the steady-state at each frequency. The phase  $\phi(\omega)$  is the measured difference in phase between input and output signals.<sup>2</sup>

A great deal can be learned about the dynamic response of a system from knowledge of the magnitude  $M(\omega)$  and the phase  $\phi(\omega)$  of its transfer function. In the obvious case, if the signal is a sinusoid, then  $M$  and  $\phi$  completely describe the response. Furthermore, if the input is periodic, then a Fourier series can be constructed to decompose the input into a sum of sinusoids, and again  $M(\omega)$  and  $\phi(\omega)$  can be used with each component to construct the total response. For transient inputs, our best path to understanding the meaning of  $M$  and  $\phi$  is to relate the frequency response  $G(j\omega)$  to the transient responses calculated by the Laplace transform. For example, in Fig. 3.16(b) we plotted the step response of a system having the transfer function

$$G(s) = \frac{1}{(s/\omega_n)^2 + 2\zeta(s/\omega_n) + 1}, \quad (6.9)$$

<sup>2</sup> Agilent Technologies produces instruments called spectral analyzers that automate this experimental procedure and greatly speed up the process.

for various values of  $\zeta$ . These transient curves were normalized with respect to time as  $\omega_n t$ . In Fig. 6.3 we plot  $M(\omega)$  and  $\phi(\omega)$  for these same values of  $\zeta$  to help us see what features of the frequency response correspond to the transient-response characteristics. Specifically, Figs. 3.16(b) and 6.3 indicate the effect of damping on system time response and the corresponding effect on the frequency response. They show that the damping of the system can be determined from the transient response overshoot or from the peak in the magnitude of the frequency response (Fig. 6.3a). Furthermore, from the frequency response, we see that  $\omega_n$  is approximately equal to the bandwidth—the frequency where the magnitude starts to fall off from its low-frequency value. (We will define bandwidth more formally in the next paragraph.) Therefore, the rise time can be estimated from the bandwidth. We also see that the peak overshoot in frequency is approximately  $1/2\zeta$  for  $\zeta < 0.5$ , so the peak overshoot in the step response can be estimated from the peak overshoot in the frequency response. Thus, we see that essentially the same information is contained in the frequency-response curve as is found in the transient-response curve.

### Bandwidth

A natural specification for system performance in terms of frequency response is the **bandwidth**, defined to be the maximum frequency at which the output of a system will track an input sinusoid in a satisfactory manner. By convention, for the system shown in Fig. 6.4 with a sinusoidal input  $r$ , the bandwidth is the frequency of  $r$  at which the output  $y$  is attenuated to a factor of 0.707 times the input.<sup>3</sup> Figure 6.5 depicts the idea graphically for the frequency response of the *closed-loop* transfer function

$$\frac{Y(s)}{R(s)} \triangleq \mathcal{T}(s) = \frac{KG(s)}{1 + KG(s)}.$$

The plot is typical of most closed-loop systems in that (1) the output follows the input [ $|\mathcal{T}| \cong 1$ ] at the lower excitation frequencies, and (2) the output ceases to follow the input [ $|\mathcal{T}| < 1$ ] at the higher excitation frequencies. The maximum value of the frequency-response magnitude is referred to as the **resonant peak**  $M_r$ .

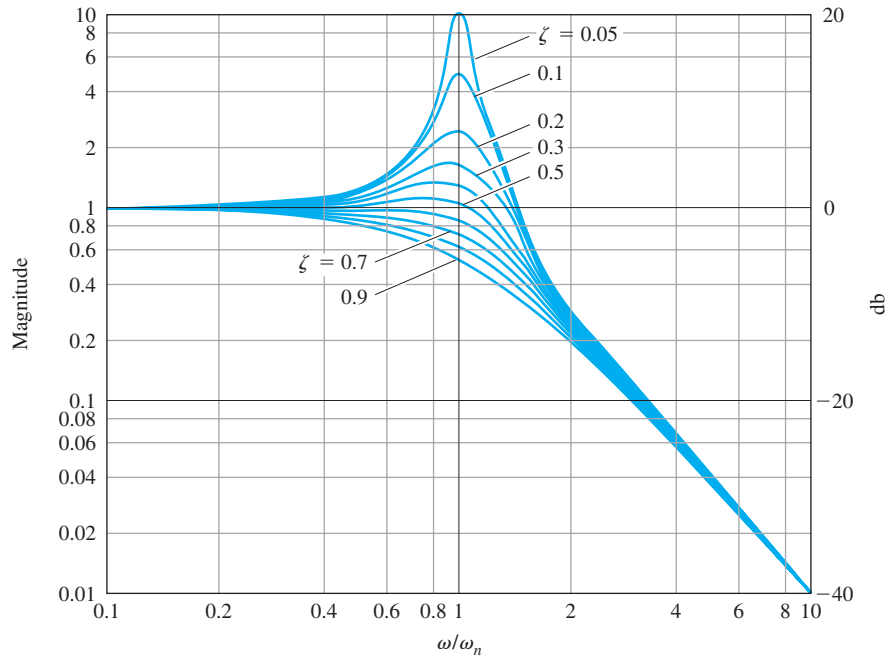
Bandwidth is a measure of speed of response and is therefore similar to time-domain measures such as rise time and peak time or the  $s$ -plane measure of dominant-root(s) natural frequency. In fact, if the  $KG(s)$  in Fig. 6.4 is such that the closed-loop response is given by Fig. 6.3, we can see that the bandwidth will equal the natural frequency of the closed-loop root (that is,  $\omega_{BW} = \omega_n$  for a closed-loop damping ratio of  $\zeta = 0.7$ ). For other damping ratios, the bandwidth is approximately equal to the natural frequency of the closed-loop roots, with an error typically less than a factor of 2.

The definition of the bandwidth stated here is meaningful for systems that have a low-pass filter behavior, as is the case for any physical control system. In other applications the bandwidth may be defined differently. Also, if the ideal

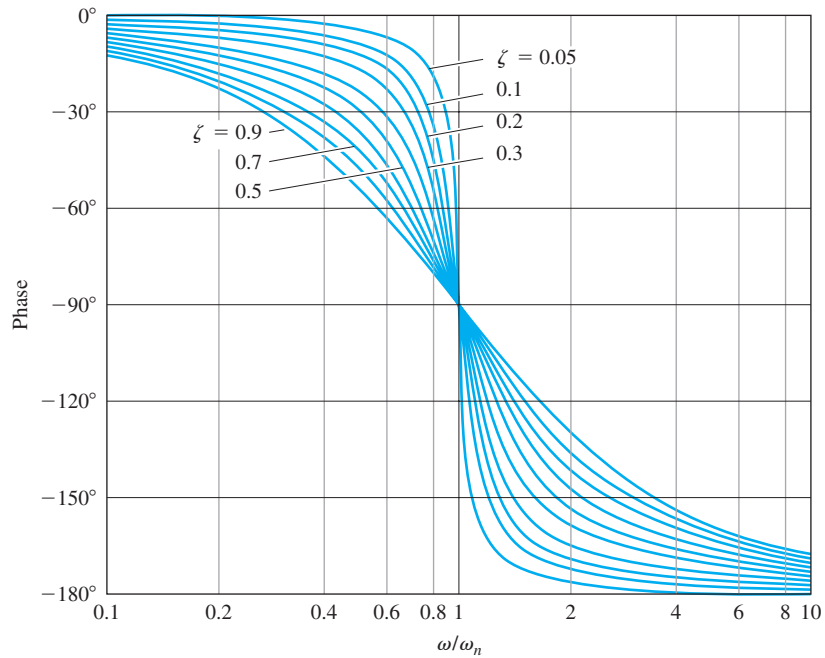
<sup>3</sup> If the output is a voltage across a  $1\Omega$  resistor, the power is  $v^2$  and when  $|v| = 0.707$ , the power is reduced by a factor of 2. By convention, this is called the half-power point.



**Figure 6.3**  
 (a) Magnitude and  
 (b) phase of Eq. (6.9)



(a)



(b)

**Figure 6.4**  
Simplified system definition

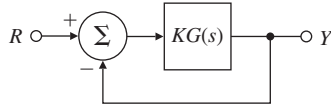
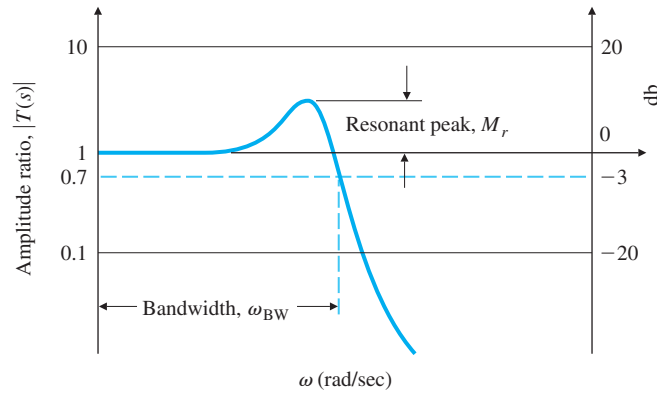


**Figure 6.5**  
Definitions of bandwidth and resonant peak



model of the system does not have a high-frequency roll-off (e.g., if it has an equal number of poles and zeros), the bandwidth is infinite; however, this does not occur in nature as nothing responds well at infinite frequencies.

In order to use the frequency response for control systems design, we need to consider an efficient and meaningful form in which to make frequency-response plots as well as find methods to relate the open-loop characteristics of  $KG$  to the closed-loop characteristics of  $\mathcal{T}(s)$ . These are the concerns of Section 6.1.1.

### 6.1.1 Bode Plot Techniques

Display of frequency response is a problem that has been studied for a long time. Before computers, this was accomplished by hand; therefore, it was useful to be able to accomplish this quickly. The most useful technique for hand plotting was developed by H. W. Bode at Bell Laboratories between 1932 and 1942. This technique allows plotting that is quick and yet sufficiently accurate for control systems design. Most control systems designers now have access to computer programs that diminish the need for hand plotting; however, it is still important to develop good intuition so that you can quickly identify erroneous computer results, and for this you need the ability to check results by hand.

The idea in Bode's method is to plot magnitude curves using a logarithmic scale and phase curves using a linear scale. This strategy allows us to plot a high-order  $G(j\omega)$  by simply adding the separate terms graphically, as discussed in Appendix B. This addition is possible because a complex expression with zero and pole factors can be written in polar (or phasor) form as

$$G(j\omega) = \frac{\vec{s}_1 \vec{s}_2}{\vec{s}_3 \vec{s}_4 \vec{s}_5} = \frac{r_1 e^{j\theta_1} r_2 e^{j\theta_2}}{r_3 e^{j\theta_3} r_4 e^{j\theta_4} r_5 e^{j\theta_5}} = \left( \frac{r_1 r_2}{r_3 r_4 r_5} \right) e^{j(\theta_1 + \theta_2 - \theta_3 - \theta_4 - \theta_5)}. \quad (6.10)$$

Composite plot from individual terms

(The overhead arrow indicates a phasor.) Note from Eq. (6.10) that the phases of the individual terms are added directly to obtain the phase of the **composite** expression,  $G(j\omega)$ . Furthermore, because

$$|G(j\omega)| = \frac{r_1 r_2}{r_3 r_4 r_5},$$

it follows that

$$\log_{10} |G(j\omega)| = \log_{10} r_1 + \log_{10} r_2 - \log_{10} r_3 - \log_{10} r_4 - \log_{10} r_5. \quad (6.11)$$

Bode plot

We see that addition of the logarithms of the individual terms provides the logarithm of the magnitude of the composite expression. The frequency response is typically presented as two curves; the logarithm of magnitude versus  $\log \omega$ , and the phase versus  $\log \omega$ . Together these two curves constitute a **Bode plot** of the system. Because

$$\log_{10} M e^{j\phi} = \log_{10} M + j\phi \log_{10} e, \quad (6.12)$$

Decibel

we see that the Bode plot shows the real and imaginary parts of the logarithm of  $G(j\omega)$ . In communications it is standard to measure the power gain in decibels (db):<sup>4</sup>

$$|G|_{\text{db}} = 10 \log_{10} \frac{P_2}{P_1}. \quad (6.13)$$

Here  $P_1$  and  $P_2$  are the input and output powers. Because power is proportional to the square of the voltage, the power gain is also given by

$$|G|_{\text{db}} = 20 \log_{10} \frac{V_2}{V_1}. \quad (6.14)$$

Hence we can present a Bode plot as the magnitude in decibels versus  $\log \omega$  and the phase in degrees versus  $\log \omega$ .<sup>5</sup> In this book we give Bode plots in the form  $\log |G|$  versus  $\log \omega$ ; also, we mark an axis in decibels on the right-hand side of the magnitude plot to give you the choice of working with the representation you prefer. However, for frequency response plots, we are not actually plotting power and use of Eq. (6.14) can be somewhat misleading. If the magnitude data are derived in terms of  $\log |G|$ , it is conventional to plot them on a log scale but identify the scale in terms of  $|G|$  only (without “log”). If the magnitude data are given in decibels, the vertical scale is linear such that each decade of  $|G|$  represents 20 db.

<sup>4</sup> Researchers at Bell Laboratories first defined the unit of power gain as a **bel** (named for Alexander Graham Bell, the founder of the company). However, this unit proved to be too large, and hence a **decibel or db** (1/10 of a bel) was selected as a more useful unit. The abbreviation dB is also sometimes used; however, Bode used db and we choose to follow his lead.

<sup>5</sup> Henceforth we will drop the base of the logarithm; it is understood to be 10.

### Advantages of Working with Frequency Response in Terms of Bode Plots

#### Advantages of Bode plots

1. Dynamic compensator design can be based entirely on Bode plots.
2. Bode plots can be determined experimentally.
3. Bode plots of systems in series (or tandem) simply add, which is quite convenient.
4. The use of a log scale permits a much wider range of frequencies to be displayed on a single plot than is possible with linear scales.

It is important for the control systems engineer to be able to hand-plot frequency responses for several reasons: This skill not only allows the engineer to deal with simple problems, but also to perform a sanity check on computer results for more complicated cases. Often approximations can be used to quickly sketch the frequency response and deduce stability, as well as to determine the form of the needed dynamic compensations. Finally, hand plotting is useful in interpreting frequency-response data that have been generated experimentally.

In Chapter 5 we wrote the open-loop transfer function in the form

$$KG(s) = K \frac{(s - z_1)(s - z_2) \cdots}{(s - p_1)(s - p_2) \cdots} \quad (6.15)$$

because it was the most convenient form for determining the degree of stability from the root locus with respect to the gain  $K$ . In working with frequency response, it is more convenient to replace  $s$  with  $j\omega$  and to write the transfer functions in the **Bode form**

#### Bode form of the transfer function

$$KG(j\omega) = K_o \frac{(j\omega\tau_1 + 1)(j\omega\tau_2 + 1) \cdots}{(j\omega\tau_a + 1)(j\omega\tau_b + 1) \cdots} \quad (6.16)$$

because the gain  $K_o$  in this form is directly related to the transfer-function magnitude at very low frequencies. In fact, for type 0 systems,  $K_o$  is the gain at  $\omega = 0$  in Eq. (6.16) and is also equal to the DC gain of the system. Although a straightforward calculation will convert a transfer function in the form of Eq. (6.15) to an equivalent transfer function in the form of Eq. (6.16), note that  $K$  and  $K_o$  will not usually have the same value in the two expressions.

Transfer functions can also be rewritten according to Eqs. (6.10) and (6.11). As an example, suppose that

$$KG(j\omega) = K_o \frac{j\omega\tau_1 + 1}{(j\omega)^2(j\omega\tau_a + 1)}. \quad (6.17)$$

Then

$$\angle KG(j\omega) = \angle K_o + \angle(j\omega\tau_1 + 1) - \angle(j\omega)^2 - \angle(j\omega\tau_a + 1) \quad (6.18)$$

and

$$\log |KG(j\omega)| = \log |K_o| + \log |j\omega\tau_1 + 1| - \log |(j\omega)^2| - \log |j\omega\tau_a + 1|. \quad (6.19)$$

In decibels, Eq. (6.19) becomes

$$\begin{aligned} |KG(j\omega)|_{\text{db}} &= 20 \log |K_o| + 20 \log |j\omega\tau_1 + 1| - 20 \log |(j\omega)^2| \\ &\quad - 20 \log |j\omega\tau_a + 1|. \end{aligned} \quad (6.20)$$

Classes of terms of transfer functions

All transfer functions for the kinds of systems we have talked about so far are composed of three classes of terms:

1.  $K_o(j\omega)^n$
2.  $(j\omega\tau + 1)^{\pm 1}$
3.  $\left[ \left( \frac{j\omega}{\omega_n} \right)^2 + 2\zeta \frac{j\omega}{\omega_n} + 1 \right]^{\pm 1}$

First we will discuss the plotting of each individual term and how the terms affect the composite plot including all the terms; then we will discuss how to draw the composite curve.

Class 1: singularities at the origin

1.  $K_o(j\omega)^n$  Because

$$\log K_o |(j\omega)^n| = \log K_o + n \log |j\omega|,$$

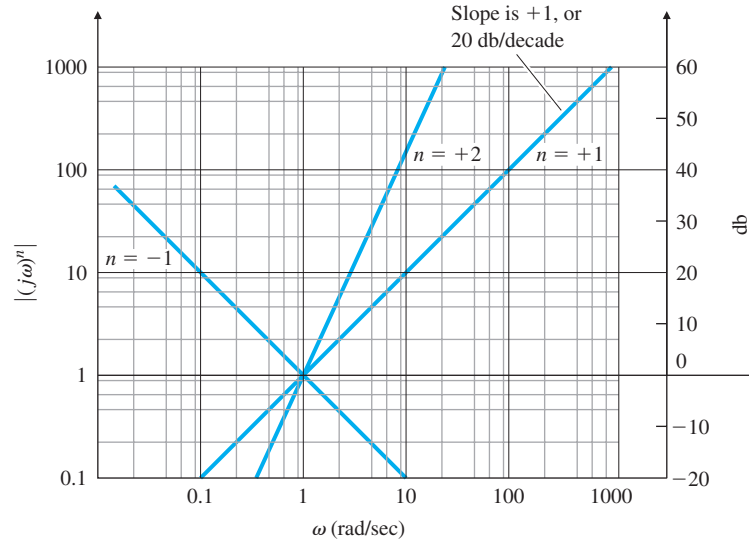
the magnitude plot of this term is a straight line with a slope  $n \times (20 \text{ db/decade})$ . Examples for different values of  $n$  are shown in Fig. 6.6.  $K_o(j\omega)^n$  is the only class of term that affects the slope at the lowest frequencies, because all other terms are constant in that region. The easiest way to draw the curve is to locate  $\omega = 1$  and plot  $\log K_o$  at that frequency. Then draw the line with slope  $n$  through that point.<sup>6</sup> The phase of  $(j\omega)^n$  is  $\phi = n \times 90^\circ$ ; it is independent of frequency and is thus a horizontal line:  $-90^\circ$  for  $n = -1$ ,  $-180^\circ$  for  $n = -2$ ,  $+90^\circ$  for  $n = +1$ , and so forth.

Class 2: first-order term

2.  $j\omega\tau + 1$  The magnitude of this term approaches one asymptote at very low frequencies and another asymptote at very high frequencies:
  - (a) For  $\omega\tau \ll 1$ ,  $j\omega\tau + 1 \cong 1$ .
  - (b) For  $\omega\tau \gg 1$ ,  $j\omega\tau + 1 \cong j\omega\tau$ .

<sup>6</sup> In decibels the slopes are  $n \times 20 \text{ db per decade}$  or  $n \times 6 \text{ db per octave}$  (an octave is a change in frequency by a factor of 2).

**Figure 6.6**  
Magnitude of  $(j\omega)^n$



**Break point**

If we call  $\omega = 1/\tau$  the **break point**, then we see that below the break point the magnitude curve is approximately constant ( $= 1$ ), while above the break point the magnitude curve behaves approximately like the class 1 term  $K_o(j\omega)$ . The example plotted in Fig. 6.7,  $G(s) = 10s + 1$ , shows how the two asymptotes cross at the break point and how the actual magnitude curve lies above that point by a factor of 1.4 (or +3 db). (If the term were in the denominator, it would be below the break point by a factor of 0.707 or -3 db.) Note that this term will have only a small effect on the composite magnitude curve below the break point, because its value is equal to 1 ( $= 0$  db) in this region. The slope at high frequencies is +1 (or +20 db/decade). The phase curve can also be easily drawn by using the following low- and high-frequency asymptotes:

- (a) For  $\omega\tau \ll 1$ ,  $\angle 1 = 0^\circ$ .
- (b) For  $\omega\tau \gg 1$ ,  $\angle j\omega\tau = 90^\circ$ .
- (c) For  $\omega\tau \cong 1$ ,  $\angle(j\omega\tau + 1) \cong 45^\circ$ .

**Figure 6.7**  
Magnitude plot for  $j\omega\tau + 1$ ;  $\tau = 10$

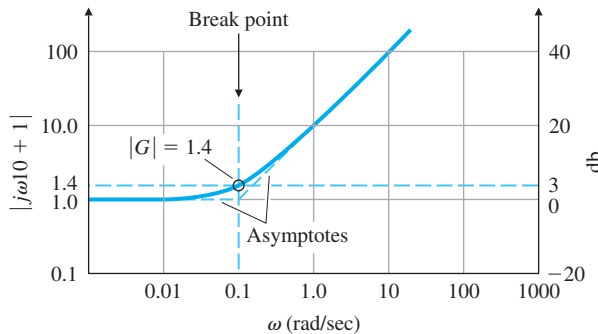
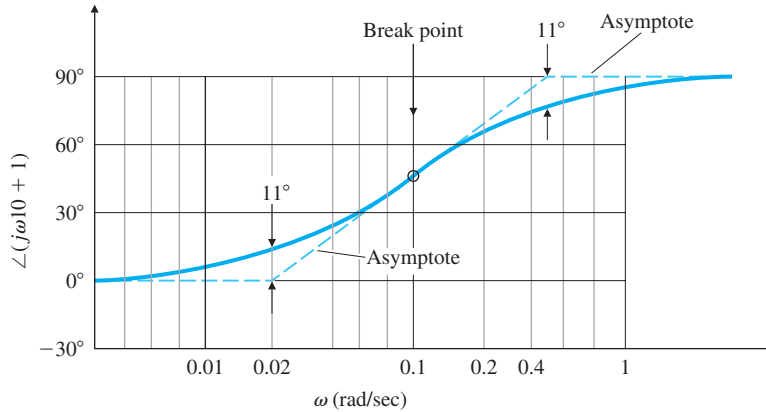


**Figure 6.8**  
Phase plot for  $j\omega\tau + 1$ ;  
 $\tau = 10$



For  $\omega\tau \cong 1$ , the  $\angle(j\omega + 1)$  curve is tangent to an asymptote going from  $0^\circ$  at  $\omega\tau = 0.2$  to  $90^\circ$  at  $\omega\tau = 5$ , as shown in Fig. 6.8. The figure also illustrates the three asymptotes (dashed lines) used for the phase plot and how the actual curve deviates from the asymptotes by  $11^\circ$  at their intersections. Both the composite phase and magnitude curves are unaffected by this class of term at frequencies below the break point by more than a factor of 10 because the term's magnitude is 1 (or 0 db) and its phase is  $0^\circ$ .

Class 3: second-order term

3.  $[(j\omega/\omega_n)^2 + 2\zeta(j\omega/\omega_n) + 1]^{\pm 1}$  This term behaves in a manner similar to the class 2 term, with differences in detail: The break point is now  $\omega = \omega_n$ . The magnitude changes slope by a factor of +2 (or +40 db per decade) at the break point (and -2, or -40 db per decade, when the term is in the denominator). The phase changes by  $\pm 180^\circ$ , and the transition through the break point region varies with the damping ratio  $\zeta$ . Figure 6.3 shows the magnitude and phase for several different damping ratios when the term is in the denominator. Note that the magnitude asymptote for frequencies above the break point has a slope of -2 (or -40 db per decade), and that the transition through the break-point region has a large dependence on the damping ratio. A rough sketch of this transition can be made by noting that

Peak amplitude

$$|G(j\omega)| = \frac{1}{2\zeta} \quad \text{at } \omega = \omega_n \tag{6.21}$$

for this class of second-order term in the denominator. If the term was in the numerator, the magnitude would be the reciprocal of the curve plotted in Fig. 6.3(a).

No such handy rule as Eq. (6.21) exists for sketching in the transition for the phase curve; therefore, we would have to resort to Fig. 6.3(b) for an accurate plot of the phase. However, a very rough idea of the transition can be gained by noting that it is a step function for  $\zeta = 0$ , while it obeys the rule for two first-order (class 2) terms when  $\zeta = 1$  with simultaneous break-point frequencies. All intermediate values of  $\zeta$  fall between these two extremes. The phase of a second-order term is always  $\pm 90^\circ$  at  $\omega_n$ .

## Composite curve

When the system has several poles and several zeros, plotting the frequency response requires that the components be combined into a composite curve. To plot the composite magnitude curve, it is useful to note that the slope of the asymptotes is equal to the sum of the slopes of the individual curves. Therefore, the composite asymptote curve has integer slope changes at each break point frequency: +1 for a first-order term in the numerator,  $-1$  for a first-order term in the denominator, and  $\pm 2$  for second-order terms. Furthermore, the lowest-frequency portion of the asymptote has a slope determined by the value of  $n$  in the  $(j\omega)^n$  term and is located by plotting the point  $K_o\omega^n$  at  $\omega = 1$ . Therefore, the complete procedure consists of plotting the lowest-frequency portion of the asymptote, then sequentially changing the asymptote's slope at each break point in order of ascending frequency, and finally drawing the actual curve by using the transition rules discussed earlier for classes 2 and 3.

The composite phase curve is the sum of the individual curves. Adding of the individual phase curves graphically is made possible by locating the curves so that the composite phase approaches the individual curve as closely as possible. A quick but crude sketch of the composite phase can be found by starting the phase curve below the lowest break point and setting it equal to  $n \times 90^\circ$ . The phase is then stepped at each break point in order of ascending frequency. The amount of the phase step is  $\pm 90^\circ$  for a first-order term and  $\pm 180^\circ$  for a second-order term. Break points in the numerator indicate a positive step in phase, while break points in the denominator indicate a negative phase step.<sup>7</sup> The plotting rules so far have only considered poles and zeros in the LHP. Changes for singularities in the RHP will be discussed at the end of the section.

## Summary of Bode Plot Rules

1. Manipulate the transfer function into the Bode form given by Eq. (6.16).
2. Determine the value of  $n$  for the  $K_o(j\omega)^n$  term (class 1). Plot the low-frequency magnitude asymptote through the point  $K_o$  at  $\omega = 1$  with a slope of  $n$  (or  $n \times 20$  db per decade).
3. Complete the composite magnitude asymptotes: Extend the low-frequency asymptote until the first frequency break point. Then step the slope by  $\pm 1$  or  $\pm 2$ , depending on whether the break point is from a first- or second-order term in the numerator or denominator. Continue through all break points in ascending order.
4. Sketch in the approximate magnitude curve: Increase the asymptote value by a factor of 1.4 (+3 db) at first-order numerator break points, and decrease it by a factor of 0.707 ( $-3$  db) at first-order denominator break points. At second-order break points, sketch in the resonant peak (or valley) according to Fig. 6.3(a) using the relation  $|G(j\omega)| = 1/2\zeta$  at denominator (or  $|G(j\omega)| = 2\zeta$  at numerator) break points.

<sup>7</sup> This approximate method was pointed out to us by our Parisian colleagues.



5. Plot the low-frequency asymptote of the phase curve,  $\phi = n \times 90^\circ$ .
6. As a guide, sketch in the approximate phase curve by changing the phase by  $\pm 90^\circ$  or  $\pm 180^\circ$  at each break point in ascending order. For first-order terms in the numerator, the change of phase is  $+90^\circ$ ; for those in the denominator the change is  $-90^\circ$ . For second-order terms, the change is  $\pm 180^\circ$ .
7. Locate the asymptotes for each individual phase curve so that their phase change corresponds to the steps in the phase toward or away from the approximate curve indicated by Step 6. Sketch in each individual phase curve as indicated by Fig. 6.8 or Fig. 6.3(b).
8. Graphically add each phase curve. Use grids if an accuracy of about  $\pm 5^\circ$  is desired. If less accuracy is acceptable, the composite curve can be done by eye. Keep in mind that the curve will start at the lowest-frequency asymptote and end on the highest-frequency asymptote and will approach the intermediate asymptotes to an extent that is determined by how close the break points are to each other.

**EXAMPLE 6.3****Bode Plot for Real Poles and Zeros**

Plot the Bode magnitude and phase for the system with the transfer function

$$KG(s) = \frac{2000(s + 0.5)}{s(s + 10)(s + 50)}.$$

**Solution.**

STEP 1. We convert the function to the Bode form of Eq. (6.16):

$$KG(j\omega) = \frac{2[(j\omega/0.5) + 1]}{j\omega[(j\omega/10) + 1][(j\omega/50) + 1]}.$$

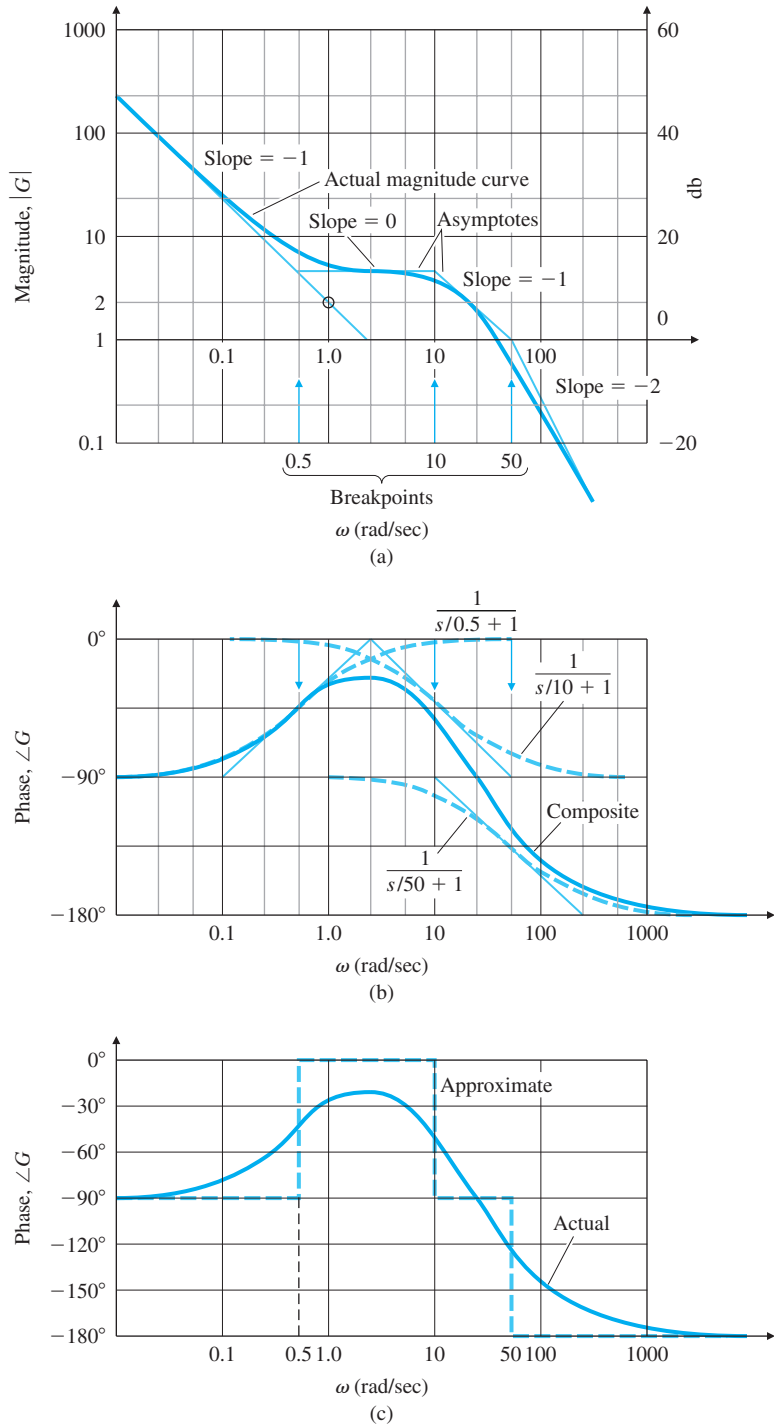
STEP 2. We note that the term in  $j\omega$  is first-order and in the denominator, so  $n = -1$ . Therefore, the low-frequency asymptote is defined by the first term:

$$KG(j\omega) = \frac{2}{j\omega}.$$

This asymptote is valid for  $\omega < 0.1$ , because the lowest break point is at  $\omega = 0.5$ . The magnitude plot of this term has the slope of  $-1$  (or  $-20$  db per decade). We locate the magnitude by passing through the value 2 at  $\omega = 1$  even though the composite curve will not go through this point because of the break point at  $\omega = 0.5$ . This is shown in Fig. 6.9(a).

STEP 3. We obtain the remainder of the asymptotes, also shown in Fig. 6.9(a): The first breakpoint is at  $\omega = 0.5$  and is a first-order term in the numerator, which thus calls for a change in slope of  $+1$ . We therefore draw a line with 0 slope that intersects the original  $-1$  slope. Then we draw a  $-1$  slope line that intersects the previous one at  $\omega = 10$ . Finally, we draw a  $-2$  slope line that intersects the previous  $-1$  slope at  $\omega = 50$ .

**Figure 6.9**  
 Composite plots:  
 (a) magnitude; (b) phase;  
 (c) approximate phase



STEP 4. We sketch in the actual curve so that it is approximately tangent to the asymptotes when far away from the break points, a factor of 1.4 (+3 db) above the asymptote at the  $\omega = 0.5$  break point, and a factor of 0.7 (−3 db) below the asymptote at the  $\omega = 10$  and  $\omega = 50$  break points.

STEP 5. Because the phase of  $\frac{2}{j\omega}$  is  $-90^\circ$ , the phase curve in Fig. 6.9(b) starts at  $-90^\circ$  at the lowest frequencies.

STEP 6. The result is shown in Fig. 6.9(c).

STEP 7. The individual phase curves, shown dashed in Fig. 6.9(b), have the correct phase change for each term and are aligned vertically so that their phase change corresponds to the steps in the phase from the approximate curve in Fig. 6.9(c). Note that the composite curve approaches each individual term.

STEP 8. The graphical addition of each dashed curve results in the solid composite curve in Fig. 6.9(b). As can be seen from the figure, the vertical placement of each individual phase curve makes the required graphical addition particularly easy because the composite curve approaches each individual phase curve in turn.

#### EXAMPLE 6.4

#### *Bode Plot with Complex Poles*

As a second example, draw the frequency response for the system

$$KG(s) = \frac{10}{s(s^2 + 0.4s + 4)}. \quad (6.22)$$

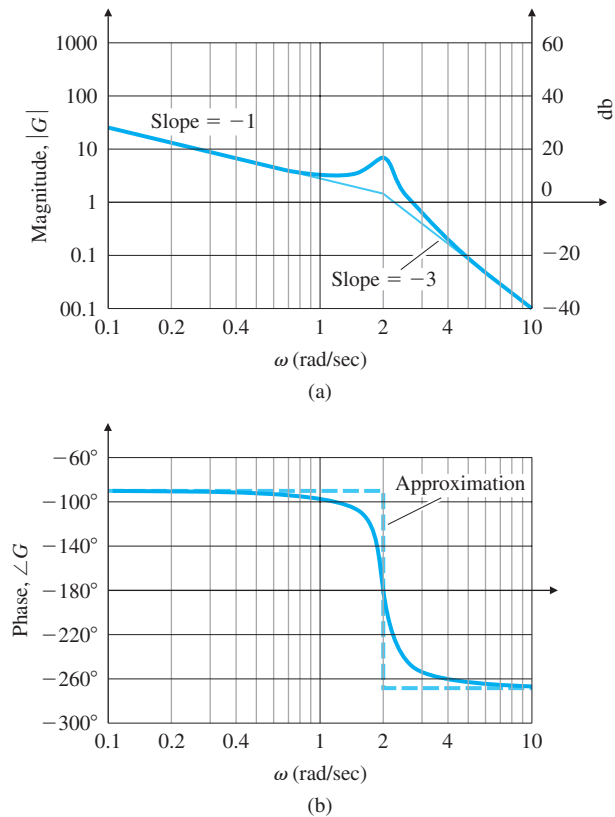
**Solution.** A system like this is more difficult to plot than the one in the previous example because the transition between asymptotes is dependent on the damping ratio; however, the same basic ideas illustrated in Example 6.3 apply.

This system contains a second-order term in the denominator. Proceeding through the steps, we convert Eq. (6.22) to the Bode form of Eq. (6.16):

$$KG(s) = \frac{10}{4} \frac{1}{s(s^2/4 + 2(0.1)s/2 + 1)}.$$

Starting with the low-frequency asymptote, we have  $n = -1$  and  $|G(j\omega)| \cong 2.5/\omega$ . The magnitude plot of this term has a slope of  $-1$  (−20 db per decade) and passes through the value of 2.5 at  $\omega = 1$  as shown in Fig. 6.10(a). For the second order pole, note that  $\omega_n = 2$  and  $\zeta = 0.1$ . At the break-point frequency of the poles,  $\omega = 2$ , the slope shifts to  $-3$  (−60 db per decade). At the pole break point the magnitude ratio above the asymptote is  $1/2\zeta = 1/0.2 = 5$ . The phase curve for this case starts at  $\phi = -90^\circ$ , corresponding to the  $1/s$  term, falls to  $\phi = -180^\circ$  at  $\omega = 2$  due to the pole as shown in Fig. 6.10(b), and then approaches  $\phi = -270^\circ$  for higher frequencies. Because the damping is small, the stepwise approximation is a very good one. The true composite phase curve is shown in Fig. 6.10(b).

**Figure 6.10**  
Bode plot for a transfer function with complex poles: (a) magnitude; (b) phase



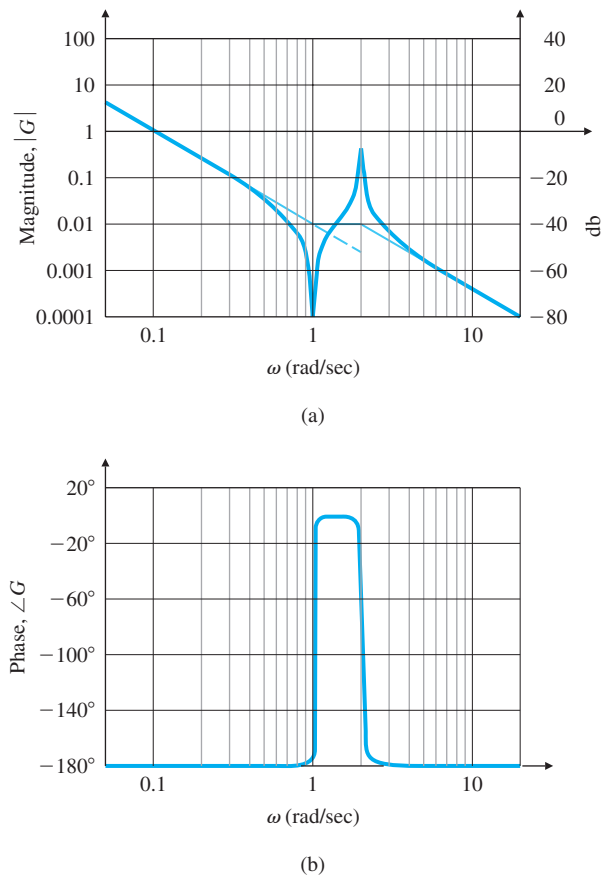
### EXAMPLE 6.5 *Bode Plot for Complex Poles and Zeros: Satellite with Flexible Appendages*

As a third example, draw the Bode plots for a system with second-order terms. The transfer function represents a mechanical system with two equal masses coupled with a lightly damped spring. The applied force and position measurement are collocated on the same mass. For the transfer function, the time scale has been chosen so that the resonant frequency of the complex zeros is equal to 1. The transfer function is

$$KG(s) = \frac{0.01(s^2 + 0.01s + 1)}{s^2[(s^2/4) + 0.02(s/2) + 1]}$$

**Solution.** Proceeding through the steps, we start with the low-frequency asymptote,  $0.01/\omega^2$ . It has a slope of  $-2$  ( $-40$  db per decade) and passes through magnitude  $= 0.01$  at  $\omega = 1$ , as shown in Fig. 6.11(a). At the break-point frequency of the zero,  $\omega = 1$ , the slope shifts to zero until the break point of the pole, which is located at  $\omega = 2$ , when

**Figure 6.11**  
Bode plot for a transfer function with complex poles and zeros: (a) magnitude; (b) phase



the slope returns to a slope of  $-2$ . To interpolate the true curve, we plot the point at the zero break point,  $\omega = 1$ , with a magnitude ratio below the asymptote of  $2\zeta = 0.01$ . At the pole break point, the magnitude ratio above the asymptote is  $1/2\zeta = 1/0.02 = 50$ . The magnitude curve is a “doublet” of a negative pulse followed by a positive pulse. Figure 6.11(b) shows that the phase curve for this system starts at  $-180^\circ$  (corresponding to the  $1/s^2$  term), jumps  $180^\circ$  to  $\phi = 0$  at  $\omega = 1$ , due to the zeros, and then falls  $180^\circ$  back to  $\phi = -180^\circ$  at  $\omega = 2$ , due to the pole. With such small damping ratios the stepwise approximation is quite good. (We haven’t drawn this on Fig. 6.11(b), because it would not be easily distinguishable from the true phase curve.) Thus, the true composite phase curve is a nearly square pulse between  $\omega = 1$  and  $\omega = 2$ .

In actual designs, most Bode plots are made with the aid of a computer. However, acquiring the ability to quickly sketch Bode plots by hand is a useful skill, because it gives the designer insight into how changes in the compensation parameters will affect the frequency response. This allows the designer to iterate to the best designs more quickly.

## EXAMPLE 6.6

**Computer-Aided Bode Plot for Complex Poles and Zeros**

Repeat Example 6.5 using MATLAB.

**Solution.** To obtain Bode plots using MATLAB, we call the function `bode` as follows:

```
numG = 0.01*[1 0.01 1];
denG = [0.25 0.01 1 0 0];
sysG = tf(numG,denG);
[mag, phase, w] = bode(sysG);
loglog(w,mag)
semilogx(w,phase)
```

These commands will result in a Bode plot that matches that in Fig. 6.11 very closely. To obtain the magnitude plot in decibels, the last three lines can be replaced with

```
bode(sysG)
```

---

**Nonminimum-Phase Systems**

A system with a zero in the right half-plane (RHP) undergoes a net change in phase when evaluated for frequency inputs between zero and infinity, which, for an associated magnitude plot, is greater than if all poles and zeros were in the left half-plane (LHP). Such a system is called **nonminimum phase**. As can be seen from the construction in Fig. B.3 in Appendix B, if the zero is in the RHP, then the phase *decreases* at the zero break point instead of exhibiting the usual phase increase that occurs for an LHP zero. Consider the transfer functions

$$G_1(s) = 10 \frac{s + 1}{s + 10},$$

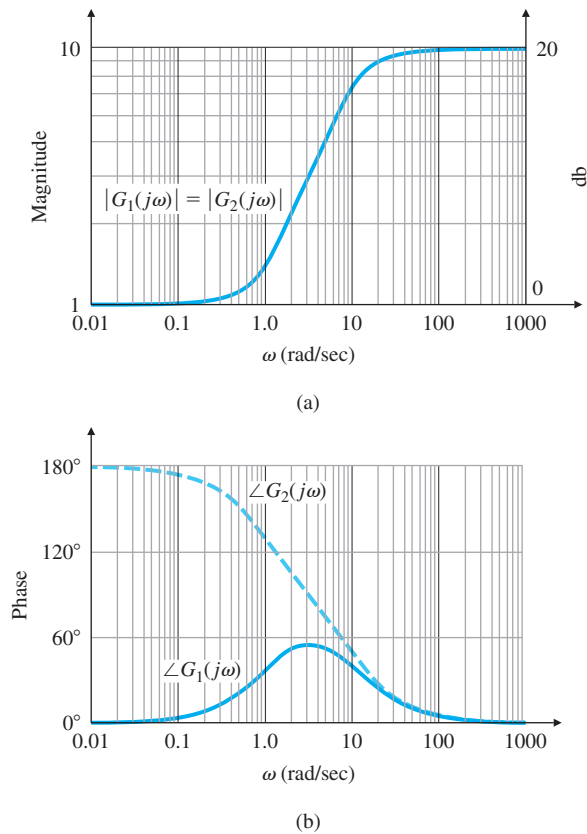
$$G_2(s) = 10 \frac{s - 1}{s + 10}.$$

Both transfer functions have the same magnitude for all frequencies; that is,

$$|G_1(j\omega)| = |G_2(j\omega)|,$$

as shown in Fig. 6.12(a). But the phases of the two transfer functions are drastically different [Fig. 6.12(b)]. A minimum-phase system (all zeros in the LHP) with a given magnitude curve will produce the smallest net change in the associated phase, as shown in  $G_1$ , compared with what the nonminimum-phase system will produce, as shown by the phase of  $G_2$ . Hence,  $G_2$  is nonminimum phase. The discrepancy between  $G_1$  and  $G_2$  with regard to the phase change would be greater if two or more zeros of the plant were in the RHP.

**Figure 6.12**  
Bode plot for minimum-  
and nonminimum-phase  
systems: (a) magnitude;  
(b) phase



### 6.1.2 Steady-State Errors

We saw in Section 4.2 that the steady-state error of a feedback system decreases as the gain of the open-loop transfer function increases. In plotting a composite magnitude curve, we saw in Section 6.1.1 that the open-loop transfer function, at very low frequencies, is approximated by

$$KG(j\omega) \cong K_o(j\omega)^n. \quad (6.23)$$

Therefore, we can conclude that the larger the value of the magnitude on the low-frequency asymptote, the lower the steady-state errors will be for the closed-loop system. This relationship is very useful in the design of compensation: Often we want to evaluate several alternate ways to improve stability and to do so we want to be able to see quickly how changes in the compensation will affect the steady-state errors.

#### Position error constant

For a system of the form given by Eq. (6.16)—that is, where  $n = 0$  in Eq. (6.23) (a type 0 system)—the low-frequency asymptote is a constant and the gain  $K_o$  of the open-loop system is equal to the position-error constant  $K_p$ . For a unity feedback system with a unit-step input, the Final Value Theorem

(Section 3.1.6) was used in Section 4.2.1 to show that the steady-state error is given by

$$e_{ss} = \frac{1}{1 + K_p}.$$

#### Velocity error coefficient

For a unity-feedback system in which  $n = -1$  in Eq. (6.23), defined to be a type 1 system in Section 4.2.1, the low-frequency asymptote has a slope of  $-1$ . The magnitude of the low-frequency asymptote is related to the gain according to Eq. (6.23); therefore, we can again read the gain,  $K_o/\omega$ , directly from the Bode magnitude plot. Equation (4.43) tells us that the velocity-error constant

$$K_v = K_o,$$

where, for a unity-feedback system with a unit-ramp input, the steady-state error is

$$e_{ss} = \frac{1}{K_v}.$$

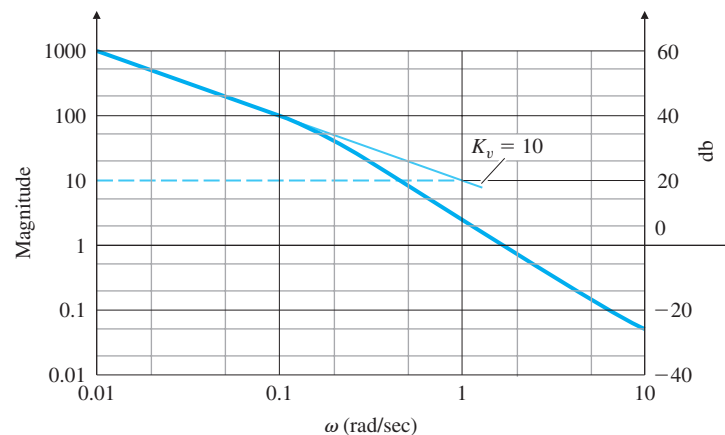
The easiest way of determining the value of  $K_v$  in a type 1 system is to read the magnitude of the low-frequency asymptote at  $\omega = 1$  rad/sec, because this asymptote is  $A(\omega) = K_v/\omega$ . In some cases the lowest-frequency break point will be below  $\omega = 1$  rad/sec; therefore, the asymptote needs to extend to  $\omega = 1$  rad/sec in order to read  $K_v$  directly. Alternately, we could read the magnitude at any frequency on the low-frequency asymptote and compute it from  $K_v = \omega A(\omega)$ .

#### EXAMPLE 6.7

#### Computation of $K_v$

As an example of the determination of steady-state errors, a Bode magnitude plot of an open-loop system is shown in Fig. 6.13. Assuming that there is unity feedback as in Fig. 6.4, find the velocity-error constant,  $K_v$ .

**Figure 6.13**  
Determination of  $K_v$  from the Bode plot for the system  $KG(s) = 10/[s(s+1)]$





**Solution.** Because the slope at the low frequencies is  $-1$ , we know that the system is type 1. The extension of the low-frequency asymptote crosses  $\omega = 1$  rad/sec at a magnitude of 10. Therefore,  $K_v = 10$  and the steady-state error to a unit ramp for a unity feedback system would be 0.1. Alternatively, at  $\omega = 0.01$  we have  $|A(\omega)| = 1000$ ; therefore, from Eq. (6.23) we have

$$K_o = K_v \cong \omega|A(\omega)| = 0.01(1000) = 10.$$

### 6.2 Neutral Stability

In the early days of electronic communications, most instruments were judged in terms of their frequency response. It is therefore natural that when the feedback amplifier was introduced, techniques to determine stability in the presence of feedback were based on this response.

Suppose the closed-loop transfer function of a system is known. We can determine the stability of a system by simply inspecting the denominator in factored form (because the factors give the system roots directly) to observe whether the real parts are positive or negative. However, the closed-loop transfer function is usually not known; in fact, the whole purpose behind understanding the root-locus technique is to be able to find the factors of the denominator in the closed-loop transfer function, given only the open-loop transfer function. Another way to determine closed-loop stability is to evaluate the frequency response of the *open-loop* transfer function  $KG(j\omega)$  and then perform a test on that response. Note that this method does not require factoring the denominator of the closed-loop transfer function. In this section we will explain the principles of this method.

Suppose we have a system defined by Fig. 6.14(a) and whose root locus behaves as shown in Fig. 6.14(b); that is, instability results if  $K$  is larger than 2. The neutrally stable points lie on the imaginary axis—that is, where  $K = 2$  and  $s = j1.0$ . Furthermore, we saw in Section 5.1 that all points on the locus have the property that

$$|KG(s)| = 1 \quad \text{and} \quad \angle G(s) = 180^\circ.$$

**Figure 6.14**  
Stability example:  
(a) system definition;  
(b) root locus

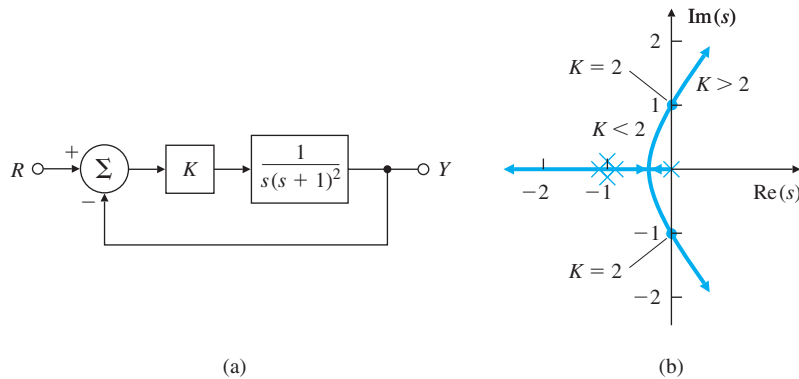
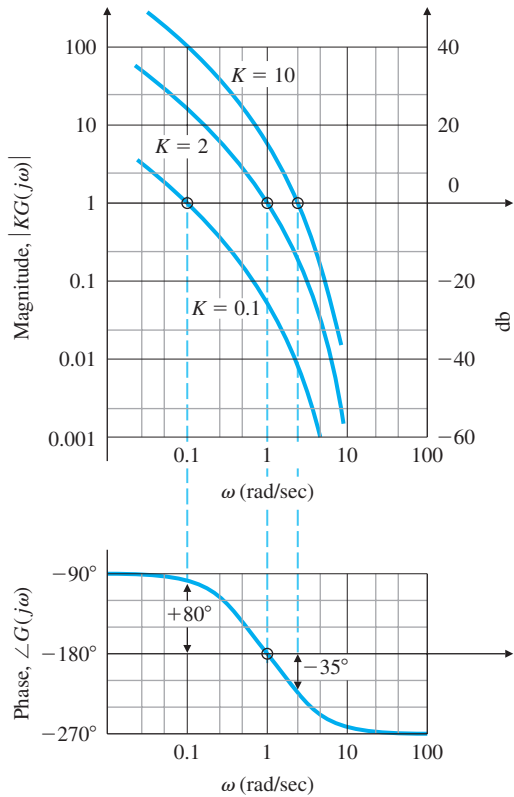


**Figure 6.15**  
 Frequency response magnitude and phase for the system in Fig. 6.14



At the point of neutral stability we see that these root-locus conditions hold for  $s = j\omega$ , so

$$|KG(j\omega)| = 1 \quad \text{and} \quad \angle G(j\omega) = 180^\circ. \tag{6.24}$$

Thus a Bode plot of a system that is neutrally stable (that is, with  $K$  defined such that a closed-loop root falls on the imaginary axis) will satisfy the conditions of Eq. (6.24). Figure 6.15 shows the frequency response for the system whose root locus is plotted in Fig. 6.14 for various values of  $K$ . The magnitude response corresponding to  $K = 2$  passes through 1 at the same frequency ( $\omega = 1$  rad/sec) at which the phase passes through  $180^\circ$ , as predicted by Eq. (6.24).

Having determined the point of neutral stability, we turn to a key question: Does increasing the gain increase or decrease the system's stability? We can see from the root locus in Fig. 6.14(b) that any value of  $K$  less than the value at the neutrally stable point will result in a stable system. At the frequency  $\omega$  where the phase  $\angle G(j\omega) = -180^\circ$  ( $\omega = 1$  rad/sec), the magnitude  $|KG(j\omega)| < 1.0$  for stable values of  $K$  and  $> 1$  for unstable values of  $K$ . Therefore, we have

## Stability condition

the following trial stability condition, based on the character of the open-loop frequency response:

$$|KG(j\omega)| < 1 \quad \text{at} \quad \angle G(j\omega) = -180^\circ. \quad (6.25)$$

This stability criterion holds for all systems for which increasing gain leads to instability and  $|KG(j\omega)|$  crosses the magnitude = 1 once, the most common situation. However, there are systems for which an increasing gain can lead from instability to stability; in this case, the stability condition is

$$|KG(j\omega)| > 1 \quad \text{at} \quad \angle G(j\omega) = -180^\circ. \quad (6.26)$$

There are also cases when  $|KG(j\omega)|$  crosses magnitude = 1 more than once. One way to resolve the ambiguity that is usually sufficient is to perform a rough sketch of the root locus. Another, more rigorous, way to resolve the ambiguity is to use the Nyquist stability criterion, the subject of the next section. However, because the Nyquist criterion is fairly complex, it is important while studying it to bear in mind the theme of this section, namely, that for most systems a simple relationship exists between closed-loop stability and the open-loop frequency response.

### 6.3 The Nyquist Stability Criterion

For most systems, as we saw in the previous section, an increasing gain eventually causes instability. In the very early days of feedback control design, this relationship between gain and stability margins was assumed to be universal. However, designers found occasionally that in the laboratory the relationship reversed itself; that is, the amplifier would become unstable when the gain was decreased. The confusion caused by these conflicting observations motivated Harry Nyquist of the Bell Telephone Laboratories to study the problem in 1932. His study explained the occasional reversals and resulted in a more sophisticated analysis with no loopholes. Not surprisingly, his test has come to be called the **Nyquist stability criterion**. It is based on a result from complex variable theory known as the **argument principle**,<sup>8</sup> as we briefly explain in this section and in more detail in Appendix B.

The Nyquist stability criterion relates the open-loop frequency response to the number of closed-loop poles of the system in the RHP. Study of the Nyquist criterion will allow you to determine stability from the frequency response of a complex system, perhaps with one or more resonances, where the magnitude curve crosses 1 several times and/or the phase crosses  $180^\circ$  several times. It is also very useful in dealing with open-loop, unstable systems, nonminimum-phase systems, and systems with pure delays (transportation lags).

<sup>8</sup> Sometimes referred to as “Cauchy’s Principle of the Argument.”

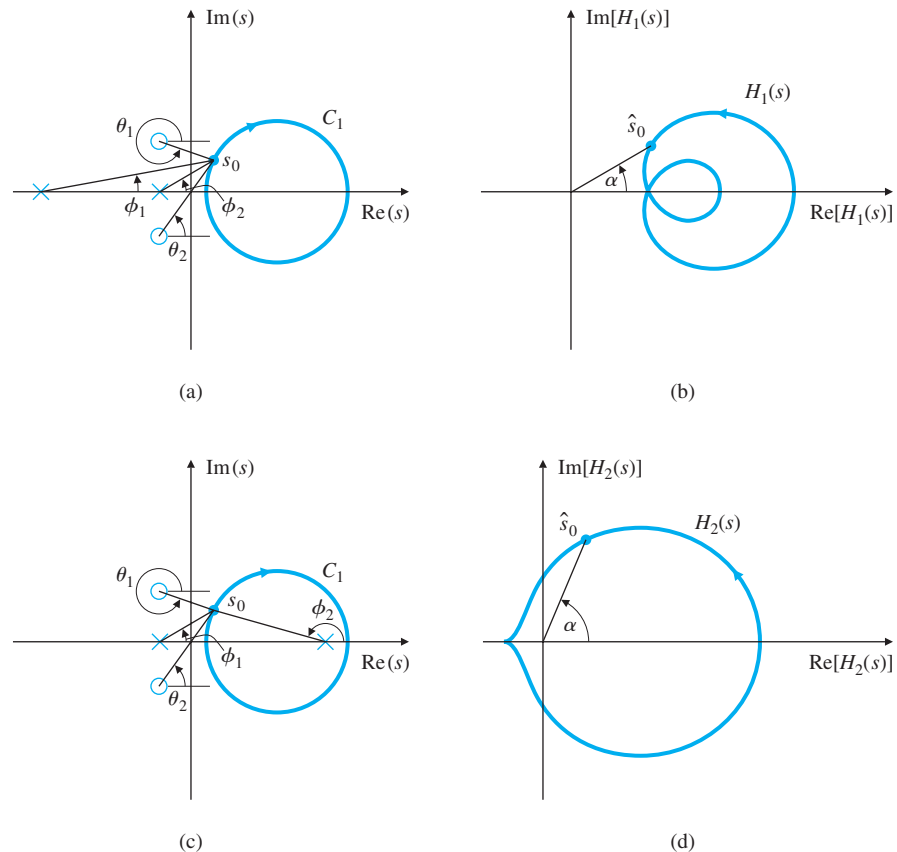
### 6.3.1 The Argument Principle

Consider the transfer function  $H_1(s)$  whose poles and zeros are indicated in the  $s$ -plane in Fig. 6.16(a). We wish to evaluate  $H_1$  for values of  $s$  on the clockwise contour  $C_1$ . (Hence this is called a **contour evaluation**.) We choose the test point  $s_o$  for evaluation. The resulting complex quantity has the form  $H_1(s_o) = \vec{v} = |\vec{v}|e^{j\alpha}$ . The value of the argument of  $H_1(s_o)$  is

$$\alpha = \theta_1 + \theta_2 - (\phi_1 + \phi_2).$$

As  $s$  traverses  $C_1$  in the clockwise direction starting at  $s_o$ , the angle  $\alpha$  of  $H_1(s)$  in Fig. 6.16(b) will change (decrease or increase), but it will not undergo a net change of  $360^\circ$  as long as there are no poles or zeros within  $C_1$ . This is because none of the angles that make up  $\alpha$  go through a net revolution. The angles  $\theta_1$ ,  $\theta_2$ ,  $\phi_1$ , and  $\phi_2$  increase or decrease as  $s$  traverses around  $C_1$ , but they return to their original values as  $s$  returns to  $s_o$  without rotating through  $360^\circ$ . This means that the plot of  $H_1(s)$  [Fig. 6.16(b)] will not encircle the origin. This

**Figure 6.16**  
Contour evaluations:  
(a)  $s$ -plane plot of poles and zeros of  $H_1(s)$  and the contour  $C_1$ ; (b)  $H_1(s)$  for  $s$  on  $C_1$ ; (c)  $s$ -plane plot of poles and zeros of  $H_2(s)$  and the contour  $C_1$ ; (d)  $H_2(s)$  for  $s$  on  $C_1$



conclusion follows from the fact that  $\alpha$  is the sum of the angles indicated in Fig. 6.16(a), so the only way that  $\alpha$  can be changed by  $360^\circ$  after  $s$  executes one full traverse of  $C_1$  is for  $C_1$  to contain a pole or zero.

Now consider the function  $H_2(s)$ , whose pole-zero pattern is shown in Fig. 6.16(c). Note that it has a singularity (pole) within  $C_1$ . Again, we start at the test point  $s_o$ . As  $s$  traverses in the clockwise direction around  $C_1$ , the contributions from the angles  $\theta_1$ ,  $\theta_2$ , and  $\phi_1$  change, but they return to their original values as soon as  $s$  returns to  $s_o$ . In contrast,  $\phi_2$ , the angle from the pole within  $C_1$ , undergoes a net change of  $-360^\circ$  after one full traverse of  $C_1$ . Therefore, the argument of  $H_2(s)$  undergoes the same change, causing  $H_2$  to encircle the origin in the counterclockwise direction, as shown in Fig. 6.16(d). The behavior would be similar if the contour  $C_1$  had enclosed a zero instead of a pole. The mapping of  $C_1$  would again enclose the origin once in the  $H_2(s)$ -plane, except it would do so in the clockwise direction.

Thus we have the essence of the argument principle:

#### Argument principle

A contour map of a complex function will encircle the origin  $Z - P$  times, where  $Z$  is the number of zeros and  $P$  is the number of poles of the function inside the contour.

For example, if the number of poles and zeros within  $C_1$  is the same, the net angles cancel and there will be no net encirclement of the origin.

### 6.3.2 Application to Control Design

To apply the principle to control design, we let the  $C_1$  contour in the  $s$ -plane encircle the entire RHP, the region in the  $s$ -plane where a pole would cause an unstable system (Fig. 6.17). The resulting evaluation of  $H(s)$  will encircle the origin only if  $H(s)$  has a RHP pole or zero.

**Figure 6.17**  
An  $s$ -plane plot of a contour  $C_1$  that encircles the entire RHP

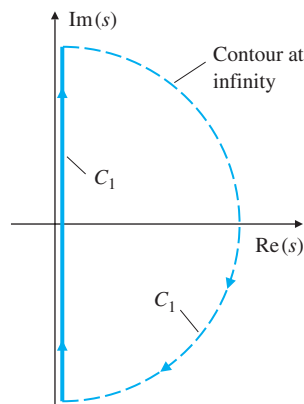
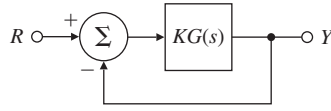


**Figure 6.18**  
Block diagram for  
 $Y(s)/R(s) =$   
 $KG(s)/[1 + KG(s)]$



As stated earlier, what makes all this contour behavior useful is that a contour evaluation of an *open-loop*  $KG(s)$  can be used to determine stability of the *closed-loop* system. Specifically, for the system in Fig. 6.18, the closed-loop transfer function is

$$\frac{Y(s)}{R(s)} = \mathcal{T}(s) = \frac{KG(s)}{1 + KG(s)}$$

Therefore, the closed-loop roots are the solutions of

$$1 + KG(s) = 0,$$

and we apply the principle of the argument to the function  $1 + KG(s)$ . If the evaluation contour of this function of  $s$  enclosing the entire RHP contains a zero or pole of  $1 + KG(s)$ , then the evaluated contour of  $1 + KG(s)$  will encircle the origin. Notice that  $1 + KG(s)$  is simply  $KG(s)$  shifted to the right 1 unit, as shown in Fig. 6.19. Therefore, if the plot of  $1 + KG(s)$  encircles the origin, the plot of  $KG(s)$  will encircle  $-1$  on the real axis. Therefore, we can plot the contour evaluation of the open-loop  $KG(s)$ , examine its encirclements of  $-1$ , and draw conclusions about the origin encirclements of the closed-loop function  $1 + KG(s)$ . Presentation of the evaluation of  $KG(s)$  in this manner is often referred to as a **Nyquist plot**, or **polar plot**, because we plot the magnitude of  $KG(s)$  versus the angle of  $KG(s)$ .

Nyquist plot; polar plot

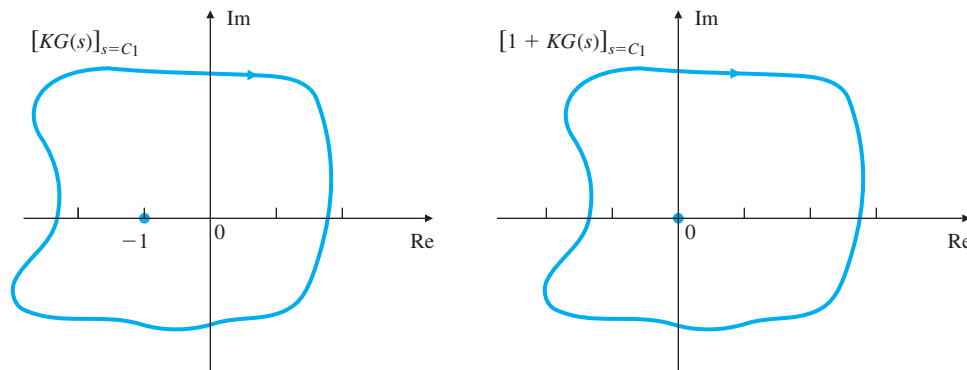


**Figure 6.19** Evaluations of  $KG(s)$  and  $1 + KG(s)$ : Nyquist plots

To determine whether an encirclement is due to a pole or zero, we write  $1 + KG(s)$  in terms of poles and zeros of  $KG(s)$ :

$$1 + KG(s) = 1 + K \frac{b(s)}{a(s)} = \frac{a(s) + Kb(s)}{a(s)}. \quad (6.27)$$

Equation (6.27) shows that the poles of  $1 + KG(s)$  are also the poles of  $G(s)$ . Because it is safe to assume that the poles of  $G(s)$  [or factors of  $a(s)$ ] are known, the (rare) existence of any of these poles in the RHP can be accounted for. Assuming for now that there are no poles of  $G(s)$  in the RHP, an encirclement of  $-1$  by  $KG(s)$  indicates a zero of  $1 + KG(s)$  in the RHP, and thus an unstable root of the closed-loop system.

We can generalize this basic idea by noting that a clockwise contour  $C_1$  enclosing a zero of  $1 + KG(s)$ —that is, a closed-loop system root—will result in  $KG(s)$  encircling the  $-1$  point in a clockwise direction. Likewise, if  $C_1$  encloses a pole of  $1 + KG(s)$ —that is, if there is an unstable open-loop pole—there will be a counterclockwise  $KG(s)$  encirclement of  $-1$ . Furthermore, if two poles or two zeros are in the RHP,  $KG(s)$  will encircle  $-1$  twice, and so on. The net number of clockwise encirclements,  $N$ , equals the number of zeros (closed-loop system roots) in the RHP,  $Z$ , minus the number of open-loop poles in the RHP,  $P$ :

$$N = Z - P.$$

This is the key concept of the Nyquist Stability Criterion.

A simplification in the plotting of  $KG(s)$  results from the fact that any  $KG(s)$  that represents a physical system will have zero response at infinite frequency (i.e., has more poles than zeros). This means that the big arc of  $C_1$  corresponding to  $s$  at infinity (Fig. 6.17) results in  $KG(s)$  being a point of infinitesimally small value near the origin for that portion of  $C_1$ . Therefore, we accomplish a complete evaluation of a physical system  $KG(s)$  by letting  $s$  traverse the imaginary axis from  $-j\infty$  to  $+j\infty$  (actually, from  $-j\omega_h$  to  $+j\omega_h$ , where  $\omega_h$  is large enough that  $|KG(j\omega)|$  is much less than 1 for all  $\omega > \omega_h$ ). The evaluation of  $KG(s)$  from  $s = 0$  to  $s = j\infty$  has already been discussed in Section 6.1 under the context of finding the frequency response of  $KG(s)$ . Because  $G(-j\omega)$  is the complex conjugate of  $G(j\omega)$ , we can easily obtain the entire plot of  $KG(s)$  by reflecting the  $0 \leq s \leq +j\infty$  portion about the real axis, to get the  $(-j\infty \leq s < 0)$  portion. Hence we see that closed-loop stability can be determined in all cases by examination of the frequency response of the open-loop transfer function on a polar plot. In some applications, models of physical systems are simplified so as to eliminate some high-frequency dynamics. The resulting reduced-order transfer function might have an equal number of poles and zeros. In that case the big arc of  $C_1$  at infinity needs to be considered.

In practice, many systems behave like those discussed in Section 6.2, so you need not carry out a complete evaluation of  $KG(s)$  with subsequent inspection of the  $-1$  encirclements; a simple look at the frequency response may suffice to

determine stability based on the gain and phase margins. However, in the case of a complex system for which the simplistic rules given in Section 6.2 become ambiguous, you will want to perform the complete analysis, summarized as follows:

Procedure for Plotting the Nyquist Plot

1. Plot  $KG(s)$  for  $-j\infty \leq s \leq +j\infty$ . Do this by first evaluating  $KG(j\omega)$  for  $\omega = 0$  to  $\omega_h$ , where  $\omega_h$  is so large that the magnitude of  $KG(j\omega)$  is negligibly small for  $\omega > \omega_h$ , then reflecting the image about the real axis and adding it to the preceding image. The magnitude of  $KG(j\omega)$  will be small at high frequencies for any physical system. The Nyquist plot will always be symmetric with respect to the real axis.
2. Evaluate the number of clockwise encirclements of  $-1$ , and call that number  $N$ . Do this by drawing a straight line in *any* direction from  $-1$  to  $\infty$ . Then count the net number of left-to-right crossings of the straight line by  $KG(s)$ . If encirclements are in the counterclockwise direction,  $N$  is negative.
3. Determine the number of unstable (RHP) poles of  $G(s)$ , and call that number  $P$ .
4. Calculate the number of unstable closed-loop roots  $Z$ :

$$Z = N + P. \tag{6.28}$$

For stability we wish to have  $Z = 0$ ; that is, no characteristic equation roots in the RHP.

Let us now examine a rigorous application of the procedure for drawing Nyquist plots for some examples.

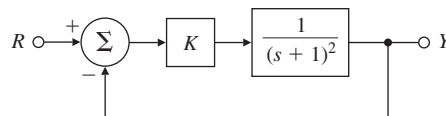
EXAMPLE 6.8

*Nyquist Plot for a Second-Order System*

Determine the stability properties of the system defined in Fig. 6.20.

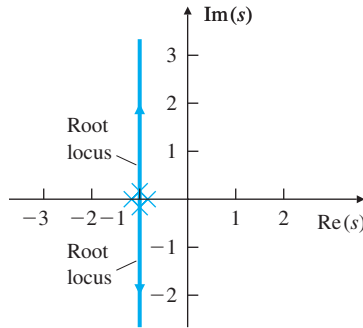
**Solution.** The root locus of the system in Fig. 6.20 is shown in Fig. 6.21. It shows that the system is stable for all values of  $K$ . The magnitude of the frequency response of  $KG(s)$  is plotted in Fig. 6.22(a) for  $K = 1$ , and the phase is plotted in Fig. 6.22(b); this is the typical Bode method of presenting frequency response and represents the evaluation of  $G(s)$  over the interesting range of frequencies. The same information is replotted in Fig. 6.23 in the Nyquist (polar) plot form. Note how the points  $A, B, C, D,$  and  $E$  are mapped from the Bode plot to the Nyquist plot in Fig. 6.23. The arc from  $G(s) = +1$  ( $\omega = 0$ ) to  $G(s) = 0$  ( $\omega = \infty$ ) that lies below the real axis is derived from Fig. 6.22. The portion of the  $C_1$  arc at infinity from Fig. 6.17 transforms into  $G(s) = 0$  in Fig. 6.23; therefore, a continuous evaluation of  $G(s)$  with  $s$  traversing  $C_1$  is completed

Figure 6.20 Control system for Example 6.8



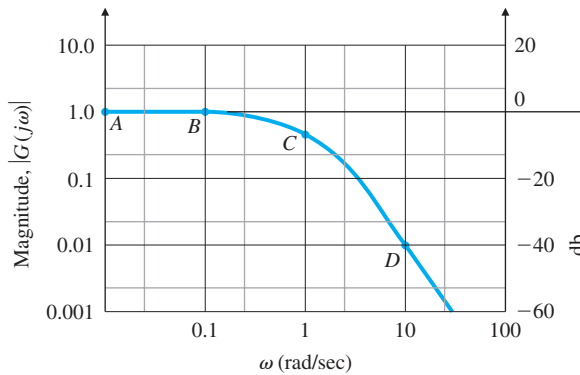


**Figure 6.21**  
 Root locus of  $G(s) = 1/(s + 1)^2$  with respect to  $K$

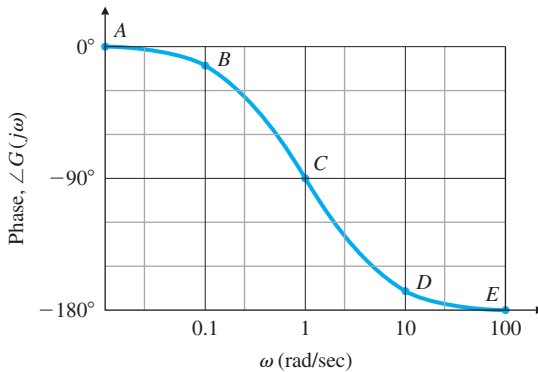


by simply reflecting the lower arc about the real axis. This creates the portion of the contour above the real axis and completes the Nyquist (polar) plot. Because the plot does not encircle  $-1$ ,  $N = 0$ . Also, there are no poles of  $G(s)$  in the RHP, so  $P = 0$ . From Eq. (6.28), we conclude that  $Z = 0$ , which indicates there are no unstable roots of the closed-loop system for  $K = 1$ . Furthermore, different values of  $K$  would simply change the magnitude of the polar plot, but no positive value of  $K$  would cause the

**Figure 6.22**  
 Open-loop Bode plot for  $G(s) = 1/(s + 1)^2$

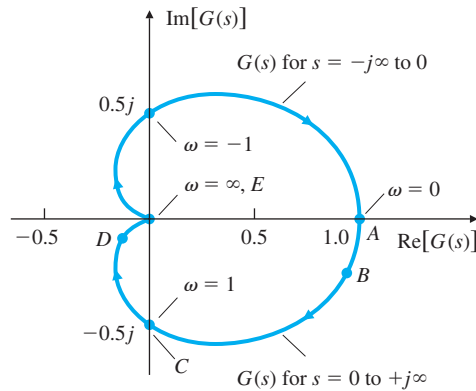


(a)



(b)

**Figure 6.23**  
Nyquist plot of the  
evaluation of  $KG(s)$  for  
 $s = C_1$  and  $K = 1$



plot to encircle  $-1$ , because the polar plot will always cross the negative real axis when  $KG(s) = 0$ . Thus the Nyquist stability criterion confirms what the root locus indicated: the closed-loop system is stable for all  $K > 0$ .

The MATLAB statements that will produce this Nyquist plot are

```
numG = 1;
denG = [1 2 1];
sysG = tf(numG,denG);
nyquist(sysG);
```

Often the control systems engineer is more interested in determining a range of gains  $K$  for which the system is stable than in testing for stability at a specific value of  $K$ . To accommodate this requirement, but to avoid drawing multiple Nyquist plots for various values of the gain, the test can be slightly modified. To do so, we scale  $KG(s)$  by  $K$  and examine  $G(s)$  to determine stability for a range of gains  $K$ . This is possible because an encirclement of  $-1$  by  $KG(s)$  is equivalent to an encirclement of  $-1/K$  by  $G(s)$ . Therefore, instead of having to deal with  $KG(s)$ , we need only consider  $G(s)$ , and count the number of the encirclements of the  $-1/K$  point.

Applying this idea to Example 6.8, we see that the Nyquist plot cannot encircle the  $-1/K$  point. For positive  $K$ , the  $-1/K$  point will move along the negative real axis, so there will not be an encirclement of  $G(s)$  for any value of  $K > 0$ .

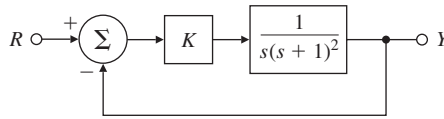
(There are also values of  $K < 0$  for which the Nyquist plot shows the system to be stable; specifically,  $-1 < K < 0$ . This result may be verified by drawing the  $0^\circ$  locus.)

### EXAMPLE 6.9

### *Nyquist Plot for a Third-Order System*

As a second example, consider the system  $G(s) = 1/s(s+1)^2$  for which the closed-loop system is defined in Fig. 6.24. Determine its stability properties using the Nyquist criterion.

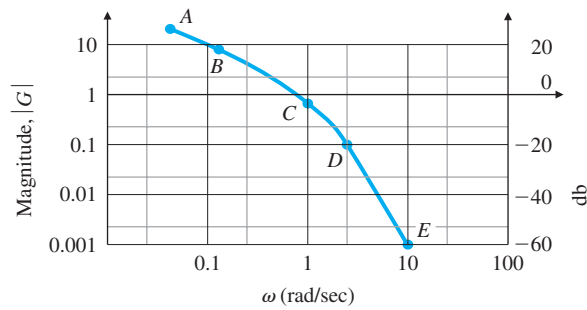
**Figure 6.24**  
Control system for  
Example 6.9



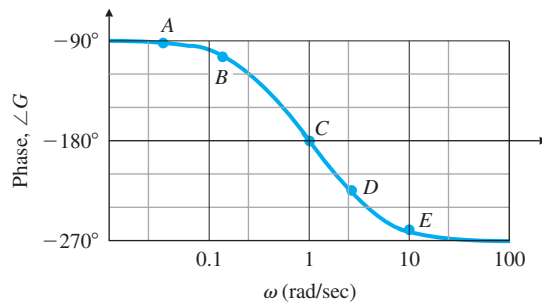
**Solution.** This is the same system discussed in Section 6.2. The root locus in Fig. 6.14(b) shows that this system is stable for small values of  $K$  but unstable for large values of  $K$ . The magnitude and phase of  $G(s)$  in Fig. 6.25 are transformed into the Nyquist plot shown in Fig. 6.26. Note how the points  $A$ ,  $B$ ,  $C$ ,  $D$ , and  $E$  on the Bode plot of Fig. 6.25 map into those on the Nyquist plot of Fig. 6.26. Also note the large arc at infinity that arises from the open-loop pole at  $s = 0$ . This pole creates an infinite magnitude of  $G(s)$  at  $\omega = 0$ ; in fact, a pole anywhere on the imaginary axis will create an arc at infinity. To correctly determine the number of  $-1/K$  point encirclements, we must draw this arc in the proper half-plane: Should it cross the *positive* real axis, as shown in Fig. 6.26, or the negative one? It is also necessary to assess whether the arc should sweep out  $180^\circ$  (as in Fig. 6.26),  $360^\circ$ , or  $540^\circ$ .

A simple artifice suffices to answer these questions. We modify the  $C_1$  contour to take a small detour around the pole either to the right (Fig. 6.27) or to the left. It makes no difference to the final stability question which way, but it is more convenient to go to the right because then no poles are introduced within the  $C_1$  contour, keeping the value of  $P$  equal to 0. Because the phase of  $G(s)$  is the negative of the sum of the angles from all of the poles, we see that the evaluation results in a Nyquist plot moving from  $+90^\circ$  for  $s$  just below the pole at  $s = 0$ , across the positive real axis to  $-90^\circ$  for  $s$  just above the pole. Had there been two poles at  $s = 0$ , the Nyquist plot at infinity would

**Figure 6.25**  
Bode plot for  
 $G(s) = 1/[s(s + 1)^2]$

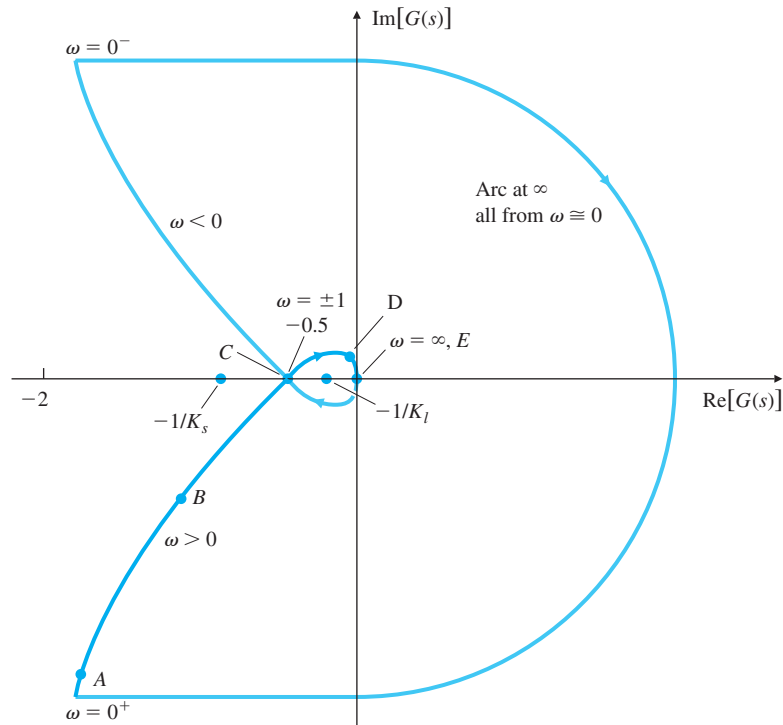


(a)



(b)

**Figure 6.26**  
Nyquist plot for  
 $G(s) = 1/[s(s+1)^2]$



have executed a full  $360^\circ$  arc, and so on for three or more poles. Furthermore, for a pole elsewhere on the imaginary axis, a  $180^\circ$  clockwise arc would also result but would be oriented differently than the example shown in Fig. 6.26.

The Nyquist plot crosses the real axis at  $\omega = 1$  with  $|G| = 0.5$ , as indicated by the Bode plot. For  $K > 0$ , there are two possibilities for the location of  $-1/K$ : inside the two loops of the Nyquist plot, or outside the Nyquist contour completely. For large values of  $K$  ( $K_l$  in Fig. 6.26),  $-0.5 < -1/K_l < 0$  will lie inside the two loops; hence  $N = 2$ , and therefore,  $Z = 2$ , indicating that there are two unstable roots. This happens for  $K > 2$ . For small values of  $K$  ( $K_s$  in Fig. 6.26),  $-1/K$  lies outside the loops; thus  $N = 0$ , and all roots are stable. All this information is in agreement with the root locus in Figure 6.14(b). (When  $K < 0$ ,  $-1/K$  lies on the positive real axis, then  $N = 1$ , which means  $Z = 1$  and the system has one unstable root. The  $0^\circ$  root locus will verify this result.)

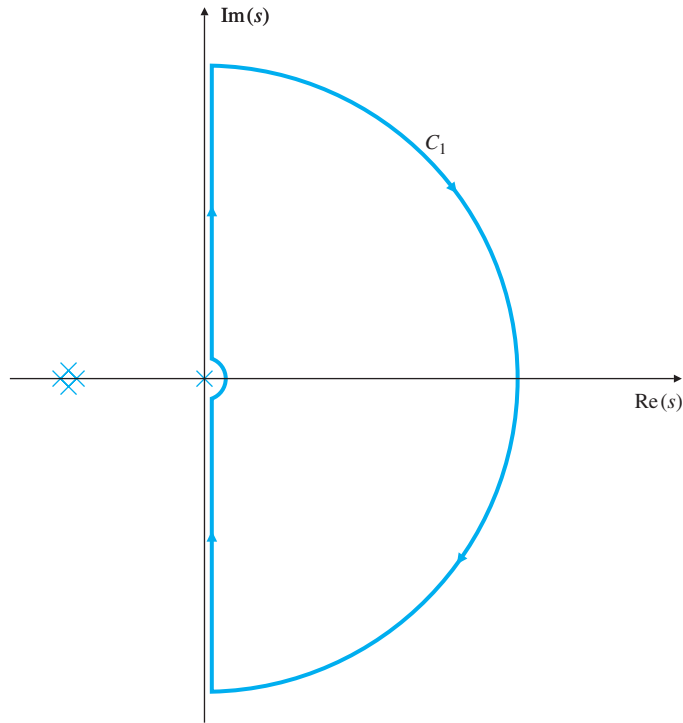
For this and many similar systems, we can see that the encirclement criterion reduces to a very simple test for stability based on the open-loop frequency response: The system is stable if  $|KG(j\omega)| < 1$  when the phase of  $G(j\omega)$  is  $180^\circ$ . Note that this relation is identical to the stability criterion given in Eq. (6.25); however, by using the Nyquist criterion, we don't require the root locus to determine whether  $|KG(j\omega)| < 1$  or  $|KG(j\omega)| > 1$ .

#### Nyquist plot via MATLAB

We draw the Nyquist plot using MATLAB with

```
numG = 1;
denG = [1 2 1 0];
sysG = tf(numG,denG);
axis([-5 5 -5 5])
```

**Figure 6.27**  
 $C_1$  contour enclosing the RHP for the system in Example 6.9



nyquist(sysG);

The axis command scaled the plot so that only points between +5 and -5 on the real and imaginary axes were included. Without manual scaling, the plot would be scaled between  $\pm\infty$  and the essential features in the vicinity of the -1 region would be lost.

For systems that are open-loop unstable, care must be taken because now  $P \neq 0$  in Eq. (6.28). We shall see that the simple rules from Section 6.2 will need to be revised in this case.

**EXAMPLE 6.10**

*Nyquist Plot for an Open-Loop Unstable System*

The third example is defined in Fig. 6.28. Determine its stability properties using the Nyquist criterion.

**Solution.** The root locus for this system is sketched in Fig. 6.29. The open-loop system is unstable because it has a pole in the RHP. The open-loop Bode plot is shown in

**Figure 6.28**  
 Control system for Example 6.10

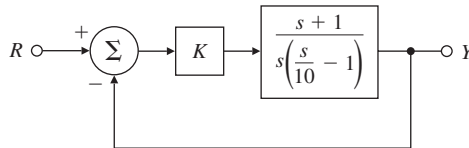


**Figure 6.29**  
 Root locus for  $G(s) = (s + 1)/[s(s/10 - 1)]$

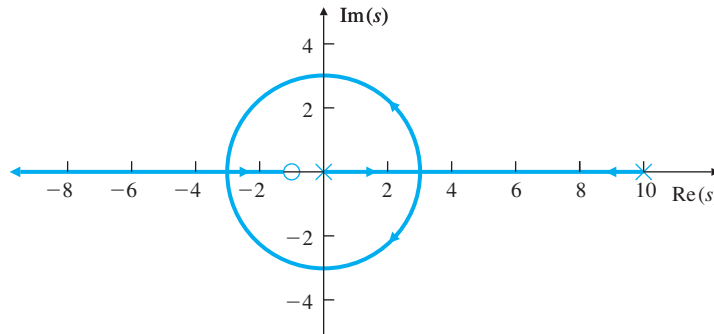
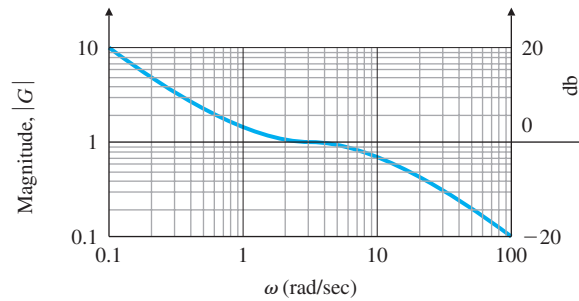


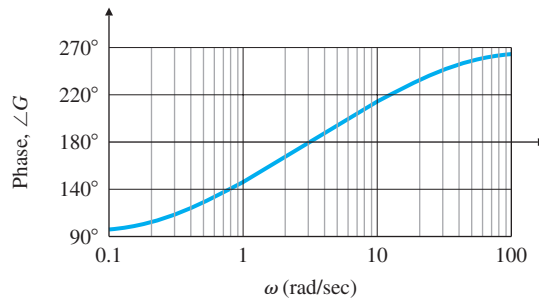
Fig. 6.30. Note in the Bode that  $|KG(j\omega)|$  behaves exactly the same as if the pole had been in the LHP. However,  $\angle G(j\omega)$  increases by  $90^\circ$  instead of the usual decrease at a pole. Any system with a pole in the RHP is unstable; hence it would be impossible to determine its frequency response experimentally because the system would never reach a steady-state sinusoidal response for a sinusoidal input. It is, however, possible to compute the magnitude and phase of the transfer function according to the rules in Section 6.1. The pole in the RHP affects the Nyquist encirclement criterion, because the value of  $P$  in Eq. (6.28) is  $+1$ .

We convert the frequency-response information of Fig. 6.30 into the Nyquist plot (Fig. 6.31) as in the previous examples. As before, the  $C_1$  detour around the pole at  $s = 0$  in Fig. 6.32 creates a large arc at infinity in Fig. 6.31. This arc crosses the *negative* real axis because of the  $180^\circ$  phase contribution of the pole in the RHP.

**Figure 6.30**  
 Bode plot for  $G(s) = (s + 1)/[s(s/10 - 1)]$

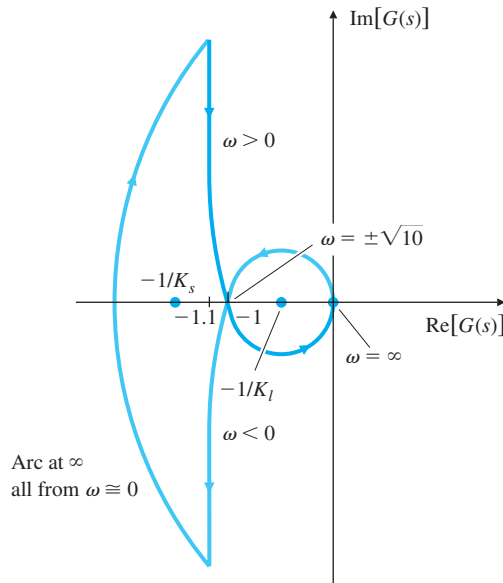


(a)



(b)

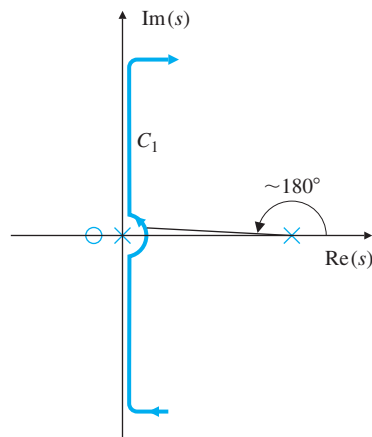
**Figure 6.31**  
Nyquist plot for  $G(s) = (s + 1)/[s(s/10 - 1)]$



The real-axis crossing occurs at  $|G(s)| = 1$  because in the Bode plot  $|G(s)| = 1$  when  $\angle G(s) = 180^\circ$ , which happens to be at  $\omega \cong 3$  rad/sec.

The contour shows two different behaviors, depending on the values of  $K (> 0)$ . For large values of  $K$  ( $K_l$  in Fig. 6.31), there is one counterclockwise encirclement; hence  $N = -1$ . However, because  $P = 1$  from the RHP pole,  $Z = N + P = 0$ , so there are no unstable system roots and the system is stable for  $K > 1$ . For small values of  $K$  ( $K_s$  in Fig. 6.31),  $N = +1$ , because of the clockwise encirclement and  $Z = 2$ , indicating two unstable roots. This happens if  $K < 1$ . These results can be verified qualitatively by the root locus in Fig. 6.29. (If  $K < 0$ ,  $-1/K$  is on the positive real axis so that  $N = 0$  and  $Z = 1$ , indicating the system will have one unstable closed-loop pole which can be verified by a  $0^\circ$  root locus.)

**Figure 6.32**  
 $C_1$  contour for Example 6.10



As with all systems, the stability boundary occurs at  $|KG(j\omega)| = 1$  for the phase of  $\angle G(j\omega) = 180^\circ$ . However, in this case,  $|KG(j\omega)|$  must be greater than 1 to yield the correct number of  $-1$  point encirclements to achieve stability.

To draw the Nyquist plot using MATLAB, use the following commands:

```
numG = [1 1];
denG = [0.1 -1 0];
sysG = tf(numG,denG);
axis([-5 5 -5 5]);
nyquist(sysG)
```

The existence of the RHP pole in Example 6.10 affected the Bode plotting rules of the phase curve and affected the relationship between encirclements and unstable closed-loop roots because  $P = 1$  in Eq. (6.28). But we apply the Nyquist stability criterion without any modifications. The same is true for systems with a RHP zero; that is, a nonminimum-phase zero has no effect on the Nyquist stability criterion, but the Bode plotting rules are affected.

## 6.4 Stability Margins

A large fraction of control system designs behave in a pattern roughly similar to that of the system in Section 6.2 and Example 6.9 in Section 6.3; that is, the system is stable for all small gain values and becomes unstable if the gain increases past a certain critical point. Two commonly used quantities that measure the stability margin for such systems are directly related to the stability criterion of Eq. (6.25): gain margin and phase margin. In this section we will define and use these two concepts to study system design. Another measure of stability, originally defined by O. J. M. Smith (1958), combines these two margins into one and gives a better indication of stability for complicated cases.

Gain margin

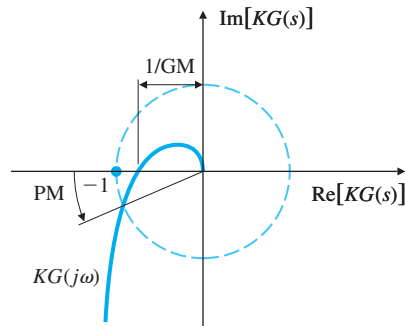
The **gain margin (GM)** is the factor by which the gain can be raised before instability results. For the typical case, it can be read directly from the Bode plot (for example, see Fig. 6.15) by measuring the vertical distance between the  $|KG(j\omega)|$  curve and the  $|KG(j\omega)| = 1$  line at the frequency where  $\angle G(j\omega) = 180^\circ$ . We see from the figure that when  $K = 0.1$ , the system is stable and  $GM = 20$  (or 26 db). When  $K = 2$ , the system is neutrally stable with  $GM = 1$  (0 db), while  $K = 10$  results in an unstable system with  $GM = 0.2$  ( $-14$  db). Note that GM is the *factor* by which the gain  $K$  can be raised before instability results; therefore,  $|GM| < 1$  (or  $|GM| < 0$  db) indicates an unstable system. The GM can also be determined from a root locus with respect to  $K$  by noting two values of  $K$ : (1) at the point where the locus crosses the  $j\omega$ -axis, and (2) at the nominal closed-loop poles. The GM is the ratio of these two values.

Phase margin

Another measure that is used to indicate the stability margin in a system is the **phase margin (PM)**. It is the amount by which the phase of  $G(j\omega)$  exceeds  $-180^\circ$  when  $|KG(j\omega)| = 1$ , which is an alternative way of measuring the degree to which the stability conditions of Eq. (6.25) are met. For the case in Fig. 6.15, we see that  $PM \cong 80^\circ$  for  $K = 0.1$ ,  $PM = 0^\circ$  for  $K = 2$ , and  $PM = -35^\circ$  for  $K = 10$ . A positive PM is required for stability.



**Figure 6.33**  
Nyquist plot for defining GM  
and PM



Note that the two stability measures, PM and GM, together determine how far the complex quantity  $G(j\omega)$  passes from the  $-1$  point, which is another way of stating the neutral-stability point specified by Eq. (6.24).

The stability margins may also be defined in terms of the Nyquist plot. Figure 6.33 shows that GM and PM are measures of how close the Nyquist plot comes to encircling the  $-1$  point. Again we can see that the GM indicates how much the gain can be raised before instability results in a system like the one in Example 6.9. The PM is the difference between the phase of  $G(j\omega)$  and  $180^\circ$  when  $KG(j\omega)$  crosses the circle  $|KG(s)| = 1$ ; the positive value of PM is assigned to the stable case (i.e., with no Nyquist encirclements).

#### Crossover frequency

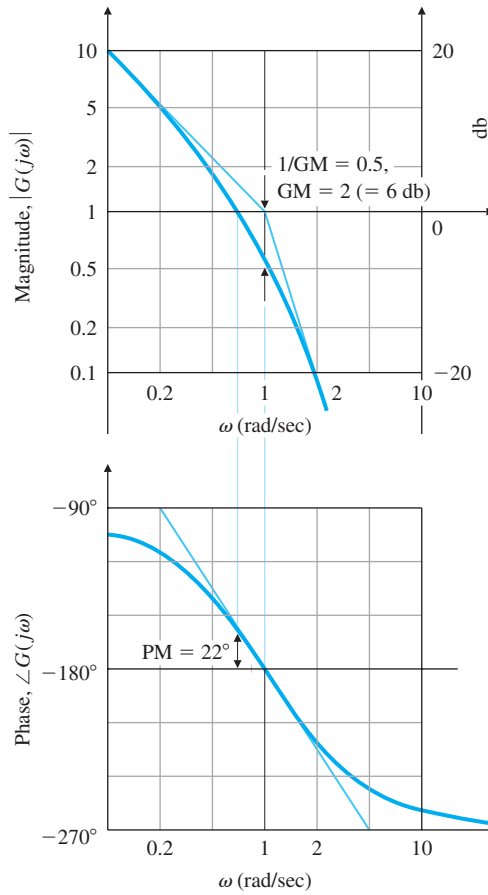
It is easier to determine these margins directly from the Bode plot than from the Nyquist plot. The term **crossover frequency**,  $\omega_c$ , is often used to refer to the frequency at which the gain is unity, or 0 db. Figure 6.34 shows the same data plotted in Fig. 6.25, but for the case with  $K = 1$ . The same values of PM ( $= 22^\circ$ ) and GM ( $= 2$ ) may be obtained from the Nyquist plot shown in Fig. 6.26. The real-axis crossing at  $-0.5$  corresponds to a GM of  $1/0.5$  or 2 and the PM could be computed graphically by measuring the angle of  $G(j\omega)$  as it crosses  $|G(j\omega)| = 1$  circle.

One of the useful aspects of frequency-response design is the ease with which we can evaluate the effects of gain changes. In fact, we can determine the PM from Fig. 6.34 for any value of  $K$  without redrawing the magnitude or phase information. We need only indicate on the figure where  $|KG(j\omega)| = 1$  for selected trial values of  $K$ , as has been done with dashed lines in Fig. 6.35. Now we can see that  $K = 5$  yields an unstable PM of  $-22^\circ$ , while a gain of  $K = 0.5$  yields a PM of  $+45^\circ$ . Furthermore, if we wish a certain PM (say  $70^\circ$ ), we simply read the value of  $|G(j\omega)|$  corresponding to the frequency that would create the desired PM (here  $\omega = 0.2$  rad/sec yields  $70^\circ$ , where  $|G(j\omega)| = 5$ ), and note that the magnitude at this frequency is  $1/K$ . Therefore, a PM of  $70^\circ$  will be achieved with  $K = 0.2$ .

The PM is more commonly used to specify control system performance because it is most closely related to the damping ratio of the system. This can be seen easily for the open-loop second-order system

$$G(s) = \frac{\omega_n^2}{s(s + 2\zeta\omega_n)}, \quad (6.29)$$

**Figure 6.34**  
GM and PM from the magnitude and phase plots



which, with unity feedback, produces the closed-loop system

$$T(s) = \frac{\omega_n^2}{s^2 + 2\zeta\omega_n s + \omega_n^2}. \tag{6.30}$$

It can be shown that the relationship between the PM and  $\zeta$  in this system is

$$PM = \tan^{-1} \left[ \frac{2\zeta}{\sqrt{\sqrt{1 + 4\zeta^4} - 2\zeta^2}} \right], \tag{6.31}$$

and this function is plotted in Fig. 6.36. Note that the function is approximately a straight line up to about  $PM = 60^\circ$ . The dashed line shows a straight-line approximation to the function, where

$$\zeta \cong \frac{PM}{100}. \tag{6.32}$$

**Figure 6.35**  
PM vs.  $K$  from the frequency-response data

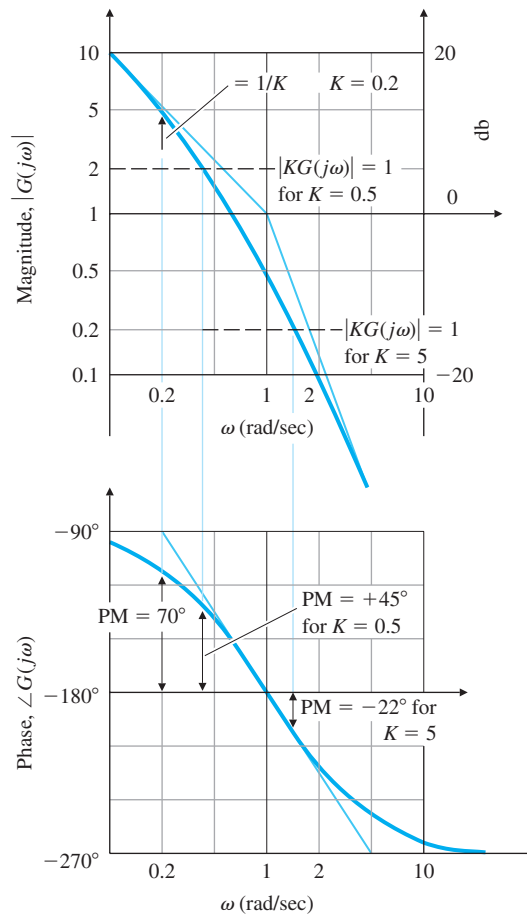
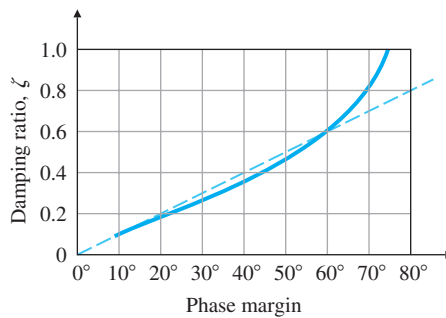


**Figure 6.36**  
Damping ratio vs. phase margin (PM)



It is clear that the approximation holds only for phase margins below about  $70^\circ$ . Furthermore, Eq. (6.31) is only accurate for the second-order system of Eq. (6.30). In spite of these limitations, Eq. (6.32) is often used as a rule of thumb for relating the closed-loop damping ratio to PM. It is useful as a starting point; however, it is important always to check the actual damping of a design, as well as other aspects of the performance, before calling the design complete.

The gain margin for the second-order system [given by Eq. (6.29)] is infinite ( $GM = \infty$ ), because the phase curve does not cross  $-180^\circ$  as the frequency increases. This would also be true for any first- or second-order system.

Additional data to aid in evaluating a control system based on its PM can be derived from the relationship between the resonant peak  $M_r$  and  $\zeta$  seen in Fig. 6.3. Note that this figure was derived for the same system [Eq. (6.9)] as Eq. (6.30). We can convert the information in Fig. 6.36 into a form relating  $M_r$  to the PM. This is depicted in Fig. 6.37, along with the step-response overshoot  $M_p$ . Therefore, we see that, given the PM, one can infer information about what the overshoot of the closed-loop step response would be.

Many engineers think directly in terms of the PM when judging whether a control system is adequately stabilized. In these terms, a  $PM = 30^\circ$  is often judged to be the lowest adequate value. In addition to testing the stability of a system design using the PM, a designer would typically also be concerned with meeting a speed-of-response specification such as bandwidth, as discussed in Section 6.1. In terms of the frequency-response parameters discussed so far, the crossover frequency would best describe a system's speed of response. This idea will be discussed further in Sections 6.6 and 6.7.

In some cases the PM and GM are not helpful indicators of stability. For first- and second-order systems, the phase never crosses the  $180^\circ$  line; hence, the GM is always  $\infty$  and not a useful design parameter. For higher-order systems it is possible to have more than one frequency where  $|KG(j\omega)| = 1$  or where  $\angle KG(j\omega) = 180^\circ$ , and the margins as previously defined need clarification. An example of this can be seen in Fig. 10.12, where the magnitude crosses 1 three times. A decision was made to define PM by the first crossing, because the PM at this crossing was the smallest of the three values and thus the most conservative assessment of stability. A Nyquist plot based on the data in Fig. 10.12 would show that the portion of the Nyquist curve closest to the  $-1$  point was the critical indicator of stability, and therefore use of the crossover frequency yielding the minimum value of PM was the logical choice. At best, a designer needs to be judicious when applying the margin definitions described in Fig. 6.33. In fact, the

**Figure 6.37**  
Transient-response overshoot ( $M_p$ ) and frequency-response resonant peak ( $M_r$ ), vs. phase margin (PM) for  $T(s) = \omega_n^2 / (s^2 + 2\zeta\omega_n s + \omega_n^2)$

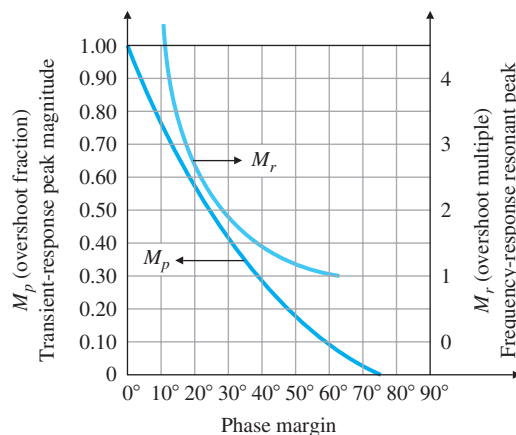
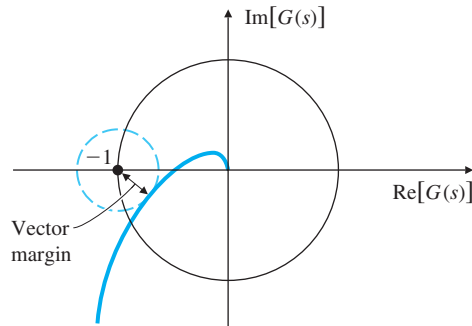


**Figure 6.38**  
Definition of the vector margin on the Nyquist plot



actual stability margin of a system can be rigorously assessed only by examining the Nyquist plot to determine its closest approach to the  $-1$  point.

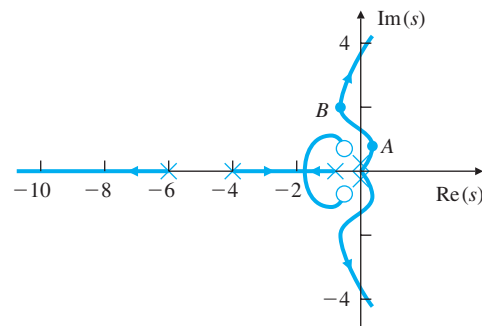
#### Vector margin

To aid in this analysis, O. J. M. Smith (1958) introduced the **vector margin**, which he defined to be the distance to the  $-1$  point from the closest approach of the Nyquist plot.<sup>9</sup> Figure 6.38 illustrates the idea graphically. Because the vector margin is a single margin parameter, it removes all the ambiguities in assessing stability that come with using GM and PM in combination. In the past it has not been used extensively due to difficulties in computing it. However, with the widespread availability of computer aids, the idea of using the vector margin to describe the degree of stability is much more feasible.

#### Conditionally stable systems

There are certain practical examples in which an increase in the gain can make the system stable. As we saw in Chapter 5, these systems are called **conditionally stable**. A representative root-locus plot for such systems is shown in Fig. 6.39. For a point on the root locus, such as  $A$ , an increase in the gain would make the system stable by bringing the unstable roots into the LHP. For point  $B$ , either a gain increase or decrease could make the system become unstable. Therefore, several gain margins exist that correspond to either gain reduction or gain increase, and the definition of the GM in Fig. 6.33 is not valid.

**Figure 6.39**  
Root locus for a conditionally stable system



<sup>9</sup> This value is closely related to the use of the sensitivity function for design and the concept of stability robustness, to be discussed in optional Section 6.9.

EXAMPLE 6.11

*Stability Properties for a Conditionally Stable System*

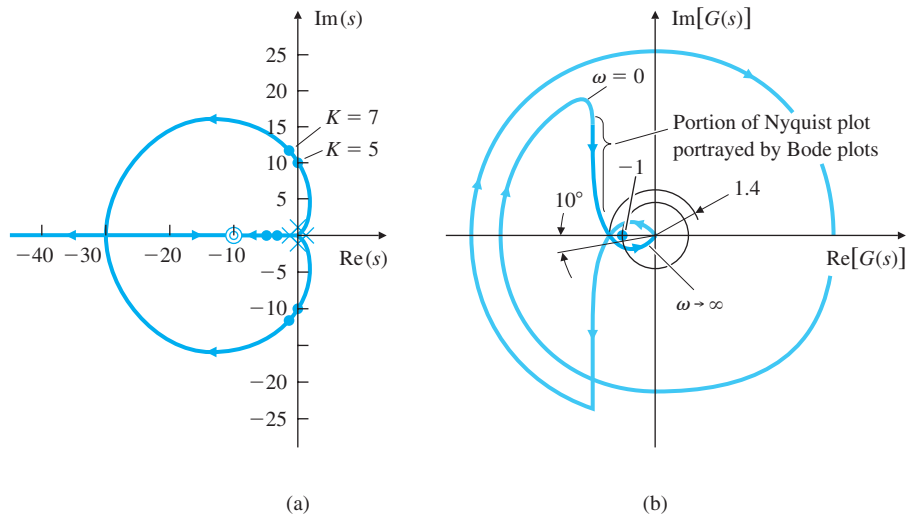
Determine the stability properties as a function of the gain  $K$  for the system with the open-loop transfer function

$$KG(s) = \frac{K(s + 10)^2}{s^3}.$$

**Solution.** This is a system for which increasing gain causes a transition from instability to stability. The root locus in Fig. 6.40(a) shows that the system is unstable for  $K < 5$  and stable for  $K > 5$ . The Nyquist plot in Fig. 6.40(b) was drawn for the stable value  $K = 7$ . Determination of the margins according to Fig. 6.33 yields  $PM = +10^\circ$  (stable) and  $GM = 0.7$  (unstable). According to the rules for stability discussed earlier, these two margins yield conflicting signals on the system's stability.

We resolve the conflict by counting the Nyquist encirclements in Fig. 6.40(b). There is one clockwise encirclement and one counterclockwise encirclement of the  $-1$  point. Hence there are no net encirclements, which confirms that the system is stable for  $K = 7$ . For systems like this it is best to resort to the root locus and/or Nyquist plot (rather than the Bode plot) to determine stability.

**Figure 6.40**  
System in which increasing gain leads from instability to stability: (a) root locus; (b) Nyquist plot



EXAMPLE 6.12

*Nyquist Plot for a System with Multiple Crossover Frequencies*

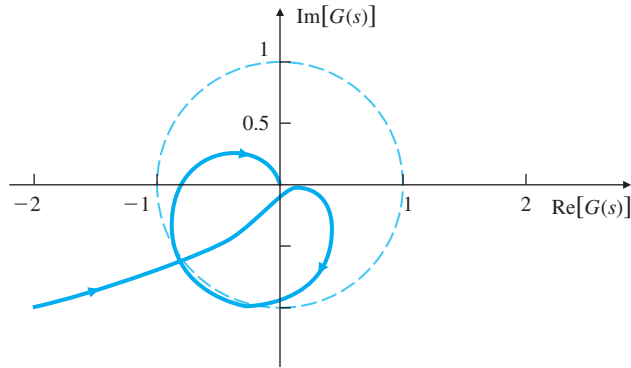
Draw the Nyquist plot for the system

$$G(s) = \frac{85(s + 1)(s^2 + 2s + 43.25)}{s^2(s^2 + 2s + 82)(s^2 + 2s + 101)}$$

$$= \frac{85(s + 1)(s + 1 \pm 6.5j)}{s^2(s + 1 \pm 9j)(s + 1 \pm 10j)},$$

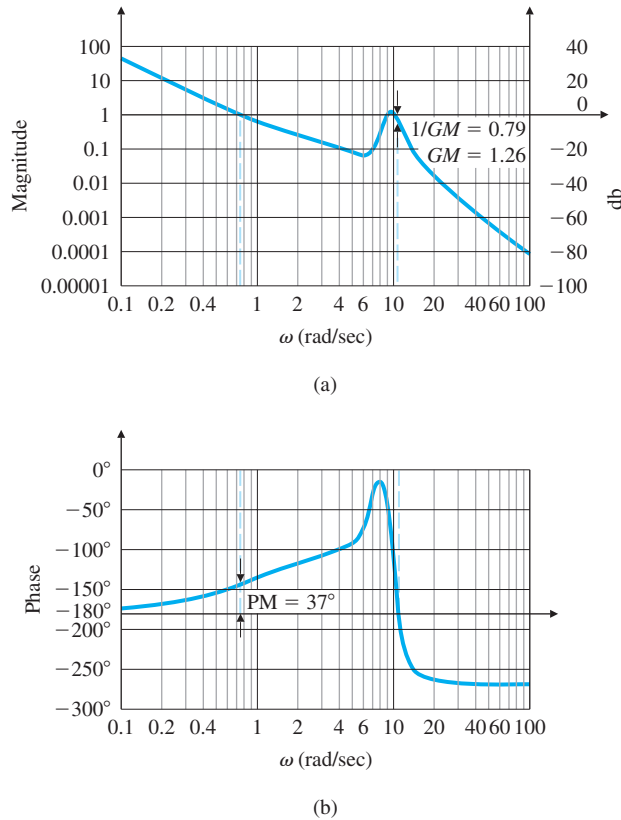
and determine the stability margins.

**Figure 6.41**  
Nyquist plot of the complex system in Example 6.12



**Solution.** The Nyquist plot (Fig. 6.41) shows that there are three crossover frequencies ( $\omega = 0.7, 8.5,$  and  $9.8$  rad/sec) with three corresponding PM values of  $37^\circ, 80^\circ,$  and  $40^\circ,$  respectively. However, the key indicator of stability is the proximity of the Nyquist plot as it approaches the  $-1$  point while crossing the real axis. In this case, only the GM indicates the poor stability margins of this system. The Bode plot for this system (Fig. 6.42) shows the same three crossings of magnitude = 1 at  $0.7, 8.5,$  and  $9.8$  rad/sec. The GM value

**Figure 6.42**  
Bode plot of the system in Example 6.12



of 1.26 from the Bode plot corresponding to  $\omega = 10.4$  rad/sec qualitatively agrees with the GM from the Nyquist plot and would be the most useful and unambiguous margin for this example.

In summary, many systems behave roughly like Example 6.9, and for them, the GM and PM are well defined and useful. There are also frequent instances of more complicated systems with multiple magnitude 1 crossovers or unstable open-loop systems for which the stability criteria defined by Fig. 6.33 are ambiguous or incorrect; therefore, we need to verify the GM and PM as previously defined, and/or modify them by reverting back to the Nyquist stability criterion.

## 6.5 Bode's Gain-Phase Relationship

One of Bode's important contributions is the following theorem:

For any stable minimum-phase system (that is, one with no RHP zeros or poles), the phase of  $G(j\omega)$  is uniquely related to the magnitude of  $G(j\omega)$ .

Bode's gain-phase relationship

When the slope of  $|G(j\omega)|$  versus  $\omega$  on a log-log scale persists at a constant value for approximately a decade of frequency, the relationship is particularly simple and is given by

$$\angle G(j\omega) \cong n \times 90^\circ, \quad (6.33)$$

where  $n$  is the slope of  $|G(j\omega)|$  in units of decade of amplitude per decade of frequency. For example, in considering the magnitude curve alone in Fig. 6.43, we see that Eq. (6.33) can be applied to the two frequencies  $\omega_1 = 0.1$  (where  $n = -2$ ) and  $\omega_2 = 10$  (where  $n = -1$ ), which are a decade removed from the change in slope, to yield the approximate values of phase,  $-180^\circ$  and  $-90^\circ$ . The exact phase curve shown in the figure verifies that indeed the approximation is quite good. It also shows that the approximation will degrade if the evaluation is performed at frequencies closer to the change in slope.

An exact statement of the Bode gain-phase theorem is

$$\angle G(j\omega_o) = \frac{1}{\pi} \int_{-\infty}^{+\infty} \left( \frac{dM}{du} \right) W(u) du \quad (\text{in radians}), \quad (6.34)$$

where

$$M = \log \text{ magnitude} = \ln |G(j\omega)|,$$

$$u = \text{normalized frequency} = \ln(\omega/\omega_o),$$

$$dM/du \cong \text{slope } n, \text{ as defined in Eq. (6.33),}$$

$$W(u) = \text{weighting function} = \ln(\coth|u|/2).$$



**Figure 6.43**  
An approximate gain–phase relationship demonstration

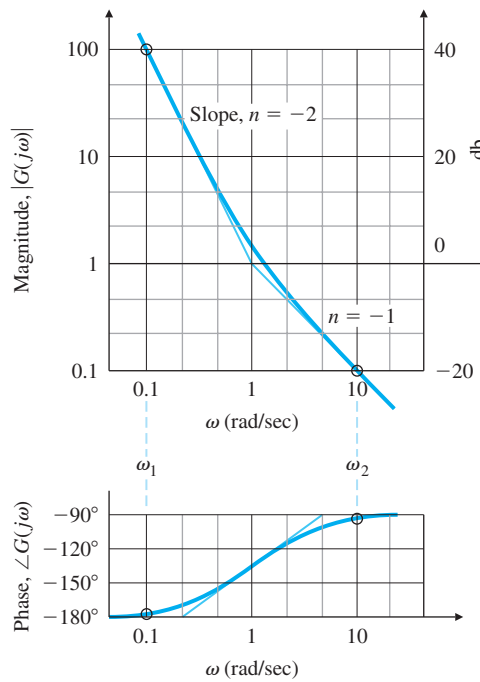
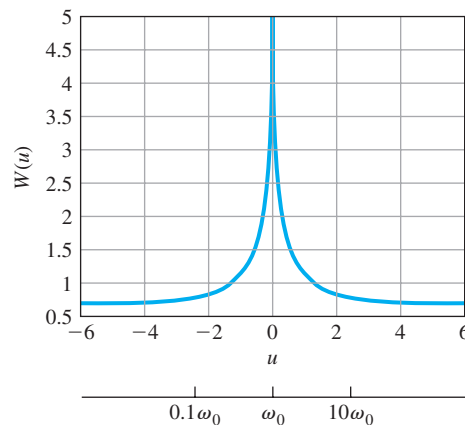


Figure 6.44 is a plot of the weighting function  $W(u)$  and shows how the phase is most dependent on the slope at  $\omega_o$ ; it is also dependent, though to a lesser degree, on slopes at neighboring frequencies. The figure also suggests that the weighting could be approximated by an impulse function centered at  $\omega_o$ . We may approximate the weighting function as

$$W(u) \cong \frac{\pi^2}{2} \delta(u),$$

**Figure 6.44**  
Weighting function in Bode's gain–phase theorem



which is precisely the approximation made to arrive at Eq. (6.33) using the “sifting” property of the impulse function (and conversion from radians to degrees).

In practice, Eq. (6.34) is never used, but Eq. (6.33) is used as a guide to infer stability from  $|G(\omega)|$  alone. When  $|KG(j\omega)| = 1$ ,

$$\angle G(j\omega) \cong -90^\circ \quad \text{if } n = -1,$$

$$\angle G(j\omega) \cong -180^\circ \quad \text{if } n = -2.$$

Crossover frequency

For stability we want  $\angle G(j\omega) > -180^\circ$  for  $PM > 0$ . Therefore, we adjust the  $|KG(j\omega)|$  curve so that it has a slope of  $-1$  at the “crossover” frequency,  $\omega_c$ , (that is, where  $|KG(j\omega)| = 1$ ). If the slope is  $-1$  for a decade above and below the crossover frequency, then  $PM \cong 90^\circ$ ; however, to ensure a reasonable PM, it is usually necessary only to insist that a  $-1$  slope ( $-20$  db per decade) persist for a decade in frequency that is centered at the crossover frequency. We therefore see that there is a very simple design criterion:

Adjust the slope of the magnitude curve  $|KG(j\omega)|$  so that it crosses over magnitude 1 with a slope of  $-1$  for a decade around  $\omega_c$ .

This criterion will usually be sufficient to provide an acceptable PM, and hence provide adequate system damping. To achieve the desired speed of response, the system gain is adjusted so that the crossover point is at a frequency that will yield the desired bandwidth or speed of response as determined by Eq. (3.49). Recall that the natural frequency  $\omega_n$ , bandwidth, and crossover frequency are all approximately equal, as will be discussed further in Section 6.6.

**EXAMPLE 6.13**

*Use of Simple Design Criterion for Spacecraft Attitude Control*

For the spacecraft attitude-control problem defined in Fig. 6.45, find a suitable expression for  $KD(s)$  that will provide good damping and a bandwidth of approximately 0.2 rad/sec.

**Solution.** The magnitude of the frequency response of the spacecraft (Fig. 6.46) clearly requires some reshaping, because it has a slope of  $-2$  (or  $-40$  db per decade) everywhere. The simplest compensation to do the job consists of using proportional and derivative terms (a PD compensator), which produces the relation

$$KD(s) = K(T_D s + 1). \tag{6.35}$$

We will adjust the gain  $K$  to produce the desired bandwidth, and adjust break point  $\omega_1 = 1/T_D$  to provide the  $-1$  slope at the crossover frequency. The actual design

**Figure 6.45**  
Spacecraft attitude-control system

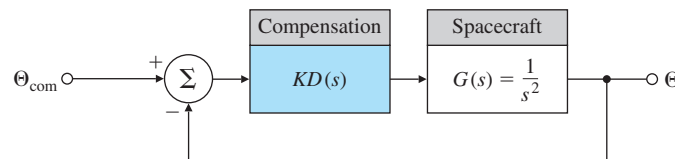
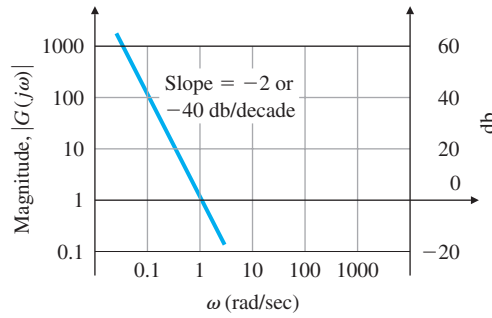


**Figure 6.46**  
Magnitude of the spacecraft's frequency response



process to achieve the desired specifications is now very simple: We pick a value of  $K$  to provide a crossover at 0.2 rad/sec and choose a value of  $\omega_1$  that is about 4 times lower than the crossover frequency, so that the slope will be  $-1$  in the vicinity of the crossover. Figure 6.47 shows the steps we take to arrive at the final compensation:

STEP 1. Plot  $|G(j\omega)|$ .

STEP 2. Modify the plot to include  $|D(j\omega)|$ , with  $\omega_1 = 0.05$  rad/sec ( $T_D = 20$ ), so that the slope will be  $\cong -1$  at  $\omega = 0.2$  rad/sec.

STEP 3. Determine that  $|DG| = 100$  where the  $|DG|$  curve crosses the line  $\omega = 0.2$  rad/sec, which is where we want magnitude 1 crossover to be.

STEP 4. In order for crossover to be at  $\omega = 0.2$  rad/sec, compute

$$K = \frac{1}{[|DG|]_{\omega=0.2}} = \frac{1}{100} = 0.01.$$

Therefore,

$$KD(s) = 0.01(20s + 1)$$

will meet the specifications, thus completing the design.

**Figure 6.47**  
Compensated open-loop transfer function

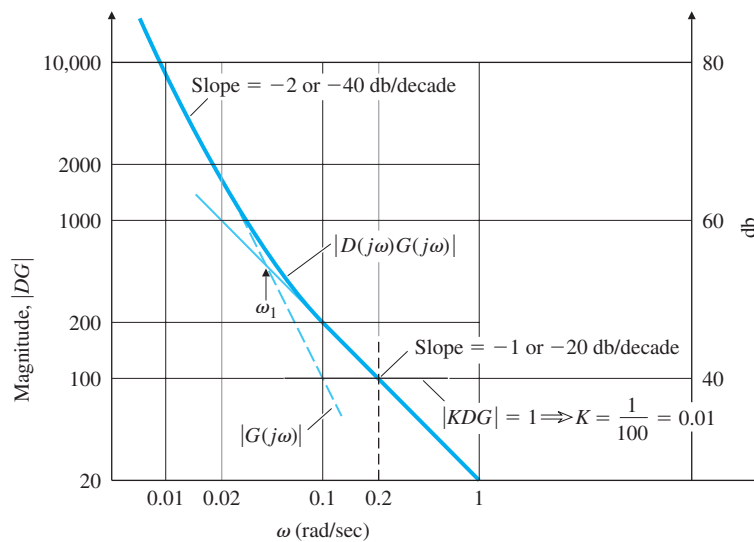


**Figure 6.48**  
Closed-loop frequency response

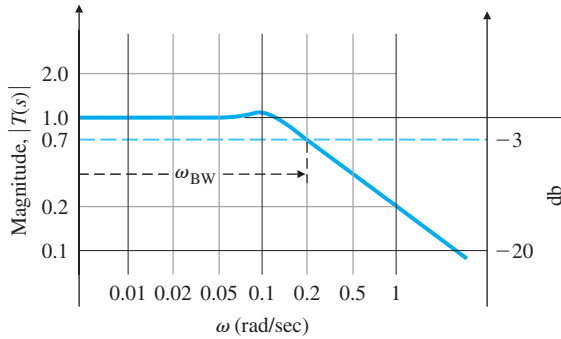
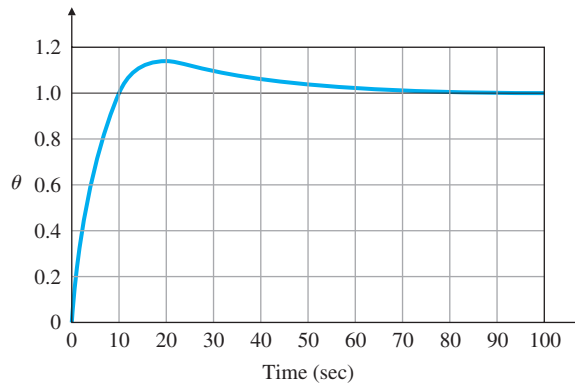


**Figure 6.49**  
Step response for PD compensation



If we were to draw the phase curve of  $KDG$ , we would find that  $PM = 75^\circ$ , which is certainly quite adequate. A plot of the closed-loop frequency-response magnitude (Fig. 6.48) shows that, indeed, the crossover frequency and the bandwidth are almost identical in this case. The step response of the closed-loop system is shown in Fig. 6.49 and its 14% overshoot confirms the adequate damping.

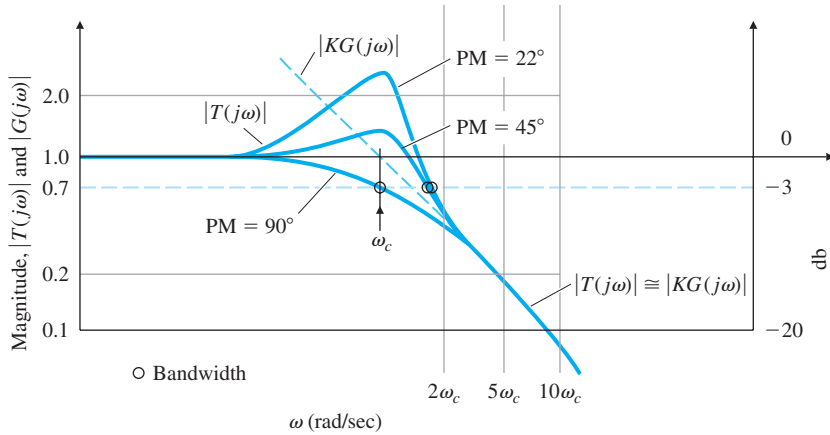
## 6.6 Closed-Loop Frequency Response

The closed-loop bandwidth was defined in Section 6.1 and in Fig. 6.5. Figure 6.3 showed that the natural frequency is always within a factor of two of the bandwidth for a second-order system. In Example 6.13, we designed the compensation so that the crossover frequency was at the desired bandwidth and verified by computation that the bandwidth was identical to the crossover frequency. Generally, the match between the crossover frequency and the bandwidth is not as good as in Example 6.13. We can help establish a more exact correspondence by making a few observations. Consider a system in which  $|KG(j\omega)|$  shows the typical behavior

$$|KG(j\omega)| \gg 1 \quad \text{for } \omega \ll \omega_c,$$

$$|KG(j\omega)| \ll 1 \quad \text{for } \omega \gg \omega_c,$$

**Figure 6.50**  
Closed-loop bandwidth with respect to PM



where  $\omega_c$  is the crossover frequency. The closed-loop frequency-response magnitude is approximated by

$$|\mathcal{T}(j\omega)| = \left| \frac{KG(j\omega)}{1 + KG(j\omega)} \right| \cong \begin{cases} 1, & \omega \ll \omega_c, \\ |KG|, & \omega \gg \omega_c. \end{cases} \quad (6.36)$$

In the vicinity of crossover, where  $|KG(j\omega)| = 1$ ,  $|\mathcal{T}(j\omega)|$  depends heavily on the PM. A PM of  $90^\circ$  means that  $\angle G(j\omega_c) = -90^\circ$ , and therefore  $|\mathcal{T}(j\omega_c)| = 0.707$ . On the other hand, PM =  $45^\circ$  yields  $|\mathcal{T}(j\omega_c)| = 1.31$ .

The approximations in Eq. (6.36) were used to generate the curves of  $|\mathcal{T}(j\omega)|$  in Fig. 6.50. It shows that the bandwidth for smaller values of PM is typically somewhat greater than  $\omega_c$ , though usually it is less than  $2\omega_c$ ; thus

$$\omega_c \leq \omega_{BW} \leq 2\omega_c.$$

Another specification related to the closed-loop frequency response is the resonant-peak magnitude  $M_r$ , defined in Fig. 6.5. Figures 6.3 and 6.37 show that, for linear systems,  $M_r$  is generally related to the damping of the system. In practice,  $M_r$  is rarely used; most designers prefer to use the PM to specify the damping of a system, because the imperfections that make systems nonlinear or cause delays usually erode the phase more significantly than the magnitude.

### 6.7 Compensation

As we discussed in Chapters 4 and 5, dynamic elements (or compensation) are typically added to feedback controllers to improve the system's stability and error characteristics because the process itself cannot be made to have acceptable characteristics with proportional feedback alone.

Section 4.3 discussed the basic types of feedback: proportional, derivative, and integral. Section 5.5 discussed three kinds of dynamic compensation:

lead compensation, which approximates proportional-derivative (PD) feedback, lag compensation, which approximates proportional-integral (PI) control, and notch compensation, which has special characteristics for dealing with resonances. In this section we discuss these and other kinds of compensation in terms of their frequency-response characteristics. In most cases, the compensation will be implemented in a microprocessor. Techniques for converting the continuous compensation  $D(s)$  into a form that can be coded in the computer was briefly discussed in Section 4.4.1. It will be illustrated further in this section and will be discussed in more detail in Chapter 8.

The frequency response stability analysis to this point has considered the closed-loop system to have the characteristic equation  $1 + KG(s) = 0$ . With the introduction of compensation, the closed-loop characteristic equation becomes  $1 + KD(s)G(s) = 0$ , and all the previous discussion in this chapter pertaining to the frequency response of  $KG(s)$  applies directly to the compensated case if we apply it to the frequency response of  $KD(s)G(s)$ . We call this quantity  $L(s)$ , the “loop gain,” or open-loop transfer function of the system, where  $L(s) = KD(s)G(s)$ .

### 6.7.1 PD Compensation

PD compensation

We will start the discussion of compensation design by using the frequency response with PD control. The compensator transfer function, given by

$$D(s) = (T_D s + 1), \quad (6.37)$$

was shown in Fig. 5.22 to have a stabilizing effect on the root locus of a second-order system. The frequency-response characteristics of Eq. (6.37) are shown in Fig. 6.51. A stabilizing influence is apparent by the increase in phase and the corresponding +1 slope at frequencies above the break point  $1/T_D$ . We use this compensation by locating  $1/T_D$  so that the increased phase occurs in the vicinity of crossover (that is, where  $|KD(s)G(s)| = 1$ ), thus increasing the phase margin.

Note that the magnitude of the compensation continues to grow with increasing frequency. This feature is undesirable because it amplifies the high-frequency noise that is typically present in any real system and, as a continuous transfer function, cannot be realized with physical elements. It is also the reason we stated in Section 5.5 that pure derivative compensation gives trouble.

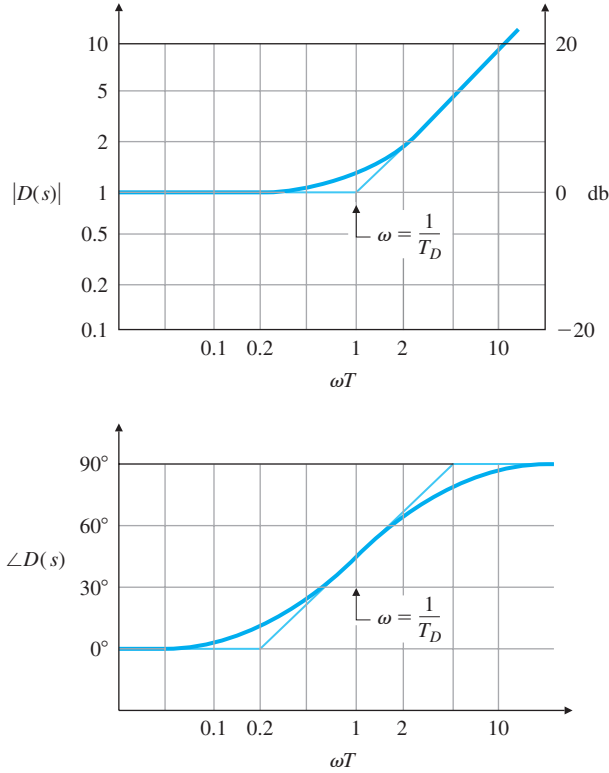
### 6.7.2 Lead Compensation

Lead compensation

In order to alleviate the high-frequency amplification of the PD compensation, a first-order pole is added in the denominator at frequencies substantially higher than the breakpoint of the PD compensator. Thus the phase increase (or lead) still occurs, but the amplification at high frequencies is limited. The resulting **lead compensation** has a transfer function of

$$D(s) = \frac{T s + 1}{\alpha T s + 1}, \quad \alpha < 1 \quad (6.38)$$

**Figure 6.51**  
Frequency response of PD control



where  $1/\alpha$  is the ratio between the pole/zero breakpoint frequencies. Figure 6.52 shows the frequency response of this lead compensation. Note that a significant amount of phase lead is still provided, but with much less amplification at high frequencies. A lead compensator is generally used whenever a substantial improvement in damping of the system is required.

The phase contributed by the lead compensation in Eq. (6.38) is given by

$$\phi = \tan^{-1}(T\omega) - \tan^{-1}(\alpha T\omega).$$

It can be shown (see Problem 6.43) that the frequency at which the phase is maximum is given by

$$\omega_{\max} = \frac{1}{T\sqrt{\alpha}}. \tag{6.39}$$

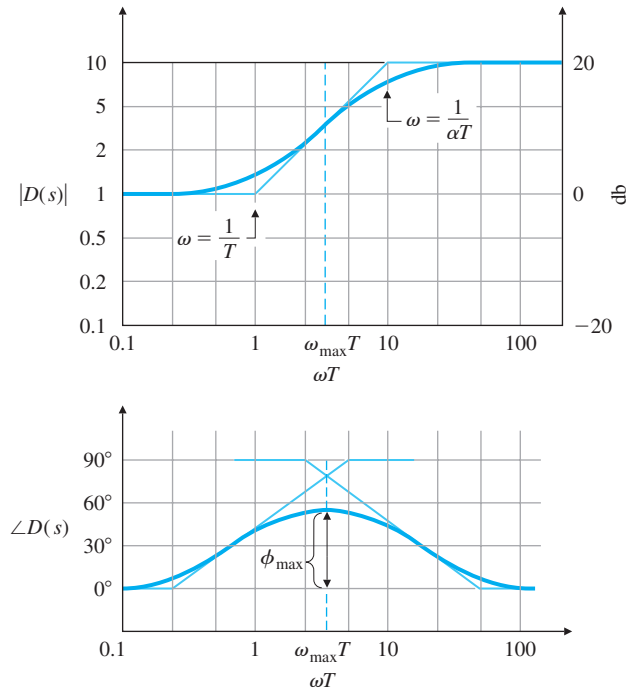
The maximum phase contribution—that is, the peak of the  $\angle D(s)$  curve in Fig. 6.52—corresponds to

$$\sin \phi_{\max} = \frac{1 - \alpha}{1 + \alpha}, \tag{6.40}$$

or

$$\alpha = \frac{1 - \sin \phi_{\max}}{1 + \sin \phi_{\max}}.$$

**Figure 6.52**  
Lead-compensation  
frequency response with  
 $1/\alpha = 10$



Another way to look at this is the following: The maximum phase occurs at a frequency that lies midway between the two break-point frequencies (sometimes called corner frequencies) on a logarithmic scale,

$$\begin{aligned}
 \log \omega_{\max} &= \log \frac{1/\sqrt{T}}{\sqrt{\alpha T}} \\
 &= \log \frac{1}{\sqrt{T}} + \log \frac{1}{\sqrt{\alpha T}} \\
 &= \frac{1}{2} \left[ \log \left( \frac{1}{T} \right) + \log \left( \frac{1}{\alpha T} \right) \right], \quad (6.41)
 \end{aligned}$$

as shown in Fig. 6.52. Alternatively, we may state these results in terms of the pole-zero locations. Rewriting  $D(s)$  in the form used for root locus analysis, we have

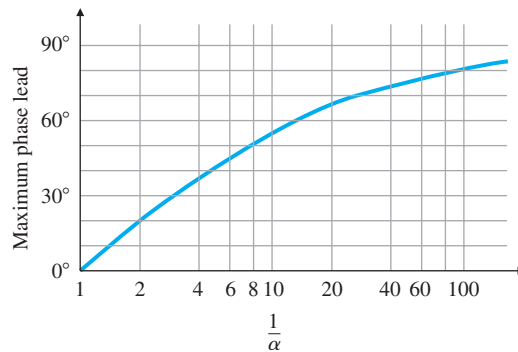
$$D(s) = \frac{s + z}{s + p}. \quad (6.42)$$

Problem 6.43 shows that

$$\omega_{\max} = \sqrt{|z| |p|} \quad (6.43)$$



**Figure 6.53**  
Maximum phase increase  
for lead compensation



and

$$\log \omega_{\max} = \frac{1}{2}(\log |z| + \log |p|). \tag{6.44}$$

These results agree with the previous ones if we let  $z = -1/T$  and  $p = -1/\alpha T$  in Eqs. (6.39) and (6.41).

For example, a lead compensator with a zero at  $s = -2$  ( $T = 0.5$ ) and a pole at  $s = -10$  ( $\alpha T = 0.1$ ) (and thus  $\alpha = \frac{1}{5}$ ) would yield the maximum phase lead at

$$\omega_{\max} = \sqrt{2 \cdot 10} = 4.47 \text{ rad/sec.}$$

The amount of phase lead at the midpoint depends only on  $\alpha$  in Eq. (6.40) and is plotted in Fig. 6.53. For  $\alpha = \frac{1}{5}$ , Fig. 6.53 shows that  $\phi_{\max} = 40^\circ$ . Note from the figure that we could increase the phase lead up to  $90^\circ$  using higher values of the **lead ratio**,  $1/\alpha$ ; however, Fig. 6.52 shows that increasing values of  $1/\alpha$  also produces higher amplifications at higher frequencies. Thus our task is to select a value of  $1/\alpha$  that is a good compromise between an acceptable phase margin and an acceptable noise sensitivity at high frequencies. Usually the compromise suggests that a lead compensation should contribute a maximum of  $60^\circ$  to the phase. If a greater phase lead is needed, then a double lead compensation would be suggested, where

Lead ratio =  $\frac{1}{\alpha}$

$$D(s) = \left( \frac{Ts + 1}{\alpha Ts + 1} \right)^2.$$

Even if a system had negligible amounts of noise present and the pure derivative compensation of Eq. (6.37) were acceptable, a continuous compensation would look more like Eq. (6.38) than Eq. (6.37) because of the impossibility of building a pure differentiator. No physical system—mechanical or electrical—responds with infinite amplitude at infinite frequencies, so there will be a limit in the frequency range (or bandwidth) for which derivative information (or phase lead) can be provided. This is also true with a digital implementation. Here, the sample rate limits the high-frequency amplification and essentially places a pole in the compensation transfer function.

## EXAMPLE 6.14

*Lead Compensation for a DC Motor*

As an example of designing a lead compensator, let us repeat the design of compensation for the DC motor with the transfer function

$$G(s) = \frac{1}{s(s+1)}$$

that was carried out in Section 5.5.1. This also represents the model of a satellite tracking antenna (see Fig. 3.52). This time we wish to obtain a steady-state error of less than 0.1 for a unit-ramp input. Furthermore, we desire an overshoot  $M_p < 25\%$ .

- Determine the lead compensation satisfying the specifications,
- determine the digital version of the compensation with  $T_s = 0.05$  sec, and
- compare the step and ramp responses of both implementations.

**Solution.**

- The steady-state error is given by

$$e_{ss} = \lim_{s \rightarrow 0} s \left[ \frac{1}{1 + KD(s)G(s)} \right] R(s), \quad (6.45)$$

where  $R(s) = 1/s^2$  for a unit ramp, so Eq. (6.45) reduces to

$$e_{ss} = \lim_{s \rightarrow 0} \left\{ \frac{1}{s + KD(s)[1/(s+1)]} \right\} = \frac{1}{KD(0)}.$$

Therefore, we find that  $KD(0)$ , the steady-state gain of the compensation, cannot be less than 10 ( $K_v \geq 10$ ) if it is to meet the error criterion, so we pick  $K = 10$ . To relate the overshoot requirement to phase margin, Fig. 6.37 shows that a PM of  $45^\circ$  should suffice. The frequency response of  $KG(s)$  in Fig. 6.54 shows that the  $PM = 20^\circ$  if no phase lead is added by compensation. If it were possible to simply add phase without affecting the magnitude, we would need an additional phase of only  $25^\circ$  at the  $KG(s)$  crossover frequency of  $\omega = 3$  rad/sec. However, maintaining the same low-frequency gain and adding a compensator zero would increase the crossover frequency; hence more than a  $25^\circ$  phase contribution will be required from the lead compensation. To be safe, we will design the lead compensator so that it supplies a maximum phase lead of  $40^\circ$ . Fig. 6.53 shows that  $1/\alpha = 5$  will accomplish that goal. We will derive the greatest benefit from the compensation if the maximum phase lead from the compensator occurs at the crossover frequency. With some trial and error, we determine that placing the zero at  $\omega = 2$  rad/sec and the pole at  $\omega = 10$  rad/sec causes the maximum phase lead to be at the crossover frequency. The compensation, therefore, is

$$KD(s) = 10 \frac{s/2 + 1}{s/10 + 1}.$$

The frequency-response characteristics of  $L(s) = KD(s)G(s)$  in Fig. 6.54 can be seen to yield a phase margin of  $45^\circ$ , which satisfies the design goals.

**Figure 6.54**  
Frequency response for lead-compensation design

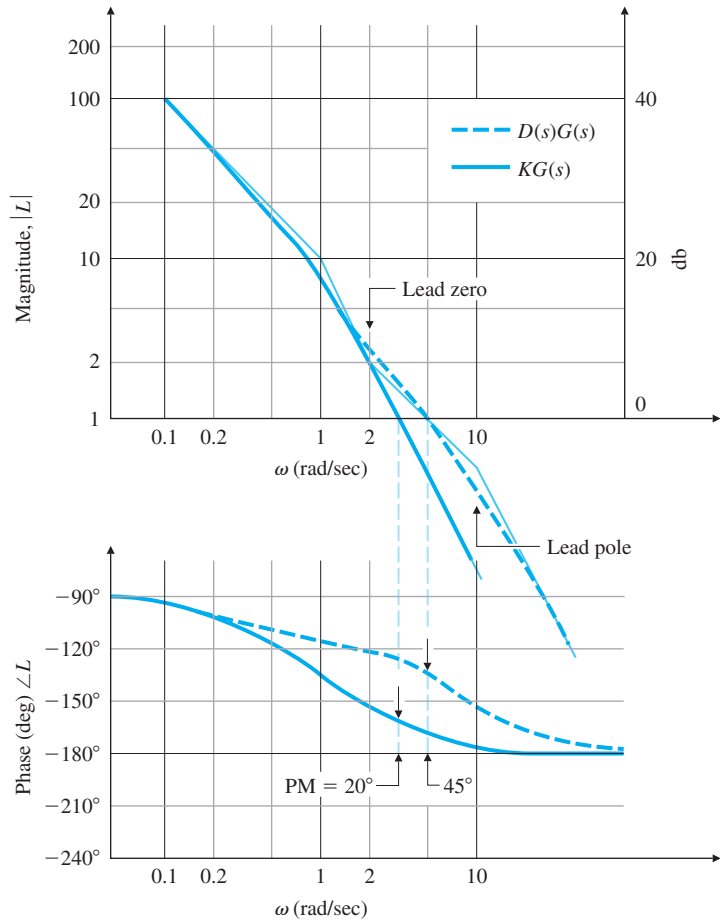
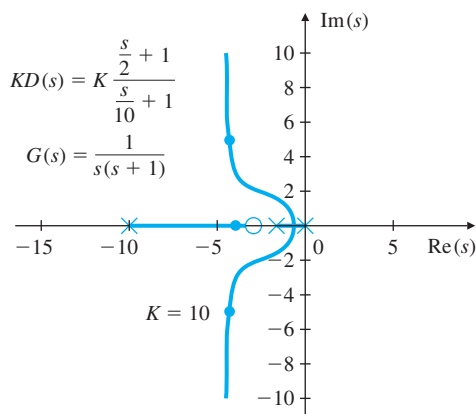


**Figure 6.55**  
Root locus for lead compensation design



The root locus for this design, originally given as Fig. 5.23, is repeated here as Fig. 6.55, with the root locations marked for  $K = 10$ . The locus is not needed for the frequency response design procedure; it is presented here only for comparison with the root locus design method presented in Chapter 5.

- (b) To find the discrete equivalent of  $D(s)$ , we use the trapezoidal rule given by Eq. (4.93). That is,

$$D_d(z) = \frac{\frac{2}{T_s} \frac{z-1}{z+1} / 2 + 1}{\frac{2}{T_s} \frac{z-1}{z+1} / 10 + 1}, \tag{6.46}$$

which, with  $T_s = 0.05$  sec, reduces to

$$D_d(z) = \frac{4.2z - 3.8}{z - 0.6}. \tag{6.47}$$

This same result can be obtained by the MATLAB statement

```
sysD = tf([0.5 1],[0.1 1]);
sysDd = c2d(sysD, 0.05, 'tustin').
```

Because

$$\frac{U(z)}{E(z)} = K D_d(z), \tag{6.48}$$

the discrete control equations that result are

$$u(k + 1) = 0.6u(k) + 10(4.2e(k + 1) - 3.8e(k)). \tag{6.49}$$

- (c) The Simulink block diagram of the continuous and discrete versions of  $D(s)$  controlling the DC motor is shown in Fig. 6.56. The step responses of the two controllers are plotted together in Fig. 6.57(a) and are reasonably close to one another; however, the discrete controller does exhibit slightly increased overshoot, as is often the case. Both overshoots are less than 25%, and thus meet the specifications. The ramp responses of the two controllers, shown in Fig. 6.57(b), are essentially identical, and both meet the 0.1 specified error.

**Figure 6.56**  
Simulink block diagram for transient response of lead-compensation design

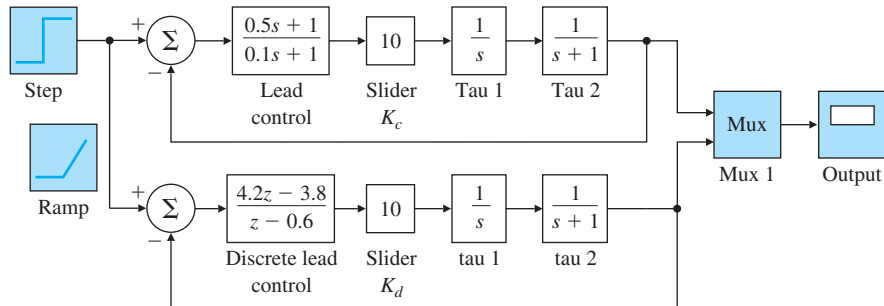
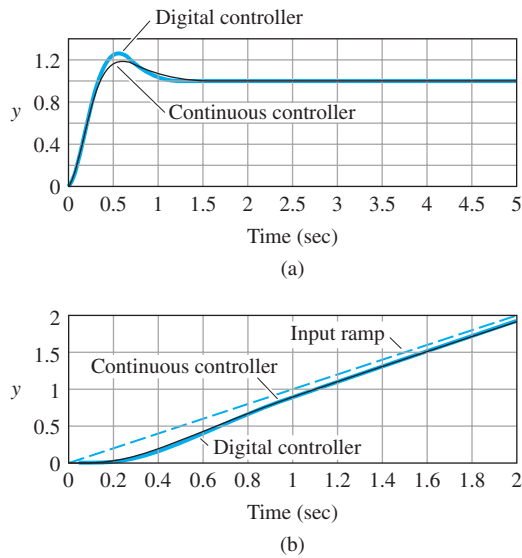


**Figure 6.57**  
Lead-compensation design:  
(a) step response; (b) ramp  
response



The design procedure used in Example 6.14 can be summarized as follows:

1. Determine the low-frequency gain so that the steady-state errors are within specification.
2. Select the combination of lead ratio  $1/\alpha$  and zero values ( $1/T$ ) that achieves an acceptable phase margin at crossover.
3. The pole location is then at  $(1/\alpha T)$ .

This design procedure will apply to many cases; however, keep in mind that the specific procedure followed in any particular design may need to be tailored to its particular set of specifications.

In Example 6.14 there were two specifications: peak overshoot and steady-state error. We transformed the overshoot specification into a PM, but the steady-state error specification we used directly. No speed-of-response type of specification was given; however, it would have impacted the design in the same way that the steady-state error specification did. The speed of response or bandwidth of a system is directly related to the crossover frequency, as we pointed out earlier in Section 6.6. Fig. 6.54 shows that the crossover frequency was  $\sim 5$  rad/sec. We could have increased it by raising the gain  $K$  and increasing the frequency of the lead compensator pole and zero in order to keep the slope of  $-1$  at the crossover frequency. Raising the gain would also have decreased the steady-state error to be better than the specified limit. The gain margin was never introduced into the problem because the stability was adequately specified by the phase margin alone. Furthermore, the gain margin would not have been useful for this system because the phase never crossed the  $180^\circ$  line and the GM was always infinite.

In lead-compensation designs there are three primary design parameters:

Design parameters for lead-networks

1. The crossover frequency  $\omega_c$ , which determines bandwidth  $\omega_{BW}$ , rise time  $t_r$ , and settling time  $t_s$ ;
2. The phase margin (PM), which determines the damping coefficient  $\zeta$  and the overshoot  $M_p$ ;
3. The low-frequency gain, which determines the steady-state error characteristics.

The design problem is to find the best values for the parameters, given the requirements. In essence, lead compensation increases the value of  $\frac{\omega_c}{L(0)}$  ( $= \frac{\omega_c}{K_v}$  for a type 1 system). That means that, if the low frequency gain is kept the same, the crossover frequency will increase. Or if the crossover frequency is kept the same, the low frequency gain will decrease. Keeping this interaction in mind, the designer can assume a fixed value of one of these three design parameters and then adjust the other two iteratively until the specifications are met. One approach is to set the low-frequency gain to meet the error specifications and add a lead compensator to increase the PM at the crossover frequency. An alternative is to pick the crossover frequency to meet a time response specification, then adjust the gain and lead characteristics so that the PM specification is met. A step-by-step procedure is outlined next for these two cases. They apply to a sizable class of problems for which a single lead is sufficient. As with all such design procedures, it provides only a starting point; the designer will typically find it necessary to go through several design iterations in order to meet all the specifications.

Design Procedure for Lead Compensation

1. Determine open-loop gain  $K$  to satisfy error or bandwidth requirements:
  - (a) to meet error requirement, pick  $K$  to satisfy error constants ( $K_p$ ,  $K_v$ , or  $K_a$ ) so that  $e_{ss}$  error specification is met, or alternatively,
  - (b) to meet bandwidth requirement, pick  $K$  so that the open-loop crossover frequency is a factor of two below the desired closed-loop bandwidth.
2. Evaluate the phase margin (PM) of the uncompensated system using the value of  $K$  obtained from Step 1.
3. Allow for extra margin (about  $10^\circ$ ), and determine the needed phase lead  $\phi_{max}$ .
4. Determine  $\alpha$  from Eq. (6.40) or Fig. 6.53.
5. Pick  $\omega_{max}$  to be at the crossover frequency; thus the zero is at  $1/T = \omega_{max}\sqrt{\alpha}$  and the pole is at  $1/\alpha T = \omega_{max}/\sqrt{\alpha}$ .
6. Draw the compensated frequency response and check the PM.
7. Iterate on the design. Adjust compensator parameters (poles, zeros, and gain) until all specifications are met. Add an additional lead compensator (that is, a double lead compensation) if necessary.

While these guidelines will not apply to all the systems you will encounter in practice, they do suggest a systematic trial-and-error process to search for a satisfactory compensator that will usually be successful.

### EXAMPLE 6.15 *Lead Compensator for a Temperature Control System*

The third-order system

$$KG(s) = \frac{K}{(s/0.5 + 1)(s + 1)(s/2 + 1)}$$

is representative of a typical temperature control system. Design a lead compensator such that  $K_p = 9$  and the phase margin is at least  $25^\circ$ .

**Solution.** Let us follow the design procedure:

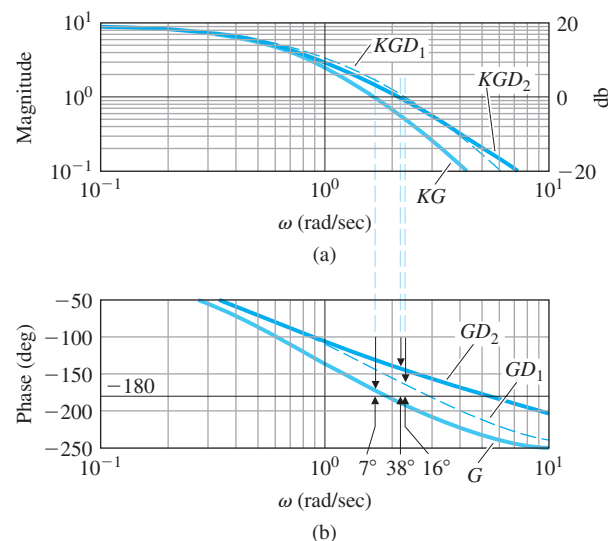
STEP 1. Given the specification for  $K_p$ , we solve for  $K$ :

$$K_p = \lim_{s \rightarrow 0} KG(s) = K = 9.$$

STEP 2. The Bode plot of the uncompensated system with  $K = 9$  can be created by the MATLAB statements below and is shown in Fig. 6.58.

```
numG = 9;
den2 = conv([1 0.5],[1 1]);
denG = conv(den2,[1 2]);
sysG = tf(numG,denG);
[mag,phas,w] = bode(sysG);
```

**Figure 6.58**  
Bode plot for the lead-compensation design in Example 6.15



It is difficult to read the PM and crossover frequencies accurately from the Bode plots; therefore, the MATLAB command

```
[GM,PM,Wcg,Wcp] = margin(mag,phas,w)
```

can be invoked. The quantity PM is the phase margin and Wcp is the frequency at which the gain crosses magnitude 1. (GM and Wcg are the open-loop gain margin and the frequency at which the phase crosses 180.) For this example, the output is

```
GM = 1.2500, PM = 7.1249, Wcg = 1.8708, Wcp = 1.6844,
```

which says that the PM of the uncompensated system is  $7^\circ$  and that this occurs at a crossover frequency of 1.7 rad/sec.

STEP 3. Allowing for  $10^\circ$  of extra margin, we want the lead compensator to contribute  $25^\circ + 10^\circ - 7^\circ = 28^\circ$  at the crossover frequency. The extra margin is typically required because the lead will increase the crossover frequency from the open-loop case, at which point more phase increase will be required.

STEP 4. From Fig. 6.53 we see that  $\alpha = 1/3$  will produce approximately  $30^\circ$  phase increase midway between the zero and pole.

STEP 5. As a first cut, let's place the zero at 1 rad/sec ( $T = 1$ ) and the pole at 3 rad/sec ( $\alpha T = 1/3$ ), thus bracketing the open-loop crossover frequency and preserving the factor of 3 between pole and zero, as indicated by  $\alpha = 1/3$ . The lead compensator is

$$D_1(s) = \frac{s+1}{s/3+1} = \frac{1}{0.333} \left( \frac{s+1}{s+3} \right).$$

STEP 6. The Bode plot of the system with  $D_1(s)$  (Fig. 6.58, middle curve) has a PM of  $16^\circ$ . We did not achieve the desired PM of  $30^\circ$ , because the lead shifted the crossover frequency from 1.7 rad/sec to 2.3 rad/sec, thus increasing the required phase increase from the lead. The step response of the system with  $D_1(s)$  (Fig. 6.59) shows a very oscillatory response, as we might expect from the low PM of  $16^\circ$ .

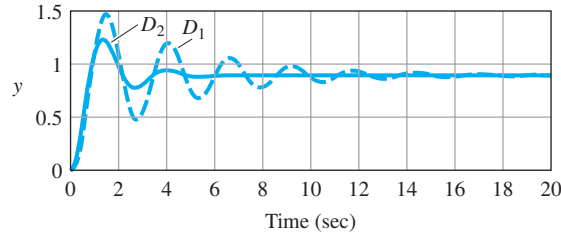
STEP 7. We repeat the design with extra phase increase and move the zero location slightly to the right so that the crossover frequency won't be shifted so much. We choose  $\alpha = \frac{1}{10}$  with the zero at  $s = -1.5$ , so

$$D_2(s) = \frac{s/1.5+1}{s/15+1} = \frac{1}{0.1} \left( \frac{s+1.5}{s+15} \right).$$

This compensation produces a PM =  $38^\circ$ , and the crossover frequency lowered slightly to 2.2 rad/sec. Figure 6.58 (upper curve) shows the frequency response of the revised design. Figure 6.59 shows a substantial reduction in the oscillations, which you should expect from the higher PM value.



**Figure 6.59**  
Step response for  
lead-compensation design



### EXAMPLE 6.16 *Lead-Compensator Design for a Type 1 Servomechanism System*

Consider the third-order system

$$KG(s) = K \frac{10}{s(s/2.5 + 1)(s/6 + 1)}.$$

This type of system would result for a DC motor with a lag in the shaft position sensor. Design a lead compensator so that the PM = 45° and  $K_v = 10$ .

**Solution.** Again, we follow the design procedure given earlier:

STEP 1. As given,  $KG(s)$  will yield  $K_v = 10$  if  $K = 1$ . Therefore, the  $K_v$  requirement is met by  $K = 1$  and the low-frequency gain of the compensation should be 1.

STEP 2. The Bode plot of the system is shown in Fig. 6.60. The phase margin of the uncompensated system (lower curve) is approximately  $-4^\circ$ , and the crossover frequency is at  $\omega_c \cong 4$  rad/sec.

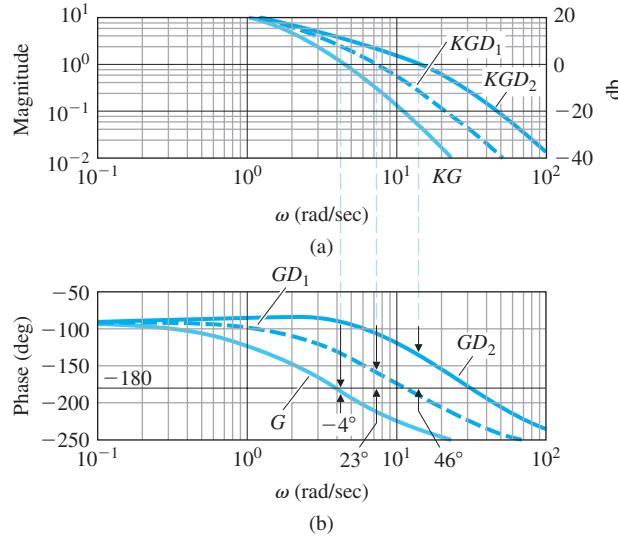
STEP 3. Allowing for  $5^\circ$  of extra phase margin, we need  $\text{PM} = 45^\circ + 5^\circ - (-4^\circ) = 54^\circ$  to be contributed by the lead compensator.

STEP 4. From Fig. 6.53 we find that  $\alpha$  must be 0.1 to achieve a maximum phase lead of  $54^\circ$ .

STEP 5. The new gain crossover frequency will be higher than the open-loop value of  $\omega_c = 4$  rad/sec, so let's select the pole and zero of the lead compensation to be at 20 and 2 rad/sec, respectively. So the candidate compensator is

$$D(s) = \frac{s/2 + 1}{s/20 + 1} = \frac{1}{0.1} \frac{s + 2}{s + 20}.$$

**Figure 6.60**  
Bode plot for the lead-compensation design in Example 6.16



STEP 6. The Bode plot of the compensated system (Fig. 6.60, middle curve) shows a PM of 23°. Further iteration will show that a single lead compensator cannot meet the specification because of the high-frequency slope of -3.

STEP 7. We need a double lead compensator in this system. If we try a compensator of the form

$$D_2(s) = \frac{1}{(0.1)^2} \frac{(s + 2)(s + 4)}{(s + 20)(s + 40)} = \frac{(s/2 + 1)(s/4 + 1)}{(s/20 + 1)(s/40 + 1)},$$

we obtain PM = 46°. The Bode plot for this case is shown as the upper curve in Fig. 6.60.

Both Examples 6.15 and 6.16 are third order. Example 6.16 was more difficult to design compensation for, because the error requirement,  $K_v$ , forced the crossover frequency,  $\omega_c$ , to be so high that a single lead could not provide enough PM.

### 6.7.3 PI Compensation

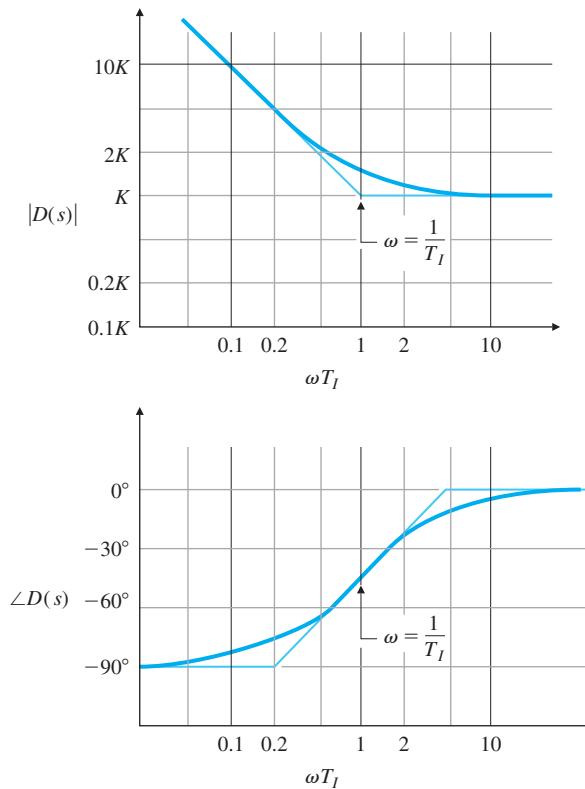
In many problems it is important to keep the bandwidth low and also to reduce the steady-state error. For this purpose, a proportional-integral (PI) or lag compensator is useful. By letting  $k_D = 0$  in Eq. (4.74), we see that PI control has the transfer function

$$D(s) = \frac{K}{s} \left( s + \frac{1}{T_I} \right), \tag{6.50}$$

which results in the frequency-response characteristics shown in Fig. 6.61. The desirable aspect of this compensation is the infinite gain at zero frequency, which

PI compensation

**Figure 6.61**  
Frequency response of PI control



reduces the steady-state errors. This is accomplished, however, at the cost of a phase decrease at frequencies lower than the break point at  $\omega = 1/T_I$ . Therefore,  $1/T_I$  is usually located at a frequency substantially less than the crossover frequency so that the system's phase margin is not affected significantly.

### 6.7.4 Lag Compensation

#### Lag compensation

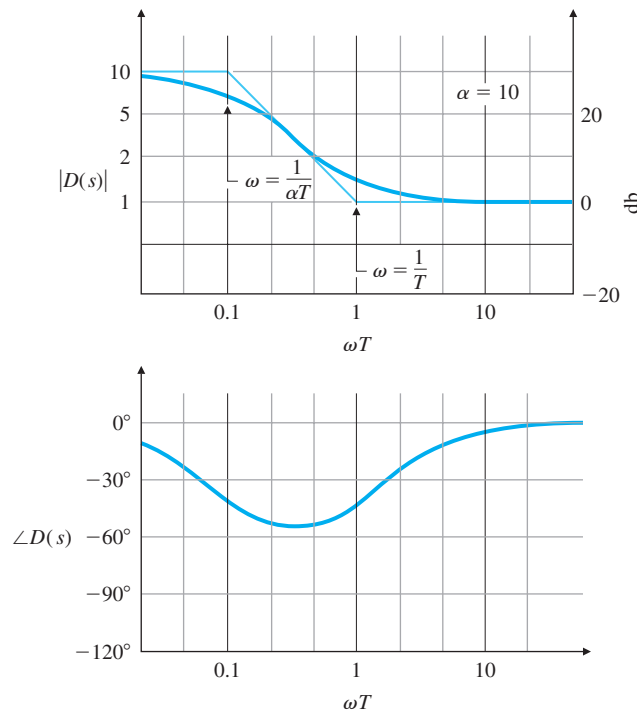
As we discussed in Section 5.5, **lag compensation** approximates PI control. Its transfer function was given by Eq. (5.91) for root-locus design, but for frequency-response design, it is more convenient to write the transfer function of the lag compensation *alone* in the Bode form

$$D(s) = \alpha \frac{T s + 1}{\alpha T s + 1}, \quad \alpha > 1, \quad (6.51)$$

where  $\alpha$  is the ratio between the zero/pole breakpoint frequencies. The complete controller will almost always include an overall gain  $K$  and perhaps other dynamics in addition to the lag compensation. Although Eq. (6.51) looks very similar to the lead compensation in Eq. (6.38), the fact that  $\alpha > 1$  causes the pole to have a lower break-point frequency than the zero. This relationship produces the low-frequency increase in amplitude and phase decrease (lag) apparent in the frequency-response plot in Fig. 6.62 and gives the compensation the essential feature of integral control—an increased low-frequency gain. The typical objective of lag-compensation design is to provide additional gain of  $\alpha$  in the low-frequency range and to leave the system sufficient phase margin (PM). Of course, phase lag is not the useful effect, and the pole and zero of the lag compensator are selected to be at much lower frequencies than the uncompensated system crossover frequency in order to keep the effect on the PM to a minimum. Thus, the lag compensator increases the open-loop DC gain, thereby improving the steady-state response characteristics, without changing the transient response characteristics significantly. If the pole and zero are relatively close together and near the origin (that is, if the value of  $T$  is large), we can increase the low-frequency gain (and thus  $K_p$ ,  $K_v$ , or  $K_a$ ) by a factor  $\alpha$  without moving the closed-loop poles appreciably. Hence, the transient response remains approximately the same while the steady-state response is improved.

We now summarize a step-by-step procedure for lag-compensator design.

**Figure 6.62**  
Frequency response of lag compensation with  $\alpha = 10$



## Design Procedure for Lag Compensation

1. Determine the open-loop gain  $K$  that will meet the phase-margin requirement without compensation.
2. Draw the Bode plot of the uncompensated system with crossover frequency from Step 1, and evaluate the low-frequency gain.
3. Determine  $\alpha$  to meet the low-frequency gain error requirement.
4. Choose the corner frequency  $\omega = 1/T$  (the zero of the lag compensator) to be one octave to one decade below the new crossover frequency  $\omega_c$ .
5. The other corner frequency (the pole location of the lag compensator) is then  $\omega = 1/\alpha T$ .
6. Iterate on the design. Adjust compensator parameters (poles, zeros, and gain) to meet all the specifications.

## EXAMPLE 6.17

*Lag-Compensator Design for Temperature Control System*

Again consider the third-order system of Example 6.15:

$$KG(s) = \frac{K}{\left(\frac{1}{0.5}s + 1\right)(s + 1)\left(\frac{1}{2}s + 1\right)}.$$

Design a lag compensator so the phase margin is at least  $40^\circ$  and  $K_p = 9$ .

**Solution.** We follow the design procedure previously enumerated.

STEP 1. From the open-loop plot of  $KG(s)$ , shown for  $K = 9$  in Fig. 6.58, it can be seen that a  $PM > 40^\circ$  will be achieved if the crossover frequency  $\omega_c \lesssim 1$  rad/sec. This will be the case if  $K = 3$ . So we pick  $K = 3$  in order to meet the PM specification.

STEP 2. The Bode plot of  $KG(s)$  in Fig. 6.63 with  $K = 3$  shows that the PM is  $\approx 50^\circ$  and the low-frequency gain is now 3. Exact calculation of the PM using MATLAB's margin shows that  $PM = 53^\circ$ .

STEP 3. The low frequency gain should be raised by a factor of 3, which means the lag compensation needs to have  $\alpha = 3$ .

STEP 4. We choose the corner frequency for the zero to be approximately a factor of 5 slower than the expected crossover frequency—that is, at 0.2 rad/sec. So,  $1/T = 0.2$ , or  $T = 5$ .

STEP 5. We then have the value for the other corner frequency:  $\omega = 1/\alpha T = \frac{1}{(3)(5)} = \frac{1}{15}$  rad/sec. The compensator is thus

$$D(s) = 3 \frac{5s + 1}{15s + 1}.$$

The compensated frequency response is also shown in Fig. 6.63. The low frequency gain of  $L(0) = KD(0)G(0) = 3K = 9$ , thus  $K_p = 9$  and the PM lowers slightly to  $44^\circ$ , which satisfies the specifications. The step response of the system, shown in Fig. 6.64, illustrates the reasonable damping that we would expect from  $PM = 44^\circ$ .

STEP 6. No iteration is required in this case.

**Figure 6.63**  
Frequency response of lag-compensation design in Example 6.17

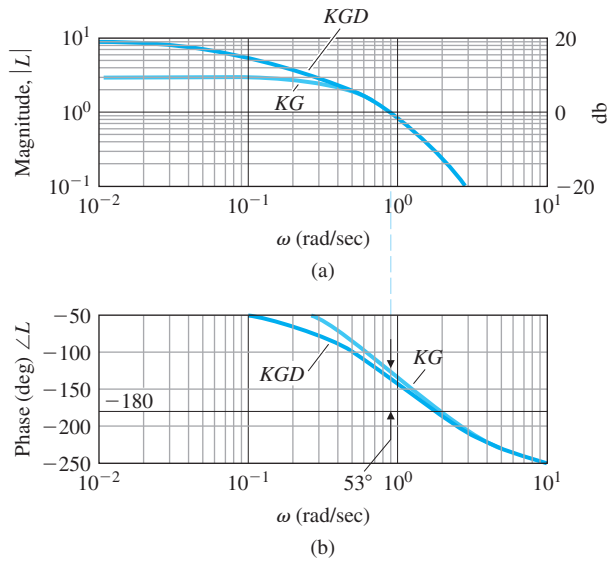
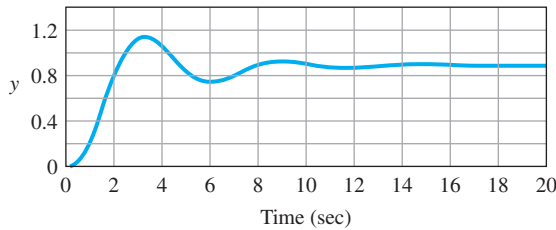


**Figure 6.64**  
Step response of lag-compensation design in Example 6.17



Note that Examples 6.15 and 6.17 are both for the same plant, and both had the same steady-state error requirement. One was compensated with lead and one was compensated with lag. The result is that the bandwidth of the lead-compensated design is approximately a factor of 3 higher than that for the lag compensated design. This result can be seen by comparing the crossover frequencies of the two designs.

A beneficial effect of lag compensation, an increase in the low-frequency gain for better error characteristics, was just demonstrated in Example 6.17. However, in essence, lag compensation reduces the value of  $\frac{\omega_c}{L(0)}$  ( $= \frac{\omega_c}{K_v}$  for a type 1 system). That means that, if the crossover frequency is kept the same, the low-frequency gain will increase. Likewise, if the low-frequency gain is kept the same, the crossover frequency will decrease. Therefore, lag compensation could also be interpreted to reduce the crossover frequency and thus obtain a better phase margin. The procedure for design in this case is partially modified. First, pick the low-frequency gain to meet error requirements, then locate the

lag compensation pole and zero in order to provide a crossover frequency with adequate PM. The next example illustrates this design procedure. The end result of the design will be the same no matter what procedure is followed.

**EXAMPLE 6.18** *Lag Compensation of the DC Motor*

Repeat the design of the DC motor control in Example 6.14, this time using lag compensation. Fix the low-frequency gain in order to meet the error requirement of  $K_v = 10$ ; then use the lag compensation to meet the PM requirement of  $45^\circ$ .

**Solution.** The frequency response of the system  $KG(s)$ , with the required gain of  $K = 10$ , is shown in Fig. 6.65. The uncompensated system has a crossover frequency at approximately 3 rad/sec where the  $PM = 20^\circ$ . The designer's task is to select the lag compensation break points so that the crossover frequency is lowered and more favorable PM results. To prevent detrimental effects from the compensation phase lag, the pole and zero position values of the compensation need to be substantially lower than the new crossover frequency. One possible choice is shown in Fig. 6.65: The lag zero is at 0.1 rad/sec, and the lag pole is at 0.01 rad/sec. This selection of parameters produces a PM of  $50^\circ$ , thus satisfying the specifications. Here the stabilization is achieved by keeping

**Figure 6.65**  
Frequency response of lag-compensation design in Example 6.18

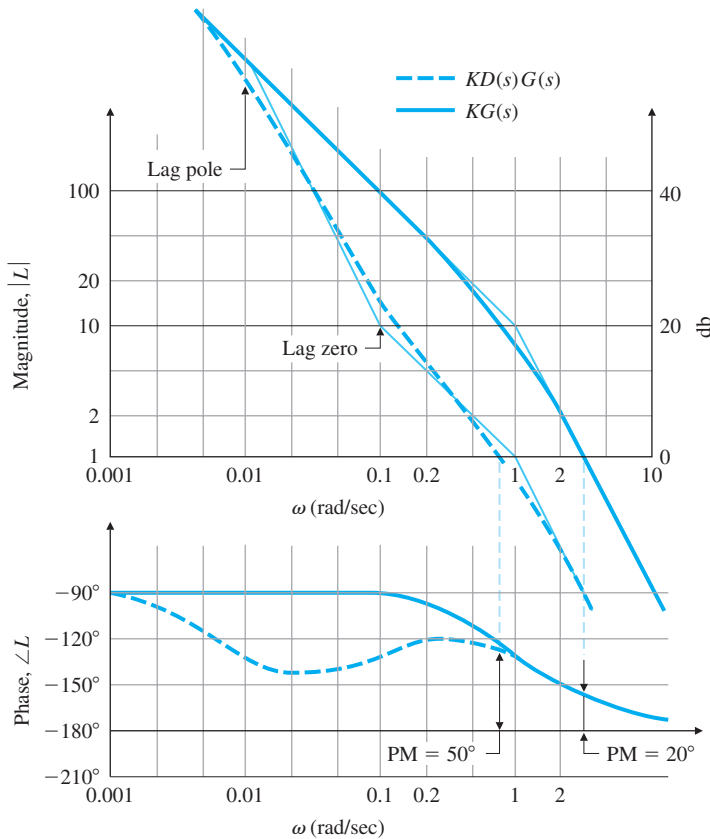
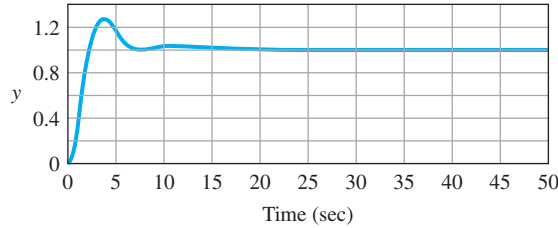


**Figure 6.66**  
Step response of  
lag-compensation design in  
Example 6.18



the crossover frequency to a region where  $G(s)$  has favorable phase characteristics. The criterion for selecting the pole and zero locations  $1/T$  is to make them low enough to minimize the effects of the phase lag from the compensation at the crossover frequency. Generally, however, the pole and zero are located no lower than necessary, because the additional system root [compare with the root locus of a similar system design in Fig. 5.29(b)] introduced by the lag will be in the same frequency range as the compensation zero and will have some effect on the output response, especially the response to disturbance inputs.

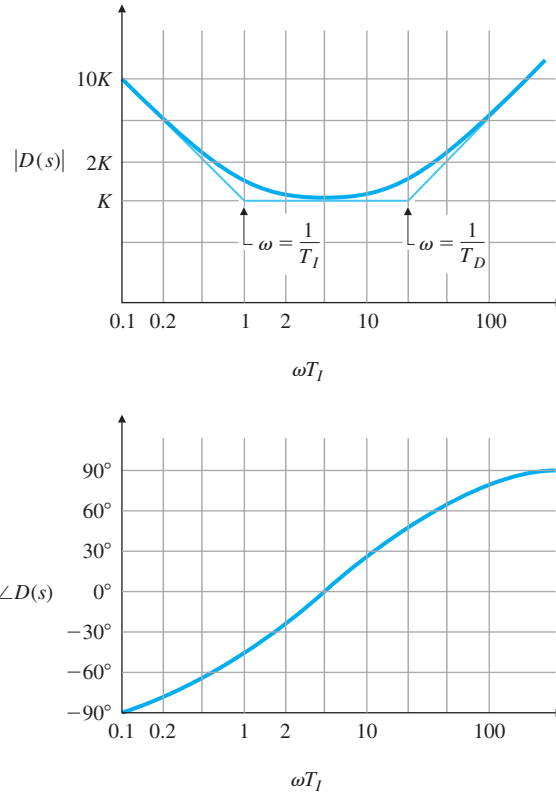
The response of the system to a step reference input is shown in Fig. 6.66. It shows no steady-state error to a step input, because this is a type 1 system. However, the introduction of the slow root from the lag compensation has caused the response to require about 25 sec to settle down to the zero steady-state value. The overshoot  $M_p$  is somewhat larger than you would expect from the guidelines, based on a second-order system shown in Fig. 6.37 for a  $PM = 50^\circ$ ; however, the performance is adequate.

As we saw previously for a similar situation, Examples 6.14 and 6.18 meet an identical set of specifications for the same plant in very different ways. In the first case the specifications are met with a lead compensation, and a crossover frequency  $\omega_c = 5$  rad/sec ( $\omega_{BW} \cong 6$  rad/sec) results. In the second case the same specifications are met with a lag compensation, and  $\omega_c \cong 0.8$  rad/sec ( $\omega_{BW} \cong 1$  rad/sec) results. Clearly, had there been specifications for rise time or bandwidth, they would have influenced the choice of compensation (lead or lag). Likewise, if the slow settling to the steady-state value was a problem, it might have suggested the use of lead compensation instead of lag.

In more realistic systems, dynamic elements usually represent the actuator and sensor as well as the process itself, so it is typically impossible to raise the crossover frequency much beyond the value representing the speed of response of the components being used. Although linear analysis seems to suggest that almost any system can be compensated, in fact, if we attempt to drive a set of components much faster than their natural frequencies, the system will saturate, the linearity assumptions will no longer be valid, and the linear design will represent little more than wishful thinking. With this behavior in mind, we see that simply increasing the gain of a system and adding lead compensators to achieve an adequate PM may not always be possible. It may be preferable to satisfy error requirements by adding a lag network so that the closed-loop bandwidth is kept at a more reasonable frequency.



**Figure 6.67**  
Frequency response of  
PID compensation with  
 $T_I/T_D = 20$



### 6.7.5 PID Compensation

For problems that need phase-margin improvement at  $\omega_c$  and low-frequency gain improvement, it is effective to use both derivative and integral control. By combining Eqs. (6.37) and (6.50), we obtain PID control. Its transfer function is

PID compensation

$$D(s) = \frac{K}{s} \left[ (T_D s + 1) \left( s + \frac{1}{T_I} \right) \right], \quad (6.52)$$

and its frequency-response characteristics are shown in Fig. 6.67. This form is slightly different from that given by Eq. (4.75); however, the effect of the difference is inconsequential. This compensation is roughly equivalent to combining lead and lag compensators in the same design, and so is sometimes referred to as a **lead-lag compensator**. Hence, it can provide simultaneous improvement in transient and steady-state responses.

#### EXAMPLE 6.19

#### *PID Compensation Design for Spacecraft Attitude Control*

A simplified design for spacecraft attitude control was presented in Section 6.5; however, here we have a more realistic situation that includes a sensor lag and a disturbing torque.

**Figure 6.68**  
Block diagram of spacecraft control using PID design, Example 6.19

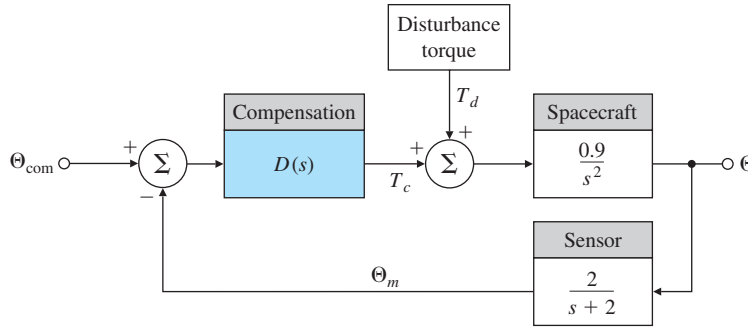


Figure 6.68 defines the system. Design a PID controller to have zero steady-state error to a constant-disturbance torque, a phase margin of  $65^\circ$ , and as high a bandwidth as is reasonably possible.

**Solution.** First, let us take care of the steady-state error. For the spacecraft to be at a steady final value, the total input torque,  $T_d + T_c$ , must equal zero. Therefore, if  $T_d \neq 0$ , then  $T_c = -T_d$ . The only way this can be true with no error ( $e = 0$ ) is for  $D(s)$  to contain an integral term. Hence, including integral control in the compensation will meet the steady-state requirement. This could also be verified mathematically by use of the Final Value Theorem (see Problem 6.46).

The frequency response of the spacecraft and sensor,

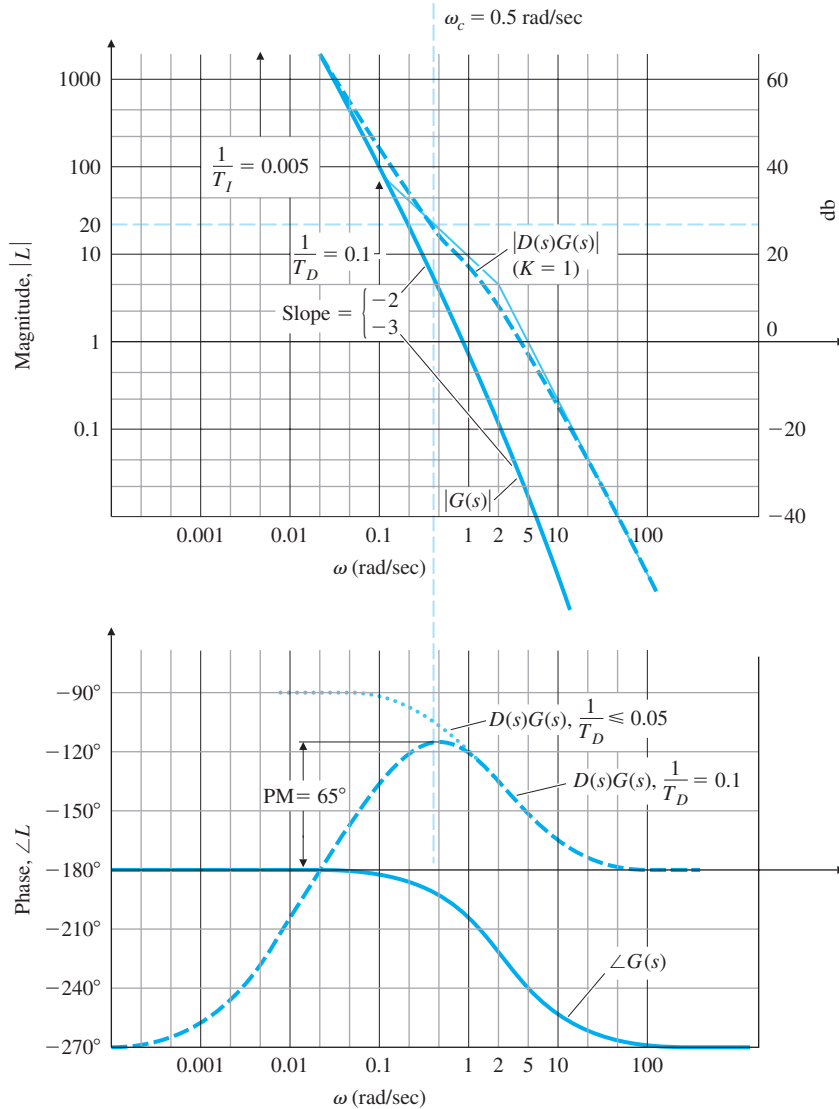
$$G(s) = \frac{0.9}{s^2} \left( \frac{2}{s+2} \right), \tag{6.53}$$

is shown in Fig. 6.69. The slopes of  $-2$  (that is,  $-40$  db per decade) and  $-3$  ( $-60$  db per decade) show that the system would be unstable for any value of  $K$  if no derivative feedback were used. This is clear because of Bode's gain-phase relationship, which shows that the phase would be  $-180^\circ$  for the  $-2$  slope and  $-270^\circ$  for the  $-3$  slope and which would correspond to a PM of  $0^\circ$  or  $-90^\circ$ . Therefore, derivative control is required to bring the slope to  $-1$  at the crossover frequency that was shown in Section 6.5 to be a requirement for stability. The problem now is to pick values for the three parameters in Eq. (6.52)— $K$ ,  $T_D$ , and  $T_I$ —that will satisfy the specifications.

The easiest approach is to work first on the phase so that  $PM = 65^\circ$  is achieved at a reasonably high frequency. This can be accomplished primarily by adjusting  $T_D$ , noting that  $T_I$  has a minor effect if sufficiently larger than  $T_D$ . Once the phase is adjusted, we establish the crossover frequency; then we can easily determine the gain  $K$ .

We examine the phase of the PID controller in Fig. 6.67 to determine what would happen to the compensated spacecraft system,  $D(s)G(s)$ , as  $T_D$  is varied. If  $1/T_D \geq 2$  rad/sec, the phase lead from the PID control would simply cancel the sensor phase lag, and the composite phase would never exceed  $-180^\circ$ , an unacceptable situation. If  $1/T_D \leq 0.01$ , the composite phase would approach  $-90^\circ$  for some range of frequencies and would exceed  $-115^\circ$  for an even wider range of frequencies; the latter threshold would provide a PM of  $65^\circ$ . In the compensated phase curve shown in Fig. 6.69,  $1/T_D = 0.1$ , which is the largest value of  $1/T_D$  that could provide the required PM of  $65^\circ$ . The phase would never cross the  $-115^\circ$  ( $65^\circ$  PM) line for any  $1/T_D > 0.1$ . For  $1/T_D = 0.1$ , the crossover frequency  $\omega_c$  that produces the  $65^\circ$  PM is  $0.5$  rad/sec. For a value of  $1/T_D \ll 0.05$ , the phase essentially follows the dotted curve in Fig. 6.69, which indicates that the maximum possible  $\omega_c$  is approximately  $1$  rad/sec and is provided by  $1/T_D =$

**Figure 6.69**  
 Compensation for PID  
 design in Example 6.19



0.05. Therefore,  $0.05 < 1/T_D < 0.1$  is the only sensible range for  $1/T_D$ ; anything less than 0.05 would provide no significant increase in bandwidth, while anything more than 0.1 could not meet the PM specification. Although the final choice is somewhat arbitrary, we have chosen  $1/T_D = 0.1$  for our final design.

Our choice for  $1/T_I$  is a factor of 20 lower than  $1/T_D$ ; that is,  $1/T_I = 0.005$ . A factor less than 20 would negatively impact the phase at crossover, thus lowering the PM. Furthermore, it is generally desirable to keep the compensated magnitude as large as possible at frequencies below  $\omega_c$  in order to have a faster transient response and smaller errors; maintaining  $1/T_D$  and  $1/T_I$  at the highest possible frequencies will bring this about.

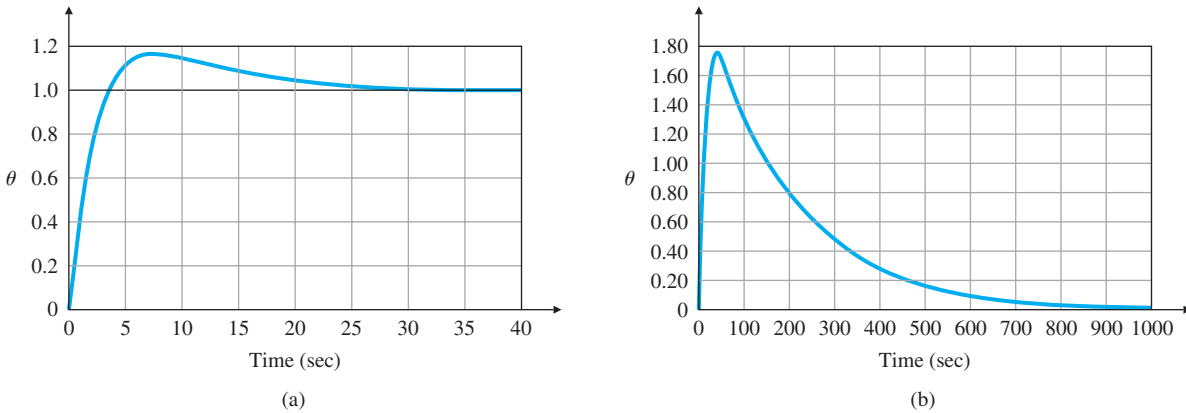


**Figure 6.70** Transient response for PID example: (a) step response; (b) step-disturbance response

The only remaining task is to determine the proportional part of the PID controller, or  $K$ . Unlike the system in Example 6.17, where we selected  $K$  in order to meet a steady-state error specification, here we select a value of  $K$  that will yield a crossover frequency at the point corresponding to the required PM of  $65^\circ$ . The basic procedure for finding  $K$ , discussed in Section 6.6, consists of plotting the compensated system amplitude with  $K = 1$ , finding the amplitude value at crossover, then setting  $1/K$  equal to that value. Figure 6.69 shows that when  $K = 1$ ,  $|D(s)G(s)| = 20$  at the desired crossover frequency  $\omega_c = 0.5$  rad/sec. Therefore,

$$\frac{1}{K} = 20, \quad \text{so} \quad K = \frac{1}{20} = 0.05.$$

The compensation equation that satisfies all of the specifications is now complete:

$$D(s) = \frac{0.05}{s} [(10s + 1)(s + 0.005)].$$

It is interesting to note that this system would become unstable if the gain were lowered so that  $\omega_c \leq 0.02$  rad/sec, the region in Fig. 6.69 where the phase of the compensated system is less than  $-180^\circ$ . As mentioned in Section 6.4, this situation is referred to as a conditionally stable system. A root locus with respect to  $K$  for this and any conditionally stable system would show the portion of the locus corresponding to very low gains in the RHP. The response of the system for a unit step  $\theta_{\text{com}}$  is shown in Fig. 6.70(a) and exhibits well damped behavior, as should be expected with a  $65^\circ$  PM.

The response of the system for a step disturbance torque  $T_d = 0.1$  N is shown in Fig. 6.70(b). Note that the integral control term does eventually drive the error to zero; however, it is slow due to the presence of a closed-loop pole in the vicinity of the zero at  $s = -0.005$ . However, recall from the design process that this zero was located in order that the integral term not impact the PM unduly. So if the slow disturbance response is not acceptable, speeding up this pole will decrease the PM and damping of the system. Compromise is often a necessity in control system design!

## Summary of Compensation Characteristics

1. *PD Control* adds phase lead at all frequencies above the break point. If there is no change in gain on the low-frequency asymptote, PD compensation will increase the crossover frequency and the speed of response. The increase in magnitude of the frequency response at the higher frequencies will increase the system's sensitivity to noise.
2. *Lead Compensation* adds phase lead at a frequency band between the two break points, which are usually selected to bracket the crossover frequency. If there is no change in gain on the low-frequency asymptote, lead compensation will increase both the crossover frequency and the speed of response over the uncompensated system.
3. *PI Control* increases the frequency-response magnitude at frequencies below the break point, thereby decreasing steady-state errors. It also contributes phase lag below the break point, which must be kept at a low enough frequency to avoid degrading the stability excessively.
4. *Lag Compensation* increases the frequency-response magnitude at frequencies below the two break points, thereby decreasing steady-state errors. Alternatively, with suitable adjustments in  $K$ , lag compensation can be used to decrease the frequency-response magnitude at frequencies above the two break points, so that  $\omega_c$  yields an acceptable phase margin. Lag compensation also contributes phase lag between the two break points, which must be kept at frequencies low enough to keep the phase decrease from degrading the PM excessively. This compensation will typically provide a slower response than using lead compensation.

## 6.7.6 Design Considerations

We have seen in the preceding designs that characteristics of the open-loop Bode plot of the loop gain,  $L(s)$  ( $= KDG$ ), determine performance with respect to steady-state errors and dynamic response. Other properties of feedback, developed in Chapter 4, include reducing the effects of sensor noise and parameter changes on the performance of the system.

The consideration of steady-state errors due to command inputs and disturbances has been an important design component in the different design methods presented. Design for acceptable steady-state errors can be thought of as placing a lower bound on the very-low-frequency gain of the system. Another aspect of the sensitivity issue concerns the high-frequency portion of the system. So far, Chapter 4 and Sections 5.5 and 6.7 have briefly discussed the idea that, to alleviate the effects of sensor noise, the gain of the system at high frequencies must be kept low. In fact, in the development of lead compensation, we added a pole to pure derivative control specifically to reduce the effects of sensor noise at the higher frequencies. It is not unusual for designers to place an extra pole in the compensation, that is, to use the relation

$$D(s) = \frac{Ts + 1}{(\alpha Ts + 1)^2},$$

in order to introduce even more attenuation for noise reduction.

A second consideration affecting high-frequency gains is that many systems have high-frequency dynamic phenomena, such as mechanical resonances, that could have an impact on the stability of a system. In very-high-performance designs, these high-frequency dynamics are included in the plant model, and a compensator is designed with a specific knowledge of those dynamics. A standard approach to designing for unknown high-frequency dynamics is to keep the high-frequency gain low, just as we did for sensor-noise reduction. The reason for this can be seen from the gain–frequency relationship of a typical system, shown in Fig. 6.71. The only way instability can result from high-frequency dynamics is if an unknown high-frequency resonance causes the magnitude to rise above 1. Conversely, if all unknown high-frequency phenomena are guaranteed to remain below a magnitude of 1, stability can be guaranteed. The likelihood of an unknown resonance in the plant  $G$  rising above 1 can be reduced if the nominal high-frequency loop gain ( $L$ ) is lowered by the addition of extra poles in  $D(s)$ . When the stability of a system with resonances is assured by tailoring the high-frequency magnitude never to exceed 1, we refer to this process as **amplitude or gain stabilization**. Of course, if the resonance characteristics are known exactly, a specially tailored compensation, such as one with a notch at the resonant frequency, can be used to change the phase at a specific frequency to avoid encirclements of  $-1$ , thus stabilizing the system even though the amplitude does exceed magnitude 1. This method of stabilization is referred to as **phase stabilization**. A drawback to phase stabilization is that the resonance information is often not available with adequate precision or varies with time; therefore, the method is more susceptible to errors in the plant model used in the design. Thus, we see that sensitivity to plant uncertainty and sensor noise are both reduced by sufficiently low loop gain at high-frequency.

Gain stabilization

Phase stabilization

These two aspects of sensitivity—high- and low-frequency behavior—can be depicted graphically, as shown in Fig. 6.72. There is a minimum low-frequency gain allowable for acceptable steady-state error performance and a maximum

**Figure 6.71**  
Effect of high-frequency plant uncertainty

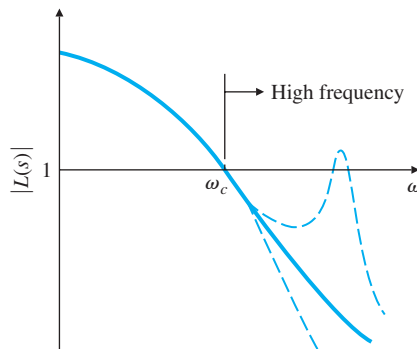
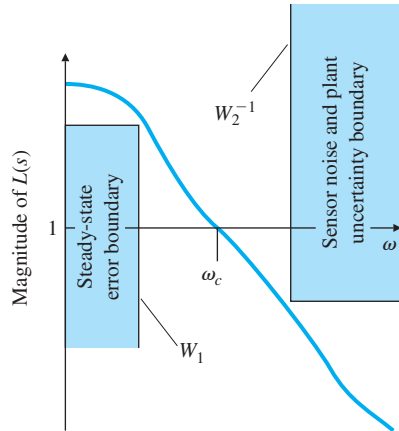


**Figure 6.72**  
Design criteria for low sensitivity



high-frequency gain allowable for acceptable noise performance and for low probability of instabilities caused by plant-modeling errors. It is sometimes convenient to define the low-frequency lower bound on the frequency response as  $W_1$  and the upper bound as  $W_2^{-1}$ , as shown in the figure. Between these two bounds the control engineer must achieve a gain crossover near the required bandwidth; as we have seen, the crossover must occur at essentially a slope of  $-1$  for good PM and hence damping.

For example, if a control system was required to follow a sine reference input with frequencies from 0 to  $\omega_d$  with errors no greater than 1%, the function  $W_1$  would be 100 from  $\omega = 0$  to  $\omega_d$ . Similar ideas enter into defining possible values for the  $W_2^{-1}$  function. These ideas will be discussed further in Section 6.9.

## ▲ 6.8 Alternative Presentations of Data

Before computers were widely available, other ways to present frequency-response data were developed to aid both in understanding design and in easing the designer's work load. The widespread availability of computers has reduced the need for these methods. Two techniques are the Nichols chart and the inverse Nyquist plot, both of which we examine in this section because of their place in history.

### 6.8.1 Nichols Chart

A rectangular plot of  $\log |G(j\omega)|$  versus  $\angle G(j\omega)$  can be drawn by simply transferring the information directly from the separate magnitude and phase portions in a Bode plot; one point on the new curve thus results from a given value of the frequency  $\omega$ . This means that the new curve is parameterized as a function of frequency. As with the Bode plots, the magnitude information is plotted on a logarithmic scale, while the phase information is plotted on a linear scale.

This template was suggested by N. Nichols and is usually referred to as a **Nichols chart**. The idea of plotting the magnitude of  $G(j\omega)$  versus its phase is similar to the concept of plotting the real and imaginary parts of  $G(j\omega)$ , which formed the basis for the Nyquist plots shown in Sections 6.3 and 6.4. However, it is difficult to capture all the pertinent characteristics of  $G(j\omega)$  on the linear scale of the Nyquist plot. The log scale for magnitude in the Nichols chart alleviates this difficulty, allowing this kind of presentation to be useful for design.

For any value of the complex transfer function  $G(j\omega)$ , Section 6.6 showed that there is a unique mapping to the unity-feedback closed-loop transfer function

$$\mathcal{T}(j\omega) = \frac{G(j\omega)}{1 + G(j\omega)}, \quad (6.54)$$

or in polar form,

$$\mathcal{T}(j\omega) = M(\omega)e^{j\alpha(\omega)}, \quad (6.55)$$

where  $M(\omega)$  is the magnitude of the closed-loop transfer function and  $\alpha(\omega)$  is the phase of the closed-loop transfer function. Specifically,

$$M = \left| \frac{G}{1 + G} \right|, \quad (6.56)$$

$$\alpha = \tan^{-1}(N) = \angle \frac{G}{1 + G}. \quad (6.57)$$

It can be proven that the contours of constant closed-loop magnitude and phase are circles when  $G(j\omega)$  is presented in the linear Nyquist plot. These circles are referred to as the **M and N circles** respectively.

M and N circles

The Nichols chart also contains contours of constant *closed-loop* magnitude and phase based on these relationships, as shown in Fig. 6.73; however, they are no longer circles, because the Nichols charts are semilog plots of magnitude vs. phase. A designer can therefore graphically determine the bandwidth of a closed-loop system from the plot of the open-loop data on a Nichols chart by noting where the open-loop curve crosses the 0.70 contour of the closed-loop magnitude and determining the frequency of the corresponding data point. Likewise, a designer can determine the resonant peak amplitude  $M_r$  by noting the value of the magnitude of the highest closed-loop contour tangent to the curve. The frequency associated with the magnitude and phase at the point of tangency is sometimes referred to as the **resonant frequency**  $\omega_r$ . Similarly, a designer can determine the gain margin (GM) by observing the value of the gain where the Nichols plot crosses the  $-180^\circ$  line, and the phase margin (PM) by observing the phase where the plot crosses the amplitude 1 line.<sup>10</sup> MATLAB provides for easy drawing of a Nichols chart via the `nicholsm`-file.

Resonant frequency

<sup>10</sup>James, H. M., N. B. Nichols, and R. S. Phillips (1947).



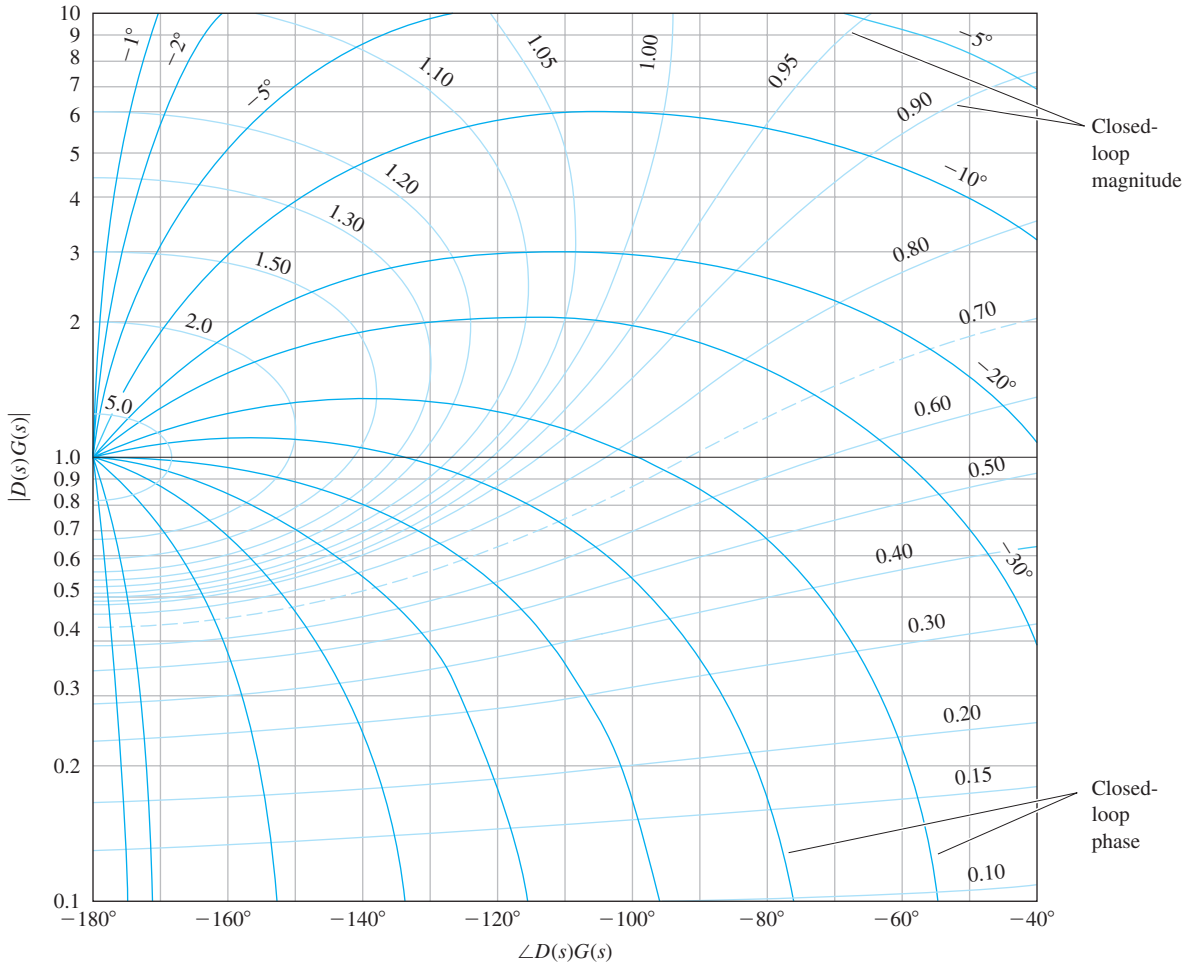
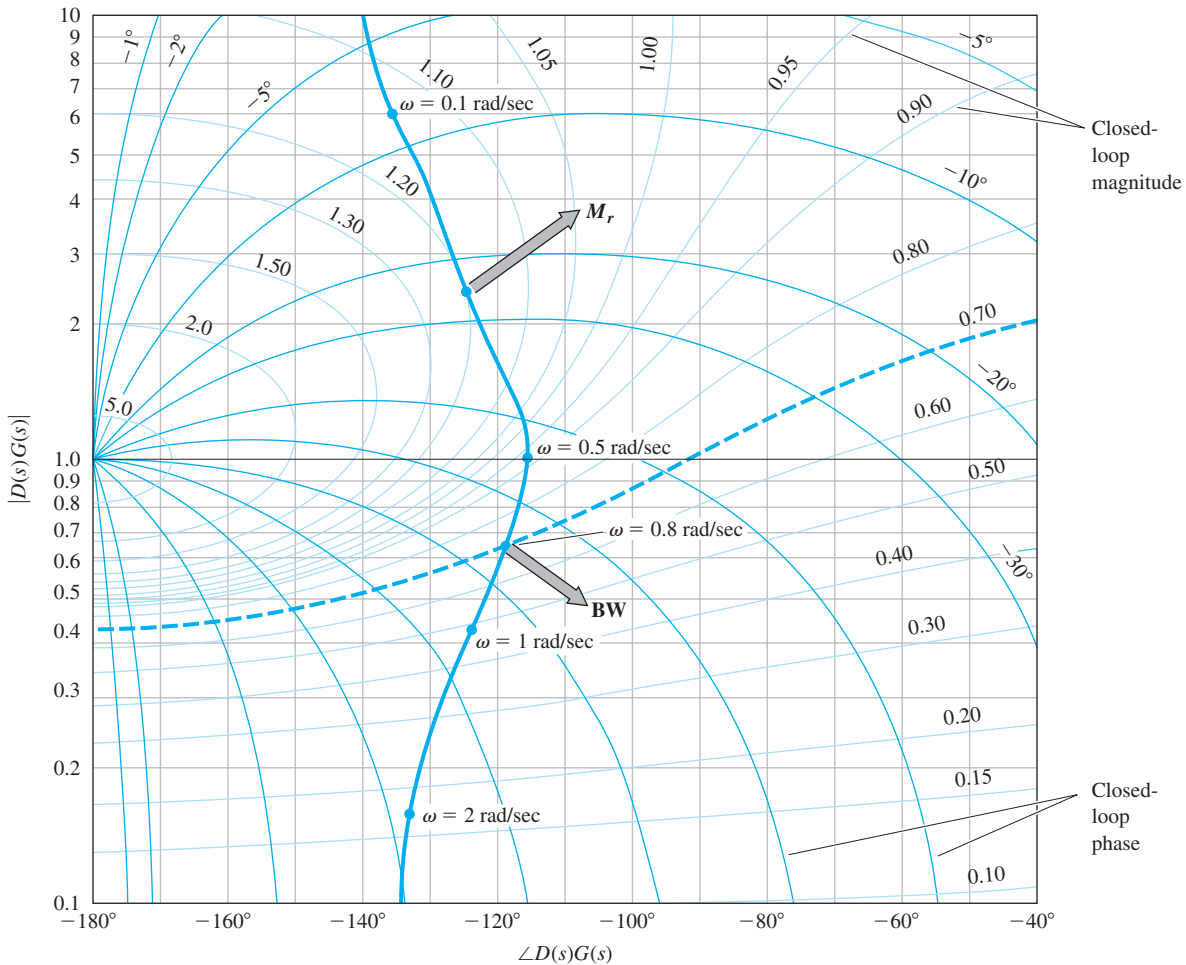


Figure 6.73 Nichols chart

EXAMPLE 6.20 *Nichols Chart for PID Example*

Determine the bandwidth and resonant peak magnitude of the compensated system whose frequency response is shown in Fig. 6.69.

**Solution.** The magnitude and phase information of the compensated design example seen in Fig. 6.69 is shown on a Nichols chart in Fig. 6.74. When comparing the two figures, it is important to divide the magnitudes in Fig. 6.69 by a factor of 20 in order to obtain  $|D(s)G(s)|$  rather than the normalized values used in Fig. 6.69. Because the curve crosses the closed-loop magnitude 0.70 contour at  $\omega = 0.8$  rad/sec, we see that the bandwidth of this system is 0.8 rad/sec. Because the largest-magnitude contour touched by the curve is 1.20, we also see that  $M_r = 1.2$ .



**Figure 6.74** Example plot on the Nichols chart for determining bandwidth and  $M_r$ .

This presentation of data was particularly valuable when a designer had to generate plots and perform calculations by hand. A change in gain, for example, could be evaluated by sliding the curve vertically on transparent paper over a standard Nichols chart. The GM, PM, and bandwidth were then easy to read off the chart, thus allowing evaluations of several values of gain with a minimal amount of effort. With access to computer-aided methods, however, we can now calculate the bandwidth and perform many repetitive evaluations of the gain or any other parameter with a few key strokes. Today the Nichols chart is used primarily as an alternative way to present the information in a Nyquist plot. For complex systems for which the  $-1$  encirclements need to be evaluated, the magnitude log scale of the Nichols chart enables us to examine a wider range of frequencies than a Nyquist plot does, as well as allowing us to read the gain and phase margins directly.

**EXAMPLE 6.21** *Stability Margins from Nichols Chart*

For the system of Example 6.12, whose Nichols plot is shown in Fig. 6.41, determine the PM and GM using the Nyquist plot.

**Solution.** Figure 6.75 shows a Nichols chart with the data from the same system shown in Fig. 6.41. Note that the PM for the magnitude 1 crossover frequency is  $36^\circ$  and the GM is 1.25 ( $= 1/0.8$ ). It is clear from this presentation of the data that the most critical portion of the curve is where it crosses the  $-180^\circ$  line; hence the GM is the most relevant stability margin in this example.

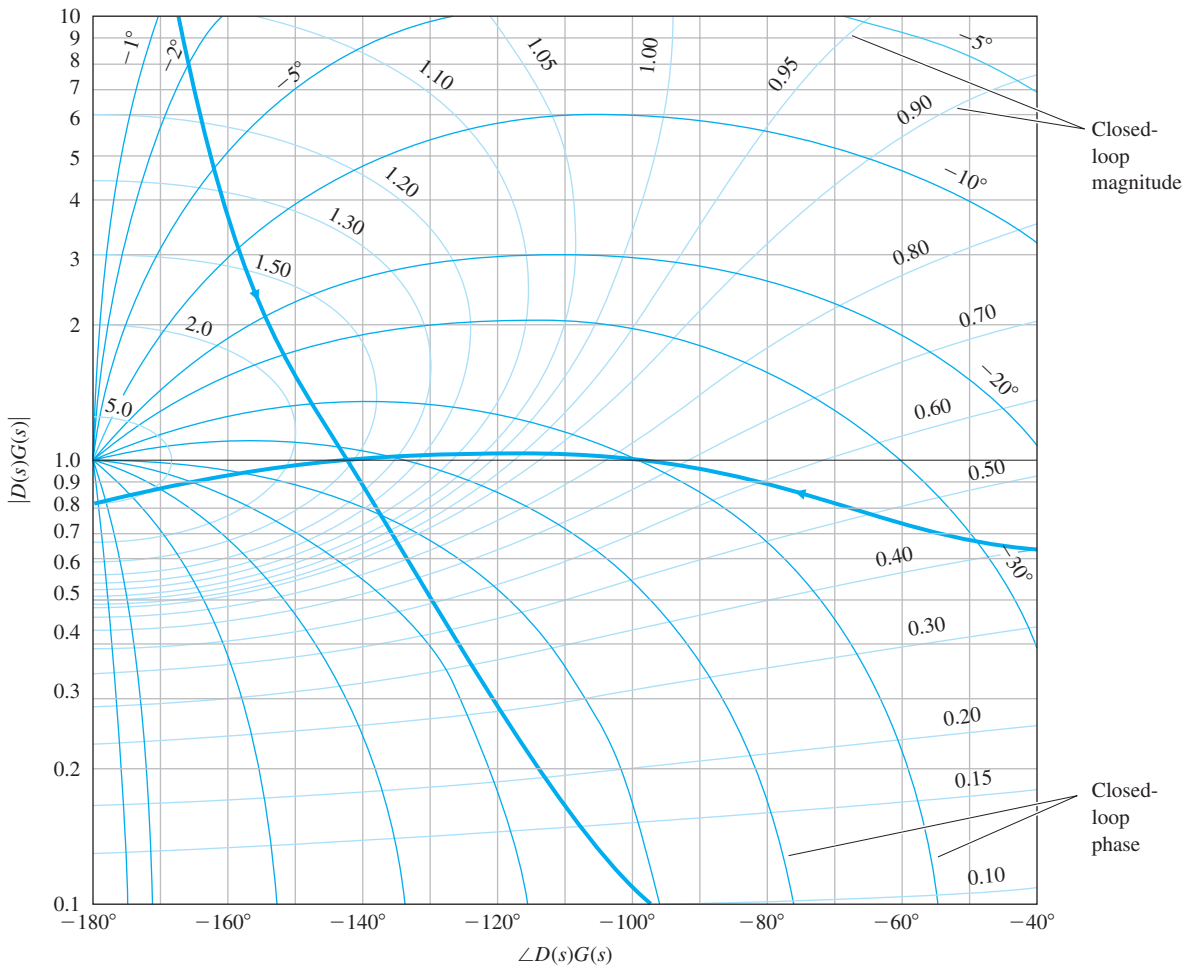
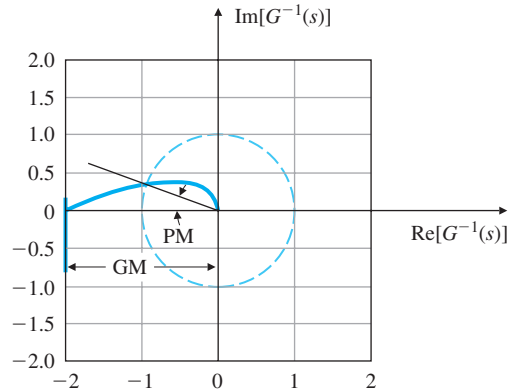


**Figure 6.75** Nichols chart of the complex system in Examples 6.12 and 6.21

**Figure 6.76**  
Inverse Nyquist plot for  
Example 6.9

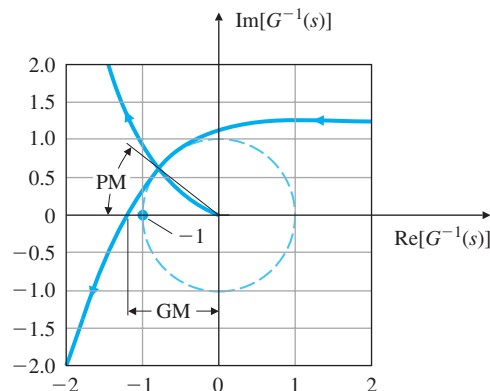


### 6.8.2 Inverse Nyquist

The **inverse Nyquist plot** is simply the reciprocal of the Nyquist plot described in Section 6.3 and used in Section 6.4 for the definition and discussion of stability margins. It is obtained most easily by computing the inverse of the magnitude from the Bode plot and plotting that quantity at an angle in the complex plane, as indicated by the phase from the Bode plot. It can be used to find the PM and GM in the same way that the Nyquist plot was used. When  $|G(j\omega)| = 1$ ,  $|G^{-1}(j\omega)| = 1$  also, so the definition of PM is identical on the two plots. However, when the phase is  $-180^\circ$  or  $+180^\circ$ , the value of  $|G^{-1}(j\omega)|$  is the GM directly; no calculation of an inverse is required, as was the case for the Nyquist plot.

The inverse Nyquist plot for the system in Fig. 6.24 (Example 6.9) is shown in Fig. 6.76 for the case where  $K = 1$  and the system is stable. Note that  $GM = 2$  and  $PM \cong 20^\circ$ . As an example of a more complex case, Fig. 6.77 shows an inverse Nyquist plot for the sixth-order case whose Nyquist plot was shown in Fig. 6.41 and whose Nichols chart was shown in Fig. 6.75. Note here

**Figure 6.77**  
Inverse Nyquist plot of the  
system whose Nyquist plot  
is in Fig. 6.41



that  $GM = 1.2$  and  $PM \cong 35^\circ$ . Had the two crossings of the unit circle not occurred at the same point, the crossing with the smallest  $PM$  would have been the appropriate one to use.

### ▲ 6.9 Specifications in Terms of the Sensitivity Function

We have seen how the gain and phase margins give useful information about the relative stability of nominal systems and can be used to guide the design of lead and lag compensations. However, the  $GM$  and  $PM$  are only two numbers and have limitations as guides to the design of realistic control problems. We can express more complete design specifications in the frequency domain if we first give frequency descriptions for the external signals, such as the reference and disturbance, and consider the sensitivity function defined in Section 4.1. For example, we have so far described dynamic performance by the transient response to simple steps and ramps. A more realistic description of the actual complex input signals is to represent them as random processes with corresponding frequency power density spectra. A less sophisticated description, which is adequate for our purposes, is to assume that the signals can be represented as a sum of sinusoids with frequencies in a specified range. For example, we can usually describe the frequency content of the reference input as a sum of sinusoids with relative amplitudes given by a magnitude function  $|R|$  such as that plotted in Fig. 6.78, which represents a signal with sinusoidal components having about the same amplitudes up to some value  $\omega_1$  and very small amplitudes for frequencies above that. With this assumption, the response tracking specification can be expressed by a statement such as “the magnitude of the

**Figure 6.78**  
Plot of typical reference spectrum

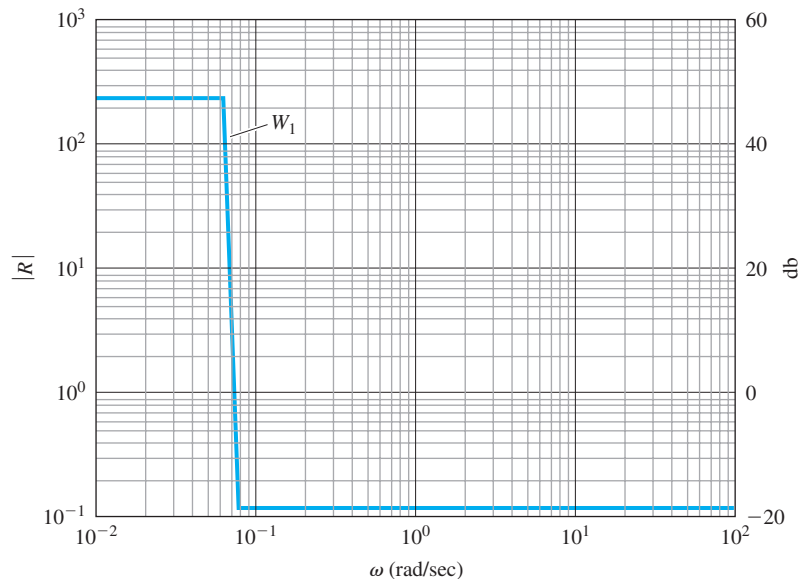
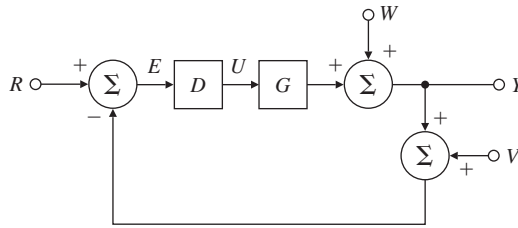


**Figure 6.79**  
Closed-loop block diagram



system error is to be less than the bound  $e_b$  (a value such as 0.01) for any sinusoid of frequency  $\omega_o$  in the range  $0 \leq \omega_o \leq \omega_1$  and of amplitude given by  $|R(j\omega_o)|$ . To express such a performance requirement in terms that can be used in design, we consider again the unity-feedback system drawn in Fig. 6.79. For this system, the error is given by

$$E(j\omega) = \frac{1}{1 + DG} R \triangleq S(j\omega)R, \tag{6.58}$$

Sensitivity function

where we have used the **sensitivity function**

$$S(j\omega) \triangleq \frac{1}{1 + DG}. \tag{6.59}$$

In addition to being the factor multiplying the system error, the sensitivity function is also the reciprocal of the distance of the Nyquist curve,  $DG$ , from the critical point  $-1$ . A large value for  $S$  indicates a Nyquist plot that comes close to the point of instability. The frequency-based error specification based on Eq. (6.58) can be expressed as  $|E| = |S| |R| \leq e_b$ . In order to normalize the problem and not need to define both the spectrum  $R$  and the error bound each time, we define the real function of frequency  $W_1(\omega) = |R|/e_b$  and the requirement can be written as

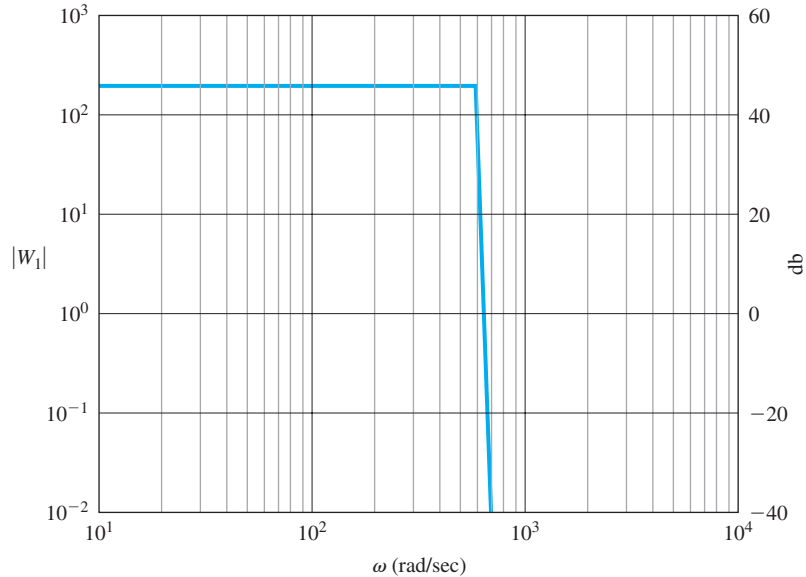
$$\boxed{|S|W_1 \leq 1.} \tag{6.60}$$

**EXAMPLE 6.22** *Performance Bound Function*

A unity feedback system is to have an error less than 0.005 for all unity amplitude sinusoids below frequency 100 Hz. Draw the performance frequency function  $W_1(\omega)$  for this design.

**Solution.** The spectrum, from the problem description, is unity for  $0 \leq \omega \leq 200\pi$ . Because  $e_b = 0.005$ , the required function is given by a rectangle of amplitude  $1/0.005 = 200$  over the given range. The function is plotted in Fig. 6.80.

**Figure 6.80**  
Plot of example  
performance function,  $W_1$



The expression in Eq. (6.60) can be translated to the more familiar Bode plot coordinates and given as a requirement on loop gain by observing that over the frequency range when errors are small the loop gain is large. In that case  $|S| \approx \frac{1}{|DG|}$ , and the requirement is approximately

$$\frac{W_1}{|DG|} \leq 1, \quad (6.61)$$

$$\boxed{|DG| \geq W_1.}$$

This requirement can be seen as an extension of the steady-state error requirement from just  $\omega = 0$  to the range  $0 \leq \omega_o \leq \omega_1$ .

In addition to the requirement on dynamic performance, the designer is usually required to design for **stability robustness**. By this we mean that, while the design is done for a nominal plant transfer function, the actual system is expected to be stable for an entire class of transfer functions that represents the range of changes that are expected to be faced as temperature, age, and other operational and environmental factors vary the plant dynamics from the nominal case. A realistic way to express this uncertainty is to describe the plant transfer function as having a multiplicative uncertainty:

$$G(j\omega) = G_o(j\omega)[1 + W_2(\omega)\Delta(j\omega)]. \quad (6.62)$$

In Eq. (6.62), the real function  $W_2$  is a magnitude function that expresses the size of changes as a function of frequency that the transfer function is expected to experience. In terms of  $G$  and  $G_o$ , the expression is

$$W_2 = \left| \frac{G - G_o}{G_o} \right|. \tag{6.63}$$

The shape of  $W_2$  is almost always very small for low frequencies (we know the model very well there) and increases substantially as we go to high frequencies, where parasitic parameters come into play and unmodeled structural flexibility is common. A typical shape is sketched in Fig. 6.81. The complex function,  $\Delta(j\omega)$ , represents the uncertainty in phase and is restricted only by the constraint

$$0 \leq |\Delta| \leq 1. \tag{6.64}$$

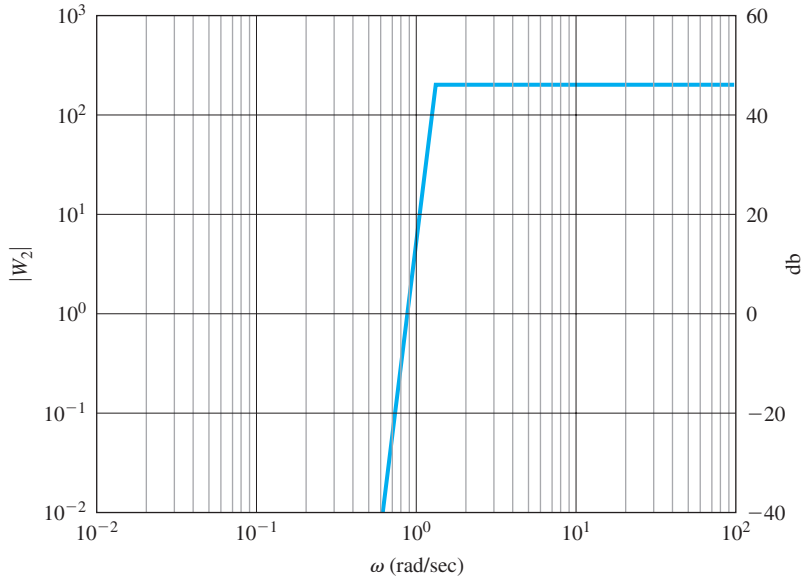
We assume that the nominal design has been done and is stable, so that the Nyquist plot of  $DG_o$  satisfies the Nyquist Stability Criterion. In this case, the nominal characteristic equation  $1 + DG_o = 0$  is never satisfied for any real frequency. If the system is to have stability robustness, the characteristic equation using the uncertain plant as described by Eq. (6.62) must not go to zero for any real frequency for any value of  $\Delta$ . The requirement can be written as

$$1 + DG \neq 0, \tag{6.65}$$

$$1 + DG_o[1 + W_2\Delta] \neq 0,$$

$$(1 + DG_o)(1 + \mathcal{I}W_2\Delta) \neq 0,$$

**Figure 6.81**  
Plot of typical plant uncertainty,  $W_2$





where we have defined the **complementary sensitivity function** as

$$\mathcal{T}(j\omega) \triangleq DG_o/(1 + DG_o) = 1 - \mathcal{S}. \quad (6.66)$$

Because the nominal system is stable, the first term in Eq. (6.65),  $(1 + DG_o)$ , is never zero. Thus, if Eq. (6.65) is not to be zero for any frequency and any  $\Delta$ , then it is necessary and sufficient that

$$|\mathcal{T}W_2\Delta| < 1,$$

which reduces to

$$|\mathcal{T}| W_2 < 1, \quad (6.67)$$

making use of Eq. (6.64). As with the performance specification, for single-input–single-output unity-feedback systems this requirement can be approximated by a more convenient form. Over the range of high frequencies where  $W_2$  is non-negligible because there is significant model uncertainty,  $DG_o$  is small. Therefore we can approximate  $\mathcal{T} \approx DG_o$ , and the constraint reduces to

$$|DG_o| W_2 < 1, \quad (6.68)$$

$$\boxed{|DG_o| < \frac{1}{W_2}}.$$

### EXAMPLE 6.23 *Typical Plant Uncertainty*

The uncertainty in a plant model is described by a function  $W_2$  that is zero until  $\omega = 3000$ , increases linearly from there to a value of 100 at  $\omega = 10,000$ , and remains at 100 for higher frequencies. Plot the constraint on  $DG_o$  to meet this requirement.

**Solution.** Where  $W_2 = 0$ , there is no constraint on the magnitude of loop gain; above  $\omega = 3000$ ,  $1/W_2 = DG_o$  is a hyperbola from  $\infty$  to 0.01 at  $\omega = 10,000$  and remains at 0.01 for  $\omega > 10,000$ . The bound is sketched in Fig. 6.82.

In practice, the magnitude of the loop gain is plotted on log–log (Bode) coordinates, and the constraints of Eqs. (6.61) and (6.68) are included on the same plot. A typical sketch is drawn in Fig. 6.83. The designer is expected to construct a loop gain that will stay above  $W_1$  for frequencies below  $\omega_1$ , cross over the magnitude 1 line ( $|DG| = 0$ ) in the range  $\omega_1 \leq \omega \leq \omega_2$ , and stay below  $1/W_2$  for frequencies above  $\omega_2$ .

**Figure 6.82**  
Plot of constraint on  $|DG_o| (= |W_2^{-1}|)$

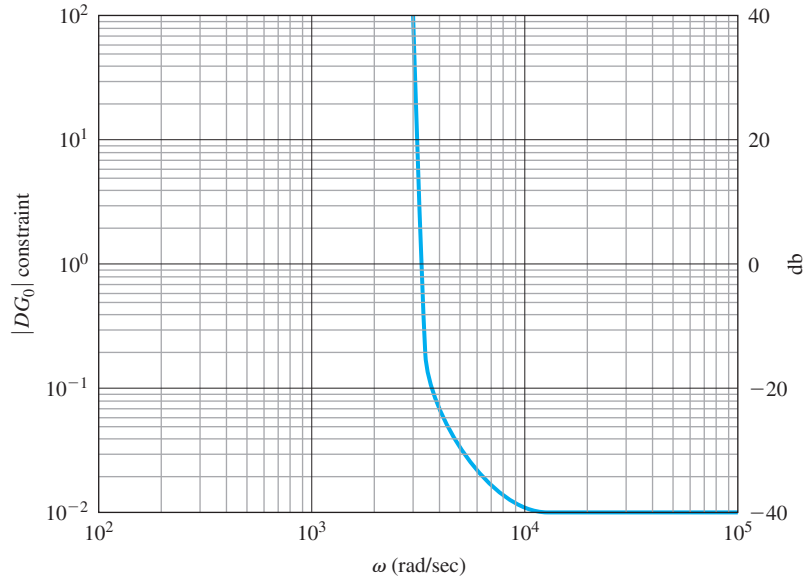
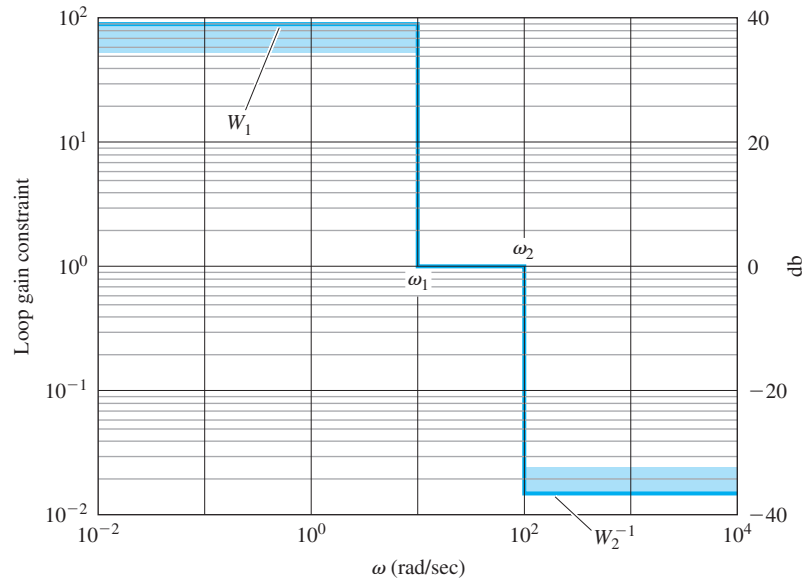


**Figure 6.83**  
Tracking and stability robustness constraints on the Bode plot



### 6.9.1 Limitations on Design in Terms of the Sensitivity Function

One of the major contributions of Bode was to derive important limitations on transfer functions that set limits on achievable design specifications. For example, one would like to have the system error kept small for the widest possible range of frequencies and yet have a system that is robustly stable for

a very uncertain plant. In terms of the plot in Fig. 6.83, we want  $W_1$  and  $W_2$  to be very large in their respective frequency ranges and for  $\omega_1$  to be pushed up close to  $\omega_2$ . Thus the loop gain is expected to plunge with a large negative slope from being greater than  $W_1$  to being less than  $1/W_2$  in a very short span, while maintaining a good phase margin to assure stability and good dynamic performance. The Bode gain–phase formula given earlier shows that this is *impossible* with a linear controller, by showing that the minimum possible phase is determined by an integral depending on the slope of the magnitude curve. If the slope is constant for a substantial range around  $\omega_o$ , then the formula can be approximated by

$$\phi(\omega_o) \approx \frac{\pi}{2} \left. \frac{dM}{du} \right|_{u=0}, \quad (6.69)$$

where  $M$  is the log magnitude and  $u = \log \frac{\omega}{\omega_o}$ . If, for example, the phase is to be kept above  $-150^\circ$  to maintain a  $30^\circ$  phase margin, then the magnitude slope near  $\omega_o$  is estimated to be

$$\begin{aligned} \frac{dM}{du} &\approx \frac{2}{\pi} \left( -150 \frac{\pi}{180} \right) \\ &\approx -1.667. \end{aligned}$$

If we try to make the average slope faster (more negative) than this, we will lose the phase margin. From this condition, there developed the design rule that the asymptotes of the Bode plot magnitude, which are restricted to be integral values for rational functions, should be made to cross over the zero-db line at a slope of  $-1$  over a frequency range of about one decade around the crossover frequency, as already discussed in Section 6.5. Modifications to this rule need of course be made in particular cases, but the limitation implied by Eq. (6.69) is a hard limit that cannot be avoided.

#### EXAMPLE 6.24 *Robustness Constraints*

If  $W_1 = W_2 = 100$ , and we want  $PM = 30^\circ$ , what is the minimum ratio of  $\omega_2/\omega_1$ ?

**Solution.** The slope is

$$\frac{\log W_1 - \log \frac{1}{W_2}}{\log \omega_1 - \log \omega_2} = \frac{2 + 2}{\log \frac{\omega_1}{\omega_2}} = -1.667.$$

Thus, the log of the ratio is  $\log \frac{\omega_1}{\omega_2} = -2.40$  and  $\omega_2 = 251\omega_1$ .

An alternative to the standard Bode plot as a design guide can be based on a plot of the sensitivity function as a function of frequency. In this format, Eq. (6.60) requires that  $|\mathcal{S}| < \frac{1}{W_1}$  over the range  $0 \leq \omega \leq \omega_1$  for performance, and Eq. (6.68) requires that  $|\mathcal{S}| \approx 1$  over the range  $\omega_2 \leq \omega$  for stability robustness. It should come as no surprise that Bode found a limitation on the possibilities in this case, too. The constraint, extended by Freudenberg and Looze, shows that an integral of the sensitivity function is determined by the presence of poles in the right half-plane. Suppose the loop gain  $DG_o$  has  $n_p$  poles,  $p_i$ , in the right half-plane and “rolls off” at high frequencies at a slope faster than  $-1$ . For rational functions, this means that there is an excess of at least two more finite poles than zeros. Then it can be shown that

$$\int_0^\infty \ln(|\mathcal{S}|) d\omega = \pi \sum_{i=1}^{n_p} \operatorname{Re}\{p_i\}. \tag{6.70}$$

If there are no right-half plane poles, then the integral is zero. This means that if we make the log of the sensitivity function very negative over some frequency band to reduce errors in that band, then, *of necessity*,  $\ln|\mathcal{S}|$  will be positive over another part of the band, and errors will be amplified there. If there are unstable poles, the situation is worse, because the positive area where sensitivity magnifies the error must *exceed* the negative area where the error is reduced by the feedback. If the system is minimum phase, then it is in principle possible to keep the magnitude of the sensitivity small by spreading the sensitivity increase over all positive frequencies to infinity, but such a design requires an excessive bandwidth and is rarely practical. If a specific bandwidth is imposed, then the sensitivity function is constrained to take on a finite, possibly large, positive value at some point below the bandwidth. As implied by the definition of the vector margin (VM) in Section 6.4 (Fig. 6.38), a large  $\mathcal{S}_{\max}$  corresponds to a Nyquist plot that comes close to the  $-1$  critical point and a system having a small vector margin, because

Vector margin

$$\text{VM} = \frac{\mathcal{S}_{\max}}{\mathcal{S}_{\max} - 1}. \tag{6.71}$$

If the system is not minimum phase, the situation is worse. An alternative to Eq. (6.70) is true if there is a nonminimum-phase zero of  $DG_o$ , a zero in the right half-plane. Suppose that the zero is located at  $z_o = \sigma_o + j\omega_o$ , where  $\sigma_o > 0$ . Again, we assume there are  $n_p$  right half-plane poles at locations  $p_i$  with conjugate values  $\bar{p}_i$ . Now the condition can be expressed as a two-sided weighted integral

$$\int_{-\infty}^\infty \ln(|\mathcal{S}|) \frac{\sigma_o}{\sigma_o^2 + (\omega - \omega_o)^2} d\omega = \pi \sum_{i=1}^{n_p} \ln \left| \frac{\bar{p}_i + z_o}{p_i - z_o} \right|. \tag{6.72}$$

In this case, we do not have the “roll-off” restriction, and there is no possibility of spreading the positive area over high frequencies, because the weighting function goes to zero with frequency. The important point about this integral is that if the nonminimum-phase zero is close to a right half-plane pole, the right side of the integral can be very large, and the excess of positive area is required to be correspondingly large. Based on this result, one expects especially great difficulty meeting both tracking and robustness specifications on sensitivity with a system having right half-plane poles and zeros close together.

### EXAMPLE 6.25 *Sensitivity Function for Antenna*

Compute and plot the sensitivity function for the design of the antenna for which  $G(s) = 1/s(s+1)$  and  $D(s) = 10(0.5s+1)/(0.1s+1)$ .

**Solution.** The sensitivity function for this case is

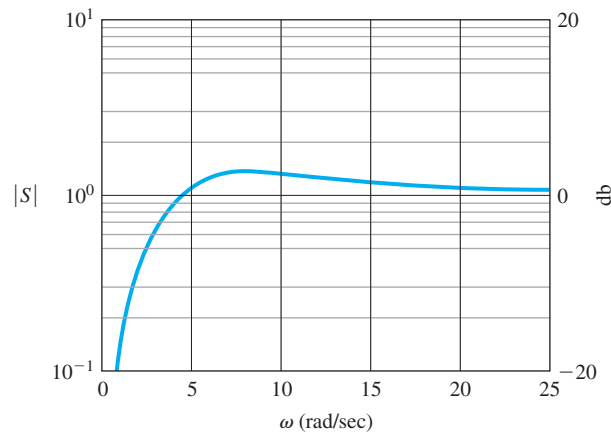
$$\mathcal{S} = \frac{s(s+1)(s+10)}{s^3 + 11s^2 + 60s + 100}, \quad (6.73)$$

and the plot shown in Fig. 6.84 is given by the MATLAB commands

```
numS = [1 11 10 0];
denS = [1 11 60 100];
sysS = tf(numS,denS);
[mag,ph,w] = bode(sysS);
semilogy(w,mag)
```

The largest value of  $\mathcal{S}$  is given by  $M = \max(\text{mag})$  and is 1.366, from which the vector margin is  $\text{VM} = 3.73$ .

**Figure 6.84**  
Sensitivity function for  
Example 6.25



## ▲ 6.10 Time Delay

The Laplace transform of a pure time delay is  $G_D(s) = e^{-sT_d}$  and was approximated by a rational function (Padé approximate) in our earlier discussion of root-locus analysis. Although this same approximation could be used with frequency-response methods, an exact analysis of the delay is possible with the Nyquist criterion and Bode plots.

Time-delay magnitude

The frequency response of the delay is given by the magnitude and phase of  $e^{-sT_d}|_{s=j\omega}$ . The magnitude is

$$|G_D(j\omega)| = |e^{-j\omega T_d}| = 1 \quad \text{for all } \omega. \quad (6.74)$$

Time-delay phase

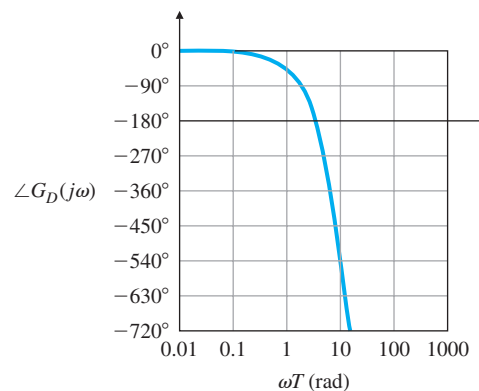
This result is expected, because a time delay merely shifts the signal in time and has no effect on its magnitude. The phase is

$$\angle G_D(j\omega) = -\omega T_d \quad (6.75)$$

in radians, and it grows increasingly negative in proportion to the frequency. This, too, is expected, because a fixed time delay  $T_d$  becomes a larger fraction or multiple of a sine wave as the period drops, due to increasing frequency. A plot of  $\angle G_D(j\omega)$  is drawn in Fig. 6.85. Note that the phase lag is greater than  $270^\circ$  for values of  $\omega T_d$  greater than about 5 rad. This trend implies that it would be virtually impossible to stabilize a system (or to achieve a positive PM) with a crossover frequency greater than  $\omega = 5/T_d$ , and it would be difficult for frequencies greater than  $\omega \cong 3/T_d$ . These characteristics essentially place a constraint on the achievable bandwidth of any system with a time delay. (See Problem 6.68 for an illustration of this constraint.)

The frequency domain concepts such as the Nyquist criterion apply directly to systems with pure time delay. This means that no approximations (Padé type or otherwise) are needed and the exact effect of time delay can be included in a Bode plot or in a Nyquist plot, as shown in the following example.

**Figure 6.85**  
Phase lag due to pure time delay



**EXAMPLE 6.26** *Nyquist Plot for System with Time Delay*

Consider the system with

$$KG(s) = \frac{Ke^{-T_d s}}{s},$$

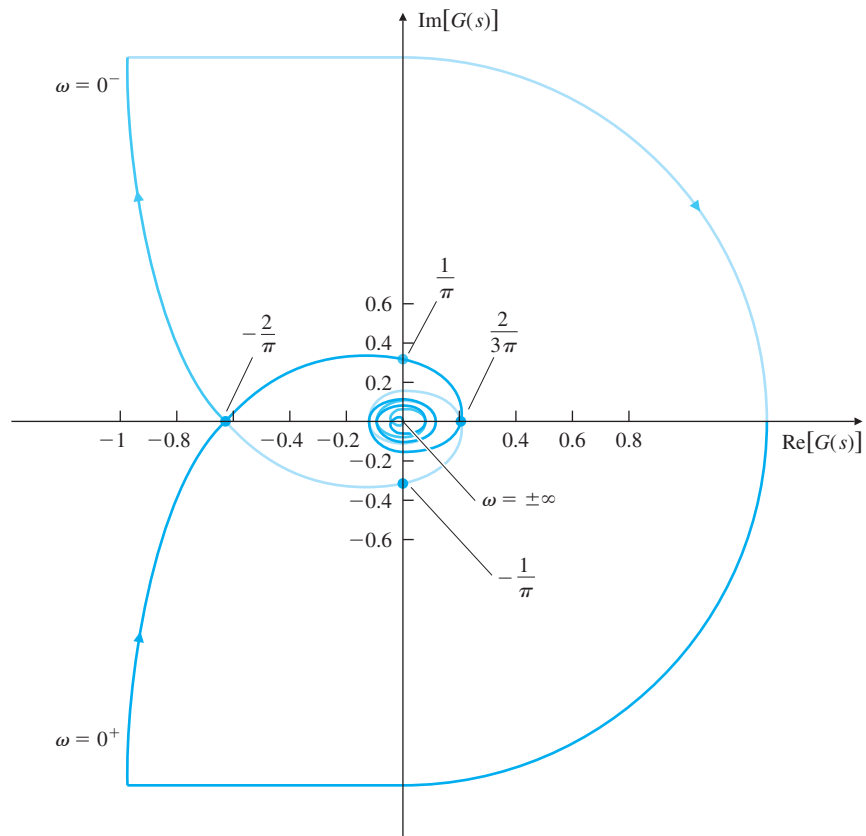
where  $T_d = 1$  sec. Determine the range of  $K$  for which the system is stable.

**Solution.** Because the Bode plotting rules do not apply for the phase of a time-delay term, we will use an analytical approach to determine the key features of the frequency response plot. As just discussed, the magnitude of the frequency response of the delay term is unity and its phase is  $-\omega$  radians. The magnitude of the frequency response of the pure integrator is  $1/\omega$ , with a constant phase of  $-\pi/2$ . Therefore,

$$\begin{aligned} G(j\omega) &= \frac{1}{\omega} e^{-j(\omega+\pi/2)} \\ &= \frac{1}{\omega} (-\sin \omega - j \cos \omega). \end{aligned} \quad (6.76)$$

Using Eq. (6.76) and substituting in different values of  $\omega$ , we can make the Nyquist plot, which is the spiral shown in Fig. 6.86.

**Figure 6.86**  
Nyquist plot for  
Example 6.26



Let us examine the shape of the spiral in more detail. We pick a Nyquist path with a small detour to the right of the origin. The effect of the pole at the origin is the large arc at infinity with a  $180^\circ$  sweep, as shown in Fig. 6.86. From Eq. (6.76), for small values of  $\omega > 0$ , the real part of the frequency response is close to  $-1$  because  $\sin \omega \cong \omega$  and  $\text{Re}[G(j\omega)] \cong -1$ . Similarly, for small values of  $\omega > 0$ ,  $\cos \omega \cong 1$  and  $\text{Im}[G(j\omega)] \cong -1/\omega$ —that is, very large negative values, as shown in Fig. 6.86. To obtain the crossover points on the real axis, we set the imaginary part equal to zero:

$$\frac{\cos \omega}{\omega} = 0. \quad (6.77)$$

The solution is then

$$\omega_0 = \frac{(2n+1)\pi}{2}, \quad n = 0, 1, 2, \dots \quad (6.78)$$

After substituting Eq. (6.78) back into Eq. (6.76), we find that

$$G(j\omega_0) = \frac{(-1)^n}{(2n+1)} \left( \frac{2}{\pi} \right), \quad n = 0, 1, 2, \dots$$

So the first crossover of the negative real axis is at  $-2/\pi$ , corresponding to  $n = 0$ . The first crossover of the positive real axis occurs for  $n = 1$  and is located at  $2/3\pi$ . As we can infer from Fig. 6.86, there are an infinite number of other crossings of the real axis. Finally, for  $\omega = \infty$ , the Nyquist plot converges to the origin. Note that the Nyquist plot for  $\omega < 0$  is the mirror image of the one for  $\omega > 0$ .

The number of poles in the RHP is zero ( $P = 0$ ), so for closed-loop stability, we need  $Z = N = 0$ . Therefore, the Nyquist plot cannot be allowed to encircle the  $-1/K$  point. It will not do so as long as

$$-\frac{1}{K} < -\frac{2}{\pi}, \quad (6.79)$$

which means that, for stability, we must have  $0 < K < \pi/2$ .

## SUMMARY

- The frequency-response **Bode plot** is a graph of the transfer function magnitude in logarithmic scale and the phase in linear scale versus frequency in logarithmic scale. For a transfer function  $G(s)$ ,

$$\begin{aligned} A &= |G(j\omega)| = |G(s)|_{s=j\omega} \\ &= \sqrt{\{\text{Re}[G(j\omega)]\}^2 + \{\text{Im}[G(j\omega)]\}^2}, \\ \phi &= \tan^{-1} \left[ \frac{\text{Im}[G(j\omega)]}{\text{Re}[G(j\omega)]} \right] = \angle G(j\omega). \end{aligned}$$



- For a transfer function in Bode form,

$$KG(\omega) = K_0 \frac{(j\omega\tau_1 + 1)(j\omega\tau_2 + 1) \cdots}{(j\omega\tau_a + 1)(j\omega\tau_b + 1) \cdots},$$

the Bode frequency response can be easily plotted by hand using the rules described in Section 6.1.1.

- Bode plots can be obtained using computer algorithms (bode in MATLAB), but hand-plotting skills are still extremely helpful.
- For a second-order system, the peak magnitude of the Bode plot is related to the damping by

$$|G(j\omega)| = \frac{1}{2\zeta} \quad \text{at } \omega = \omega_n.$$

- A method of determining the stability of a closed-loop system based on the frequency response of the system's open-loop transfer function is the **Nyquist stability criterion**. Rules for plotting the **Nyquist plot** are described in Section 6.3. The number of RHP closed-loop roots is given by

$$Z = N + P,$$

where

$N$  = number of clockwise encirclements of the  $-1$  point,

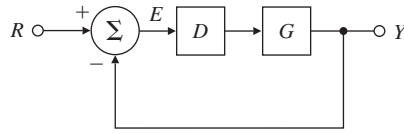
$P$  = number of open-loop poles in the RHP.

- The Nyquist plot may be obtained using computer algorithms (nyquist in MATLAB).
- The **gain margin** (GM) and **phase margin** (PM) can be determined directly by inspecting the open-loop Bode plot or the Nyquist plot. Also, use of MATLAB's margin function determines the values directly.
- For a standard second-order system, the PM is related to the closed-loop damping by Eq. (6.32),

$$\zeta \cong \frac{\text{PM}}{100}.$$

- The **bandwidth** of the system is a measure of speed of response. For control systems, it is defined as the frequency corresponding to 0.707 ( $-3$  db) in the closed-loop magnitude Bode plot and is approximately given by the crossover frequency  $\omega_c$ , which is the frequency at which the open-loop gain curve crosses magnitude 1.
- The **vector margin** is a single-parameter stability margin based on the closest point of the Nyquist plot to the critical point  $-1/K$ .

**Figure 6.87**  
Typical system



- For a stable minimum-phase system, Bode's gain–phase relationship uniquely relates the phase to the gain of the system and is approximated by Eq. (6.33),

$$\angle G(j\omega) \cong n \times 90^\circ,$$

where  $n$  is the slope of  $|G(j\omega)|$  in units of decade of amplitude per decade of frequency. The relationship shows that, in most cases, stability is ensured if the gain plot crosses the magnitude 1 line with a slope of  $-1$ .

- Experimental frequency-response data of the open-loop system can be used directly for analysis and design of a closed-loop control system with no analytical model.
- For the system shown in Fig. 6.87, the open-loop Bode plot is the frequency response of  $GD$ , and the closed-loop frequency response is obtained from  $\mathcal{T}(s) = GD/(1 + GD)$ .
- The frequency-response characteristics of several types of compensation have been described, and examples of design using these characteristics have been discussed. Design procedures were given for lead and lag compensators in Section 6.7. The examples in that section show the ease of selecting specific values of design variables, a result of using frequency-response methods. A summary was provided at the end of Section 6.7.5.
- **Lead compensation**, given by Eq. (6.38),

$$D(s) = \frac{T_s + 1}{\alpha T_s + 1}, \quad \alpha < 1,$$

is a high-pass filter and approximates PD control. It is used whenever substantial improvement in damping of the system is required. It tends to increase the speed of response of a system for a fixed low-frequency gain.

- **Lag compensation**, given by Eq. (6.51),

$$D(s) = \alpha \frac{T_s + 1}{\alpha T_s + 1}, \quad \alpha > 1, \quad (6.80)$$

is a low-pass filter and approximates PI control. It is usually used to increase the low-frequency gain of the system so as to improve steady-state response for fixed bandwidth. For a fixed low-frequency gain, it will decrease the speed of response of a system.

- ▲ • The **Nichols plot** is an alternate representation of the frequency response as a plot of gain versus phase and is parameterized as a function of frequency.
- ▲ • Tracking-error reduction and disturbance rejection can be specified in terms of the low-frequency gain of the Bode plot. Sensor-noise rejection can be specified in terms of high-frequency attenuation of the Bode plot (see Fig. 6.72).
- ▲ • Time delay can be analyzed exactly in a Bode plot or a Nyquist plot.

### End-of-Chapter Questions

1. Why did Bode suggest plotting the magnitude of a frequency response on log-log coordinates?
2. Define a decibel.
3. What is the transfer function magnitude if the gain is listed as 14 db?
4. Define gain crossover.
5. Define phase crossover.
6. Define phase margin, PM.
7. Define gain margin, GM.
8. What Bode plot characteristic is the best indicator of the closed-loop step response overshoot?
9. What Bode plot characteristic is the best indicator of the closed-loop step response rise time?
10. What is the principal effect of a lead compensation on Bode plot performance measures?
11. What is the principal effect of a lag compensation on Bode plot performance measures?
12. How do you find the  $K_v$  of a type 1 system from its Bode plot?
13. Why do we need to know beforehand the number of open-loop unstable poles in order to tell stability from the Nyquist plot?
14. What is the main advantage in control design of counting the encirclements of  $-\frac{1}{K}$  of  $D(j\omega)G(j\omega)$  rather than encirclements of  $-1$  of  $KD(j\omega)G(j\omega)$ ?
15. Define a conditionally stable feedback system. How can you identify one on a Bode plot?
- ▲ 16. A certain control system is required to follow sinusoids, which may be any frequency in the range  $0 \leq \omega \leq 450$  rad/sec and have amplitudes up to 5 units, with (sinusoidal) steady-state error to be never more than 0.01. Sketch (or describe) the corresponding performance function  $W_1(\omega)$ .

## Problems

## Problems for Section 6.1: Frequency Response

- 6.1. (a) Show that  $\alpha_0$  in Eq. (6.2), with  $A = U_o$  and  $\omega_o = \omega$ , is

$$\alpha_0 = \left[ G(s) \frac{U_0 \omega}{s - j\omega} \right] \Big|_{s=-j\omega} = -U_0 G(-j\omega) \frac{1}{2j}$$

and

$$\alpha_0^* = \left[ G(s) \frac{U_0 \omega}{s + j\omega} \right] \Big|_{s=+j\omega} = U_0 G(j\omega) \frac{1}{2j}.$$

- (b) By assuming the output can be written as

$$y(t) = \alpha_0 e^{-j\omega t} + \alpha_0^* e^{j\omega t},$$

derive Eqs. (6.4)–(6.6).

- 6.2. (a) Calculate the magnitude and phase of

$$G(s) = \frac{1}{s + 10}$$

by hand for  $\omega = 1, 2, 5, 10, 20, 50$ , and  $100$  rad/sec.

- (b) Sketch the asymptotes for  $G(s)$  according to the Bode plot rules, and compare these with your computed results from part (a).

- 6.3. Sketch the asymptotes of the Bode plot magnitude and phase for each of the following open-loop transfer functions. After completing the hand sketches, verify your result using MATLAB. Turn in your hand sketches and the MATLAB results on the same scales.

(a)  $L(s) = \frac{2000}{s(s + 200)}$

(b)  $L(s) = \frac{100}{s(0.1s + 1)(0.5s + 1)}$

(c)  $L(s) = \frac{1}{s(s + 1)(0.02s + 1)}$

(d)  $L(s) = \frac{1}{(s + 1)^2(s^2 + 2s + 4)}$

(e)  $L(s) = \frac{10(s + 4)}{s(s + 1)(s^2 + 2s + 5)}$

(f)  $L(s) = \frac{1000(s + 0.1)}{s(s + 1)(s^2 + 8s + 64)}$

(g)  $L(s) = \frac{(s + 5)(s + 3)}{s(s + 1)(s^2 + s + 4)}$

(h)  $L(s) = \frac{4s(s + 10)}{(s + 100)(4s^2 + 5s + 4)}$

(i)  $L(s) = \frac{s}{(s + 1)(s + 10)(s^2 + 2s + 2500)}$

- 6.4. Real poles and zeros.** Sketch the asymptotes of the Bode plot magnitude and phase for each of the listed open-loop transfer functions. After completing the hand sketches, verify your result using MATLAB. Turn in your hand sketches and the MATLAB results on the same scales.

$$(a) L(s) = \frac{1}{s(s+1)(s+5)(s+10)}$$

$$(b) L(s) = \frac{(s+2)}{s(s+1)(s+5)(s+10)}$$

$$(c) L(s) = \frac{(s+2)(s+6)}{s(s+1)(s+5)(s+10)}$$

$$(d) L(s) = \frac{(s+2)(s+4)}{s(s+1)(s+5)(s+10)}$$

- 6.5. Complex poles and zeros.** Sketch the asymptotes of the Bode plot magnitude and phase for each of the listed open-loop transfer functions, and approximate the transition at the second-order break point, based on the value of the damping ratio. After completing the hand sketches, verify your result using MATLAB. Turn in your hand sketches, and the MATLAB results on the same scales.

$$(a) L(s) = \frac{1}{s^2 + 3s + 10}$$

$$(b) L(s) = \frac{1}{s(s^2 + 3s + 10)}$$

$$(c) L(s) = \frac{(s^2 + 2s + 8)}{s(s^2 + 2s + 10)}$$

$$(d) L(s) = \frac{(s^2 + 2s + 12)}{s(s^2 + 2s + 10)}$$

$$(e) L(s) = \frac{(s^2 + 1)}{s(s^2 + 4)}$$

$$(f) L(s) = \frac{(s^2 + 4)}{s(s^2 + 1)}$$

- 6.6. Multiple poles at the origin.** Sketch the asymptotes of the Bode plot magnitude and phase for each of the listed open-loop transfer functions. After completing the hand sketches, verify your result with MATLAB. Turn in your hand sketches and the MATLAB results on the same scales.

$$(a) L(s) = \frac{1}{s^2(s+8)}$$

$$(b) L(s) = \frac{1}{s^3(s+8)}$$

$$(c) L(s) = \frac{1}{s^4(s+8)}$$

$$(d) L(s) = \frac{(s+3)}{s^2(s+8)}$$

$$(e) L(s) = \frac{(s+3)}{s^3(s+4)}$$

$$(f) L(s) = \frac{(s+1)^2}{s^3(s+4)}$$

$$(g) L(s) = \frac{(s+1)^2}{s^3(s+10)^2}$$

- 6.7. Mixed real and complex poles.** Sketch the asymptotes of the Bode plot magnitude and phase for each of the listed open-loop transfer functions. Embellish the asymptote plots with a rough estimate of the transitions for each break point. After completing the hand sketches, verify your result with MATLAB. Turn in your hand sketches and the MATLAB results on the same scales.

$$(a) L(s) = \frac{(s+2)}{s(s+10)(s^2+2s+2)}$$

$$(b) L(s) = \frac{(s+2)}{s^2(s+10)(s^2+6s+25)}$$

$$(c) L(s) = \frac{(s+2)^2}{s^2(s+10)(s^2+6s+25)}$$

$$(d) L(s) = \frac{(s+2)(s^2+4s+68)}{s^2(s+10)(s^2+4s+85)}$$

$$(e) L(s) = \frac{[(s+1)^2+1]}{s^2(s+2)(s+3)}$$

- 6.8. Right half-plane poles and zeros.** Sketch the asymptotes of the Bode plot magnitude and phase for each of the listed open-loop transfer functions. Make sure that the phase asymptotes properly take the RHP singularity into account by sketching the complex plane to see how the  $\angle L(s)$  changes as  $s$  goes from 0 to  $+j\infty$ . After completing the hand sketches, verify your result with MATLAB. Turn in your hand sketches and the MATLAB results on the same scales.

$$(a) L(s) = \frac{s+2}{s+10} \frac{1}{s^2-1};$$
 The model for a case of magnetic levitation with lead compensation.

$$(b) L(s) = \frac{s+2}{s(s+10)} \frac{1}{(s^2-1)};$$
 The magnetic levitation system with integral control and lead compensation.

$$(c) L(s) = \frac{s-1}{s^2}$$

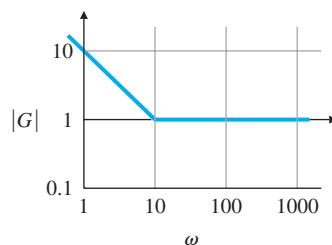
$$(d) L(s) = \frac{s^2+2s+1}{s(s+20)^2(s^2-2s+2)}$$

$$(e) L(s) = \frac{(s+2)}{s(s-1)(s+6)^2}$$

$$(f) L(s) = \frac{1}{(s-1)[(s+2)^2+3]}$$

- 6.9.** A certain system is represented by the asymptotic Bode diagram shown in Fig. 6.88. Find and sketch the response of this system to a unit-step input (assuming zero initial conditions).

**Figure 6.88**  
Magnitude portion of Bode plot for Problem 6.9



- 6.10.** Prove that a magnitude slope of  $-1$  in a Bode plot corresponds to  $-20$  db per decade or  $-6$  db per octave.
- 6.11.** A normalized second-order system with a damping ratio  $\zeta = 0.5$  and an additional zero is given by

$$G(s) = \frac{s/a + 1}{s^2 + s + 1}.$$

Use MATLAB to compare the  $M_p$  from the step response of the system for  $a = 0.01, 0.1, 1, 10,$  and  $100$  with the  $M_r$  from the frequency response of each case. Is there a correlation between  $M_r$  and  $M_p$ ?

- 6.12.** A normalized second-order system with  $\zeta = 0.5$  and an additional pole is given by

$$G(s) = \frac{1}{[(s/p) + 1](s^2 + s + 1)}.$$

Draw Bode plots with  $p = 0.01, 0.1, 1, 10,$  and  $100$ . What conclusions can you draw about the effect of an extra pole on the bandwidth compared with the bandwidth for the second-order system with no extra pole?

- 6.13.** For the closed-loop transfer function

$$T(s) = \frac{\omega_n^2}{s^2 + 2\zeta\omega_n s + \omega_n^2},$$

derive the following expression for the bandwidth  $\omega_{BW}$  of  $T(s)$  in terms of  $\omega_n$  and  $\zeta$ :

$$\omega_{BW} = \omega_n \sqrt{1 - 2\zeta^2 + \sqrt{2 + 4\zeta^4 - 4\zeta^2}}.$$

Assuming that  $\omega_n = 1$ , plot  $\omega_{BW}$  for  $0 \leq \zeta \leq 1$ .

- 6.14.** Consider the system whose transfer function is

$$G(s) = \frac{A_0\omega_0 s}{Qs^2 + \omega_0 s + \omega_0^2 Q}.$$

This is a model of a tuned circuit with *quality factor*  $Q$ .

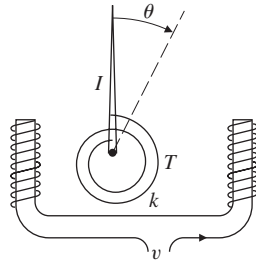
- (a) Compute the magnitude and phase of the transfer function analytically, and plot them for  $Q = 0.5, 1, 2,$  and  $5$  as a function of the normalized frequency  $\omega/\omega_0$ .
- (b) Define the bandwidth as the distance between the frequencies on either side of  $\omega_0$  where the magnitude drops to 3 db below its value at  $\omega_0$ , and show that the bandwidth is given by

$$\text{BW} = \frac{1}{2\pi} \left( \frac{\omega_0}{Q} \right).$$

- (c) What is the relation between  $Q$  and  $\zeta$ ?

- 6.15. A DC voltmeter schematic is shown in Fig. 6.89. The pointer is damped so that its maximum overshoot to a step input is 10%.

Figure 6.89  
Voltmeter schematic



$$\begin{aligned}
 I &= 40 \times 10^{-6} \text{ kg} \cdot \text{m}^2 \\
 k &= 4 \times 10^{-6} \text{ kg} \cdot \text{m}^2/\text{sec}^2 \\
 T &= \text{input torque} = K_m v \\
 v &= \text{input voltage} \\
 K_m &= 1 \text{ N} \cdot \text{m}/\text{V}
 \end{aligned}$$

- What is the undamped natural frequency of the system?
- What is the damped natural frequency of the system?
- Plot the frequency response using MATLAB to determine what input frequency will produce the largest magnitude output?
- Suppose this meter is now used to measure a 1-V AC input with a frequency of 2 rad/sec. What amplitude will the meter indicate after initial transients have died out? What is the phase lag of the output with respect to the input? Use a Bode plot analysis to answer these questions. Use the `lsim` command in MATLAB to verify your answer in part (d).

#### Problems for Section 6.2: Neutral Stability

- 6.16. Determine the range of  $K$  for which each of the listed systems is stable by making a Bode plot for  $K = 1$  and imagining the magnitude plot sliding up or down until instability results. Verify your answers by using a very rough sketch of a root-locus plot.

(a)  $KG(s) = \frac{K(s+2)}{s+20}$

(b)  $KG(s) = \frac{K}{(s+10)(s+1)^2}$

(c)  $KG(s) = \frac{K(s+10)(s+1)}{(s+100)(s+5)^3}$



- 6.17.** Determine the range of  $K$  for which each of the listed systems is stable by making a Bode plot for  $K = 1$  and imagining the magnitude plot sliding up or down until instability results. Verify your answers by using a very rough sketch of a root-locus plot.

(a)  $KG(s) = \frac{K(s+1)}{s(s+5)}$

(b)  $KG(s) = \frac{K(s+1)}{s^2(s+10)}$

(c)  $KG(s) = \frac{K}{(s+2)(s^2+9)}$

(d)  $KG(s) = \frac{K(s+1)^2}{s^3(s+10)}$

#### Problems for Section 6.3: The Nyquist Stability Criterion

- 6.18.** (a) Sketch the Nyquist plot for an open-loop system with transfer function  $1/s^2$ ; that is, sketch

$$\left. \frac{1}{s^2} \right|_{s=C_1},$$

where  $C_1$  is a contour enclosing the entire RHP, as shown in Fig. 6.17. (*Hint:* Assume  $C_1$  takes a small detour around the poles at  $s = 0$ , as shown in Fig. 6.27.)

- (b) Repeat part (a) for an open-loop system whose transfer function is  $G(s) = 1/(s^2 + \omega_0^2)$ .
- 6.19.** Sketch the Nyquist plot based on the Bode plots for each of the following systems, and then compare your result with that obtained by using the MATLAB command `nyquist`:
- (a)  $KG(s) = \frac{K(s+2)}{s+10}$
- (b)  $KG(s) = \frac{K}{(s+10)(s+2)^2}$
- (c)  $KG(s) = \frac{K(s+10)(s+1)}{(s+100)(s+2)^3}$
- (d) Using your plots, estimate the range of  $K$  for which each system is stable, and qualitatively verify your result by using a rough sketch of a root-locus plot.

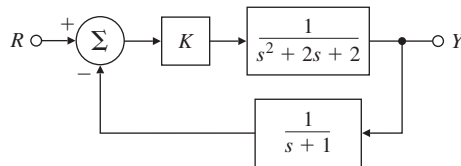
6.20. Draw a Nyquist plot for

$$KG(s) = \frac{K(s+1)}{s(s+3)}, \quad (6.81)$$

choosing the contour to be to the right of the singularity on the  $j\omega$ -axis. Next, using the Nyquist criterion, determine the range of  $K$  for which the system is stable. Then redo the Nyquist plot, this time choosing the contour to be to the left of the singularity on the imaginary axis. Again, using the Nyquist criterion, check the range of  $K$  for which the system is stable. Are the answers the same? Should they be?

6.21. Draw the Nyquist plot for the system in Fig. 6.90. Using the Nyquist stability criterion, determine the range of  $K$  for which the system is stable. Consider both positive and negative values of  $K$ .

**Figure 6.90**  
Control system for  
Problem 6.21



6.22. (a) For  $\omega = 0.1$  to 100 rad/sec, sketch the phase of the minimum-phase system

$$G(s) = \frac{s+1}{s+10} \Big|_{s=j\omega}$$

and the nonminimum-phase system

$$G(s) = -\frac{s-1}{s+10} \Big|_{s=j\omega},$$

noting that  $\angle(j\omega - 1)$  decreases with  $\omega$  rather than increasing.

- (b) Does a RHP zero affect the relationship between the  $-1$  encirclements on a polar plot and the number of unstable closed-loop roots in Eq. (6.28)?
- (c) Sketch the phase of the following unstable system for  $\omega = 0.1$  to 100 rad/sec:

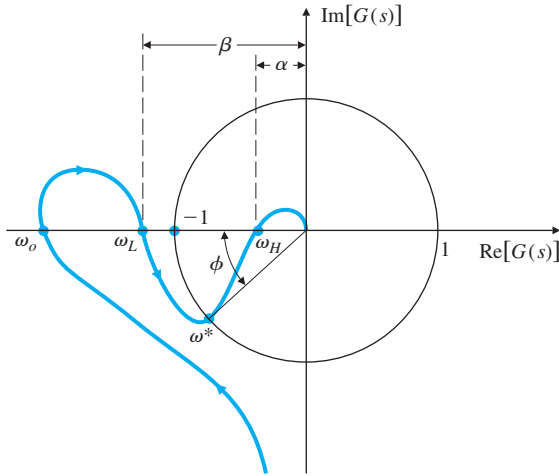
$$G(s) = \frac{s+1}{s-10} \Big|_{s=j\omega}.$$

- (d) Check the stability of the systems in (a) and (c) using the Nyquist criterion on  $KG(s)$ . Determine the range of  $K$  for which the closed-loop system is stable, and check your results qualitatively by using a rough root-locus sketch.

Problems for Section 6.4: Stability Margins

6.23. The Nyquist plot for some actual control systems resembles the one shown in Fig. 6.91. What are the gain and phase margin(s) for the system of Fig. 6.91, given that  $\alpha = 0.4$ ,  $\beta = 1.3$ , and  $\phi = 40^\circ$ . Describe what happens to the stability of the system as the gain goes from zero to a very large value. Sketch what the corresponding root locus must look like for such a system. Also, sketch what the corresponding Bode plots would look like for the system.

Figure 6.91  
Nyquist plot for  
Problem 6.23



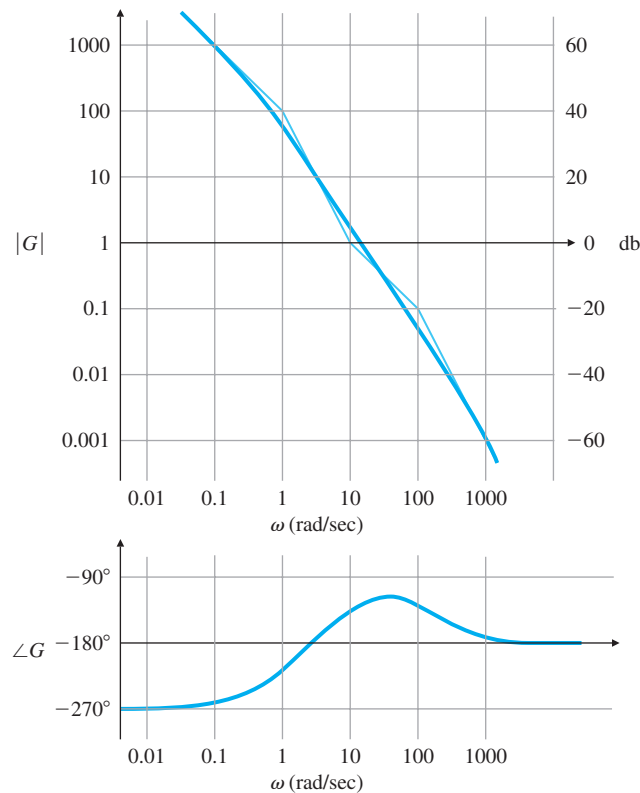
6.24. The Bode plot for

$$G(s) = \frac{100[(s/10) + 1]}{s[(s/1) - 1][(s/100) + 1]}$$

is shown in Fig. 6.92.

- (a) Why does the phase start at  $270^\circ$  at the low frequencies?
- (b) Sketch the Nyquist plot for  $G(s)$ .
- (c) Is the closed-loop system shown in Fig. 6.92 stable?
- (d) Will the system be stable if the gain is lowered by a factor of 100? Make a rough sketch of a root locus for the system, and qualitatively confirm your answer.

**Figure 6.92**  
Bode plot for Problem 6.24

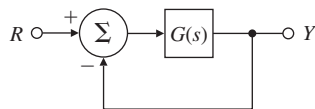


**6.25.** Suppose that in Fig. 6.93,

$$G(s) = \frac{25(s+1)}{s(s+2)(s^2+2s+16)}.$$

Use MATLAB's margin to calculate the PM and GM for  $G(s)$  and, on the basis of the Bode plots, conclude which margin would provide more useful information to the control designer for this system.

**Figure 6.93**  
Control system for  
Problem 6.25

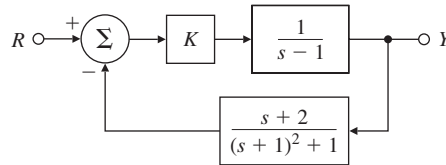


**6.26.** Consider the system given in Fig. 6.94.

- (a) Use MATLAB to obtain Bode plots for  $K = 1$ , and use the plots to estimate the range of  $K$  for which the system will be stable.
- (b) Verify the stable range of  $K$  by using margin to determine PM for selected values of  $K$ .

- (c) Use `rlocus` and `rlocfind` to determine the values of  $K$  at the stability boundaries.
- (d) Sketch the Nyquist plot of the system, and use it to verify the number of unstable roots for the unstable ranges of  $K$ .
- (e) Using Routh's criterion, determine the ranges of  $K$  for closed-loop stability of this system.

**Figure 6.94**  
Control system for  
Problem 6.26



**6.27.** Suppose that in Fig. 6.93,

$$G(s) = \frac{3.2(s+1)}{s(s+2)(s^2+0.2s+16)}.$$

Use MATLAB's `margin` to calculate the PM and GM for  $G(s)$ , and comment on whether you think this system will have well-damped closed-loop roots.

- 6.28.** For a given system, show that the ultimate period  $P_u$  and the corresponding ultimate gain  $K_u$  for the Zeigler–Nichols method can be found by using the following:
- (a) Nyquist diagram
  - (b) Bode plot
  - (c) Root locus
- 6.29.** If a system has the open-loop transfer function

$$G(s) = \frac{\omega_n^2}{s(s+2\zeta\omega_n)}$$

with unity feedback, then the closed-loop transfer function is given by

$$T(s) = \frac{\omega_n^2}{s^2 + 2\zeta\omega_n s + \omega_n^2}.$$

Verify the values of the PM shown in Fig. 6.36 for  $\zeta = 0.1, 0.4,$  and  $0.7$ .

**6.30.** Consider the unity feedback system with the open-loop transfer function

$$G(s) = \frac{K}{s(s+1)[(s^2/25) + 0.4(s/5) + 1]}.$$

- (a) Use MATLAB to draw the Bode plots for  $G(j\omega)$ , assuming that  $K = 1$ .
- (b) What gain  $K$  is required for a PM of  $45^\circ$ ? What is the GM for this value of  $K$ ?
- (c) What is  $K_v$  when the gain  $K$  is set for PM =  $45^\circ$ ?
- (d) Create a root locus with respect to  $K$ , and indicate the roots for a PM of  $45^\circ$ .

- 6.31. For the system depicted in Fig. 6.95(a), the transfer-function blocks are defined by

$$G(s) = \frac{1}{(s+2)^2(s+4)} \quad \text{and} \quad H(s) = \frac{1}{s+1}.$$

- Using rlocus and rlocfind, determine the value of  $K$  at the stability boundary.
- Using rlocus and rlocfind, determine the value of  $K$  that will produce roots with damping corresponding to  $\zeta = 0.707$ .
- What is the gain margin of the system if the gain is set to the value determined in part (b)? Answer this question *without* using any frequency response methods.
- Create the Bode plots for the system, and determine the gain margin that results for  $\text{PM} = 65^\circ$ . What damping ratio would you expect for this PM?
- Sketch a root locus for the system shown in Fig. 6.95(b). How does it differ from the one in part (a)?
- For the systems in Figs. 6.95(a) and (b), how does the transfer function  $Y_2(s)/R(s)$  differ from  $Y_1(s)/R(s)$ ? Would you expect the step response to  $r(t)$  to be different for the two cases?

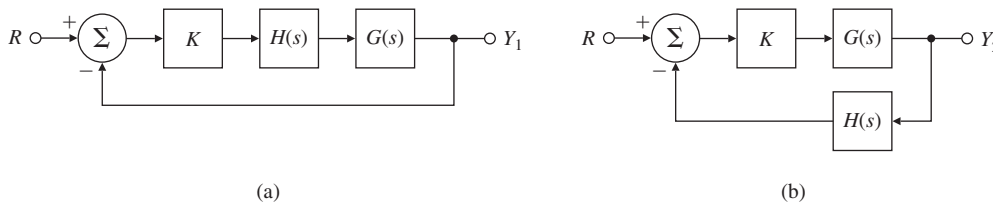
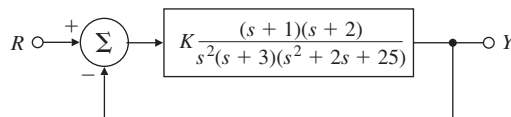


Figure 6.95 Block diagram for Problem 6.31: (a) unity feedback; (b)  $H(s)$  in feedback

- 6.32. For the system shown in Fig. 6.96, use Bode and root-locus plots to determine the gain and frequency at which instability occurs. What gain (or gains) gives a PM of  $20^\circ$ ? What is the gain margin when  $\text{PM} = 20^\circ$ ?

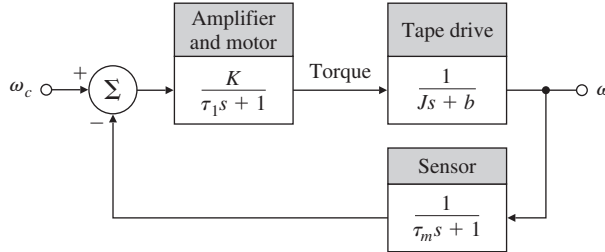
Figure 6.96  
Control system for  
Problem 6.32



- 6.33. A magnetic tape-drive speed-control system is shown in Fig. 6.97. The speed sensor is slow enough that its dynamics must be included. The speed-measurement time constant is  $\tau_m = 0.5$  sec; the reel time constant is  $\tau_r = J/b = 4$  sec, where  $b$  = the output shaft damping constant = 1 N·m·sec; and the motor time constant is  $\tau_1 = 1$  sec.

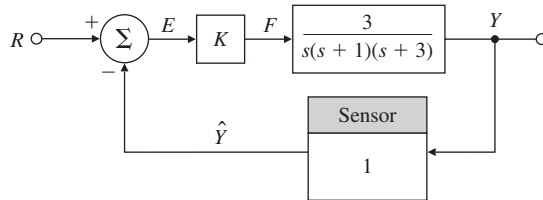
- (a) Determine the gain  $K$  required to keep the steady-state speed error to less than 7% of the reference-speed setting.
- (b) Determine the gain and phase margins of the system. Is this a good system design?

**Figure 6.97**  
Magnetic tape-drive speed control



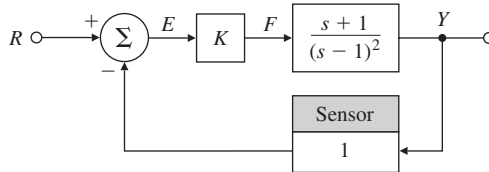
- 6.34.** For the system in Fig. 6.98, determine the Nyquist plot and apply the Nyquist criterion
- (a) to determine the range of values of  $K$  (positive and negative) for which the system will be stable, and
  - (b) to determine the number of roots in the RHP for those values of  $K$  for which the system is unstable. Check your answer by using a rough root-locus sketch.

**Figure 6.98**  
Control system for Problems 6.34, 6.61, and 6.62



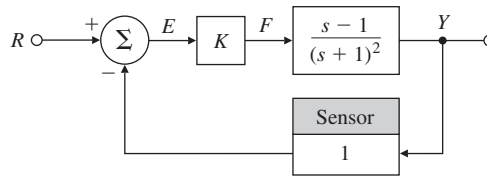
- 6.35.** For the system shown in Fig. 6.99, determine the Nyquist plot and apply the Nyquist criterion
- (a) to determine the range of values of  $K$  (positive and negative) for which the system will be stable, and
  - (b) to determine the number of roots in the RHP for those values of  $K$  for which the system is unstable. Check your answer by using a rough root-locus sketch.

**Figure 6.99**  
Control system for Problem 6.35



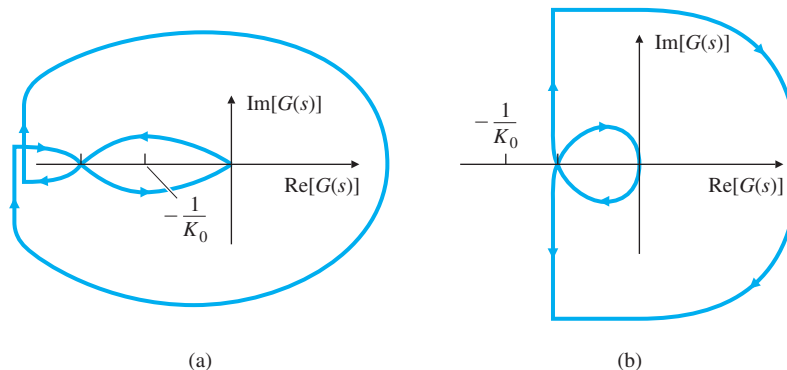
- 6.36.** For the system shown in Fig. 6.100, determine the Nyquist plot and apply the Nyquist criterion
- (a) to determine the range of values of  $K$  (positive and negative) for which the system will be stable, and
  - (b) to determine the number of roots in the RHP for those values of  $K$  for which the system is unstable. Check your answer by using a rough root-locus sketch.

**Figure 6.100**  
Control system for  
Problem 6.36



- 6.37.** The Nyquist diagrams for two stable, open-loop systems are sketched in Fig. 6.101. The proposed operating gain is indicated as  $K_0$ , and arrows indicate increasing frequency. In each case give a rough estimate of the following quantities for the closed-loop (unity feedback) system:
- Phase margin
  - Damping ratio
  - Range of gain for stability (if any)
  - System type (0, 1, or 2)

**Figure 6.101**  
Nyquist plots for  
Problem 6.37



- 6.38.** The steering dynamics of a ship are represented by the transfer function

$$\frac{V(s)}{\delta_r(s)} = G(s) = \frac{K[-(s/0.142) + 1]}{s(s/0.325 + 1)(s/0.0362 + 1)},$$

where  $v$  is the ship's lateral velocity in meters per second, and  $\delta_r$  is the rudder angle in radians.

- Use the MATLAB command `bode` to plot the log magnitude and phase of  $G(j\omega)$  for  $K = 0.2$ .
- On your plot, indicate the crossover frequency, PM, and GM.
- Is the ship steering system stable with  $K = 0.2$ ?
- What value of  $K$  would yield a PM of  $30^\circ$  and what would the crossover frequency be?



6.39. For the open-loop system

$$KG(s) = \frac{K(s+1)}{s^2(s+10)^2},$$

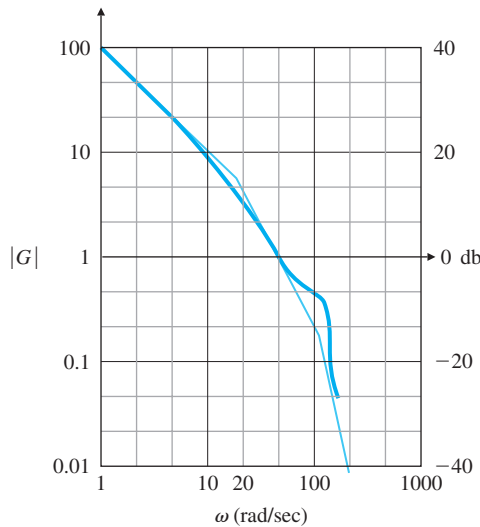
determine the value for  $K$  at the stability boundary and the values of  $K$  at the points where  $PM = 30^\circ$ .

Problems for Section 6.5: Bode's Gain-Phase Relationship

6.40. The frequency response of a plant in a unity feedback configuration is sketched in Fig. 6.102. Assume that the plant is open-loop stable and minimum phase.

- (a) What is the velocity constant  $K_v$  for the system as drawn?
- (b) What is the damping ratio of the complex poles at  $\omega = 100$ ?
- (c) Approximately what is the system error in tracking (following) a sinusoidal input of  $\omega = 3$  rad/sec?
- (d) What is the PM of the system as drawn? (Estimate to within  $\pm 10^\circ$ .)

Figure 6.102  
Magnitude frequency  
response for Problem 6.40



6.41. For the system

$$G(s) = \frac{100(s/a + 1)}{s(s+1)(s/b + 1)},$$

where  $b = 10a$ , find the approximate value of  $a$  that will yield the best PM by sketching only candidate values of the frequency response magnitude.

Problem for Section 6.6: Closed-Loop Frequency Response

6.42. For the open-loop system

$$KG(s) = \frac{K(s+1)}{s^2(s+10)^2},$$

determine the value for  $K$  that will yield  $PM \geq 30^\circ$  and the maximum possible closed-loop bandwidth. Use MATLAB to find the bandwidth.

## Problems for Section 6.7: Compensation Design

**6.43.** For the lead compensator

$$D(s) = \frac{Ts + 1}{\alpha Ts + 1},$$

where  $\alpha < 1$ ,

(a) Show that the phase of the lead compensator is given by

$$\phi = \tan^{-1}(T\omega) - \tan^{-1}(\alpha T\omega).$$

(b) Show that the frequency where the phase is maximum is given by

$$\omega_{\max} = \frac{1}{T\sqrt{\alpha}}$$

and that the maximum phase corresponds to

$$\sin \phi_{\max} = \frac{1 - \alpha}{1 + \alpha}.$$

(c) Rewrite your expression for  $\omega_{\max}$  to show that the maximum-phase frequency occurs at the geometric mean of the two corner frequencies on a logarithmic scale:

$$\log \omega_{\max} = \frac{1}{2} \left( \log \frac{1}{T} + \log \frac{1}{\alpha T} \right).$$

(d) To derive the same results in terms of the pole-zero locations, rewrite  $D(s)$  as

$$D(s) = \frac{s + z}{s + p},$$

and then show that the phase is given by

$$\phi = \tan^{-1} \left( \frac{\omega}{|z|} \right) - \tan^{-1} \left( \frac{\omega}{|p|} \right),$$

such that

$$\omega_{\max} = \sqrt{|z||p|}.$$

Hence the frequency at which the phase is maximum is the square root of the product of the pole and zero locations.

**6.44.** For the third-order servo system

$$G(s) = \frac{50,000}{s(s + 10)(s + 50)},$$

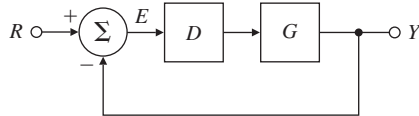
use Bode plot sketches to design a lead compensator so that  $\text{PM} \geq 50^\circ$  and  $\omega_{\text{BW}} \geq 20$  rad/sec. Then verify and refine your design by using MATLAB.

- 6.45. For the system shown in Fig. 6.103, suppose that

$$G(s) = \frac{5}{s(s+1)(s/5+1)}.$$

Use Bode plot sketches to design a lead compensation  $D(s)$  with unity DC gain so that  $PM \geq 40^\circ$ . Then verify and refine your design by using MATLAB. What is the approximate bandwidth of the system?

**Figure 6.103**  
Control system for  
Problem 6.45



ePIV

- 6.46. Derive the transfer function from  $T_d$  to  $\theta$  for the system in Fig. 6.68. Then apply the Final Value Theorem (assuming  $T_d = \text{constant}$ ) to determine whether  $\theta(\infty)$  is nonzero for the following two cases:
- When  $D(s)$  has no integral term:  $\lim_{s \rightarrow 0} D(s) = \text{constant}$ ;
  - When  $D(s)$  has an integral term:

$$D(s) = \frac{D'(s)}{s},$$

In this case,  $\lim_{s \rightarrow 0} D'(s) = \text{constant}$ .

- 6.47. The inverted pendulum has a transfer function given by Eq. (2.91), which is similar to

$$G(s) = \frac{1}{s^2 - 1}.$$

- Use Bode plot sketches to design a lead compensator to achieve a PM of  $30^\circ$ . Then verify and refine your design by using MATLAB.
  - Sketch a root locus and correlate it with the Bode plot of the system.
  - Could you obtain the frequency response of this system experimentally?
- 6.48. The open-loop transfer function of a unity feedback system is

$$G(s) = \frac{K}{s(s/5+1)(s/50+1)}.$$

- Use Bode plot sketches to design a lag compensator for  $G(s)$  so that the closed-loop system satisfies the following specifications:
  - The steady-state error to a unit-ramp reference input is less than 0.01.
  - $PM \geq 40^\circ$
- Verify and refine your design by using MATLAB.

6.49. The open-loop transfer function of a unity feedback system is

$$G(s) = \frac{K}{s(s/5 + 1)(s/200 + 1)}.$$

- (a) Use Bode plot sketches to design a lead compensator for  $G(s)$  so that the closed-loop system satisfies the following specifications:
- i. The steady-state error to a unit-ramp reference input is less than 0.01.
  - ii. For the dominant closed-loop poles, the damping ratio  $\zeta \geq 0.4$ .
- (b) Verify and refine your design using MATLAB, including a direct computation of the damping of the dominant closed-loop poles.

6.50. A DC motor with negligible armature inductance is to be used in a position control system. Its open-loop transfer function is given by

$$G(s) = \frac{50}{s(s/5 + 1)}.$$

- (a) Use Bode plot sketches to design a compensator for the motor so that the closed-loop system satisfies the following specifications:
- i. The steady-state error to a unit-ramp input is less than 1/200.
  - ii. The unit-step response has an overshoot of less than 20%.
  - iii. The bandwidth of the compensated system is no less than that of the uncompensated system.
- (b) Verify and/or refine your design using MATLAB, including a direct computation of the step-response overshoot.

6.51. The open-loop transfer function of a unity-feedback system is

$$G(s) = \frac{K}{s(1 + s/5)(1 + s/20)}.$$

- (a) Sketch the system block diagram, including input reference commands and sensor noise.
- (b) Use Bode plot sketches to design a compensator for  $G(s)$  so that the closed-loop system satisfies the following specifications:
- i. The steady-state error to a unit-ramp input is less than 0.01.
  - ii.  $PM \geq 45^\circ$
  - iii. The steady-state error for sinusoidal inputs with  $\omega < 0.2$  rad/sec is less than 1/250.
  - iv. Noise components introduced with the sensor signal at frequencies greater than 200 rad/sec are to be attenuated at the output by at least a factor of 100.
- (c) Verify and/or refine your design using MATLAB, including a computation of the closed-loop frequency response to verify (iv).

6.52. Consider a type I unity-feedback system with

$$G(s) = \frac{K}{s(s+1)}.$$

Use Bode plot sketches to design a lead compensator so that  $K_v = 20 \text{ sec}^{-1}$  and  $\text{PM} > 40^\circ$ . Use MATLAB to verify and/or refine your design so that it meets the specifications.

6.53. Consider a satellite attitude-control system with the transfer function

$$G(s) = \frac{0.05(s+25)}{s^2(s^2+0.1s+4)}.$$

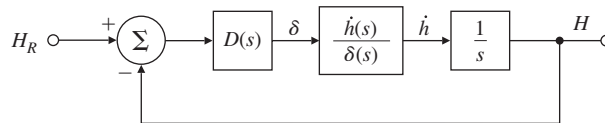
Amplitude-stabilize the system using lead compensation so that  $\text{GM} \geq 2$  (6 db), and  $\text{PM} \geq 45^\circ$ , keeping the bandwidth as high as possible with a single lead.

6.54. In one mode of operation, the autopilot of a jet transport is used to control altitude. For the purpose of designing the altitude portion of the autopilot loop, only the long-period airplane dynamics are important. The linearized relationship between altitude and elevator angle for the long-period dynamics is

$$G(s) = \frac{h(s)}{\delta(s)} = \frac{20(s+0.01)}{s(s^2+0.01s+0.0025)} \frac{\text{ft/sec}}{\text{deg}}.$$

The autopilot receives from the altimeter an electrical signal proportional to altitude. This signal is compared with a command signal (proportional to the altitude selected by the pilot), and the difference provides an error signal. The error signal is processed through compensation, and the result is used to command the elevator actuators. A block diagram of this system is shown in Fig. 6.104. You have been given the task of designing the compensation. Begin by considering a proportional control law  $D(s) = K$ .

**Figure 6.104**  
Control system for  
Problem 6.54



- Use MATLAB to draw a Bode plot of the open-loop system for  $D(s) = K = 1$ .
- What value of  $K$  would provide a crossover frequency (i.e., where  $|G| = 1$ ) of 0.16 rad/sec?
- For this value of  $K$ , would the system be stable if the loop were closed?
- What is the PM for this value of  $K$ ?
- Sketch the Nyquist plot of the system, and locate carefully any points where the phase angle is  $180^\circ$  or the magnitude is unity.
- Use MATLAB to plot the root locus with respect to  $K$ , and locate the roots for your value of  $K$  from part (b).

- (g) What steady-state error would result if the command was a step change in altitude of 1000 ft?

For parts (h) and (i), assume a compensator of the form

$$D(s) = K \frac{Ts + 1}{\alpha Ts + 1}.$$

- (h) Choose the parameters  $K$ ,  $T$ , and  $\alpha$  so that the crossover frequency is 0.16 rad/sec and the PM is greater than  $50^\circ$ . Verify your design by superimposing a Bode plot of  $D(s)G(s)/K$  on top of the Bode plot you obtained for part (a), and measure the PM directly.
- (i) Use MATLAB to plot the root locus with respect to  $K$  for the system including the compensator you designed in part (h). Locate the roots for your value of  $K$  from part (h).
- (j) Altitude autopilots also have a mode in which the rate of climb is sensed directly and commanded by the pilot.
- Sketch the block diagram for this mode.
  - Define the pertinent  $G(s)$ .
  - Design  $D(s)$  so that the system has the same crossover frequency as the altitude hold mode and the PM is greater than  $50^\circ$ .

- 6.55. For a system with open-loop transfer function

$$G(s) = \frac{10}{s[(s/1.4) + 1][(s/3) + 1]},$$

design a lag compensator with unity DC gain so that  $PM \geq 40^\circ$ . What is the approximate bandwidth of this system?

- 6.56. For the ship-steering system in Problem 6.38,

- (a) Design a compensator that meets the following specifications:
- Velocity constant  $K_v = 2$ ,
  - $PM \geq 50^\circ$ ,
  - Unconditional stability ( $PM > 0$  for all  $\omega \leq \omega_c$ , the crossover frequency).
- (b) For your final design, draw a root locus with respect to  $K$ , and indicate the location of the closed-loop poles.

- 6.57. Consider a unity-feedback system with

$$G(s) = \frac{1}{s(\frac{s}{20} + 1)(\frac{s^2}{100^2} + 0.5\frac{s}{100} + 1)}. \quad (6.82)$$

- (a) A lead compensator is introduced with  $\alpha = 1/5$  and a zero at  $1/T = 20$ . How must the gain be changed to obtain crossover at  $\omega_c = 31.6$  rad/sec, and what is the resulting value of  $K_v$ ?
- (b) With the lead compensator in place, what is the required value of  $K$  for a lag compensator that will readjust the gain to a  $K_v$  value of 100?

- (c) Place the pole of the lag compensator at 3.16 rad/sec, and determine the zero location that will maintain the crossover frequency at  $\omega_c = 31.6$  rad/sec. Plot the compensated frequency response on the same graph.
- (d) Determine the PM of the compensated design.
- 6.58.** Golden Nugget Airlines had great success with their free bar near the tail of the airplane. (See Problem 5.41.) However, when they purchased a much larger airplane to handle the passenger demand, they discovered that there was some flexibility in the fuselage that caused a lot of unpleasant yawing motion at the rear of the airplane when in turbulence, which caused the revelers to spill their drinks. The approximate transfer function for the Dutch roll mode (Section 10.3.1) is

$$\frac{r(s)}{\delta_r(s)} = \frac{8.75(4s^2 + 0.4s + 1)}{(s/0.01 + 1)(s^2 + 0.24s + 1)},$$

where  $r$  is the airplane's yaw rate and  $\delta_r$  is the rudder angle. In performing a finite element analysis (FEA) of the fuselage structure and adding those dynamics to the Dutch roll motion, they found that the transfer function needed additional terms which reflected the fuselage lateral bending that occurred due to excitation from the rudder and turbulence. The revised transfer function is

$$\frac{r(s)}{\delta_r(s)} = \frac{8.75(4s^2 + 0.4s + 1)}{(s/0.01 + 1)(s^2 + 0.24s + 1)} \cdot \frac{1}{\left(\frac{s^2}{\omega_b^2} + 2\zeta\frac{s}{\omega_b} + 1\right)},$$

where  $\omega_b$  is the frequency of the bending mode ( $= 10$  rad/sec) and  $\zeta$  is the bending mode damping ratio ( $= 0.02$ ). Most swept-wing airplanes have a “yaw damper,” which essentially feeds back yaw rate measured by a rate gyro to the rudder with a simple proportional control law. For the new Golden Nugget airplane, the proportional feedback gain  $K = 1$ , where

$$\delta_r(s) = -Kr(s). \quad (6.83)$$

- (a) Make a Bode plot of the open-loop system, determine the PM and GM for the nominal design, and plot the step response and Bode magnitude of the closed-loop system. What is the frequency of the lightly damped mode that is causing the difficulty?
- (b) Investigate remedies to quiet down the oscillations, but maintain the same low-frequency gain in order not to affect the quality of the Dutch roll damping provided by the yaw rate feedback. Specifically, investigate each of the following one at a time:
- i. Increasing the damping of the bending mode from  $\zeta = 0.02$  to  $\zeta = 0.04$  (would require adding energy-absorbing material in the fuselage structure).
  - ii. Increasing the frequency of the bending mode from  $\omega_b = 10$  rad/sec to  $\omega_b = 20$  rad/sec (would require stronger and heavier structural elements).

- iii. Adding a low-pass filter in the feedback—that is, replacing  $K$  in Eq. (6.83) with  $KD(s)$ , where

$$D(s) = \frac{1}{s/\tau_p + 1}. \quad (6.84)$$

Pick  $\tau_p$  so that the objectionable features of the bending mode are reduced while maintaining the  $\text{PM} \geq 60^\circ$ .

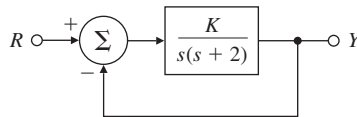
- iv. Adding a notch filter as described in Section 5.5.3. Pick the frequency of the notch zero to be at  $\omega_b$ , with a damping of  $\zeta = 0.04$ , and pick the denominator poles to be  $(s/100 + 1)^2$ , keeping the DC gain of the filter = 1.
- (c) Investigate the sensitivity of the preceding two compensated designs (iii and iv) by determining the effect of a reduction in the bending mode frequency of  $-10\%$ . Specifically, reexamine the two designs by tabulating the GM, PM, closed-loop bending mode damping ratio and resonant-peak amplitude, and qualitatively describe the differences in the step response.
- (d) What do you recommend to Golden Nugget to help their customers quit spilling their drinks? (Telling them to get back in their seats is not an acceptable answer for this problem! Make the recommendation in terms of improvements to the yaw damper.)



#### Problems for Section 6.8: Alternative Presentations of Data

- 6.59. A feedback control system is shown in Fig. 6.105. The closed-loop system is specified to have an overshoot of less than 30% to a step input.

**Figure 6.105**  
Control system for  
Problem 6.59



- (a) Determine the corresponding PM specification in the frequency domain and the corresponding closed-loop resonant-peak value  $M_r$ . (See Fig. 6.37.)
- (b) From Bode plots of the system, determine the maximum value of  $K$  that satisfies the PM specification.
- (c) Plot the data from the Bode plots [adjusted by the  $K$  obtained in part (b)] on a copy of the Nichols chart in Fig. 6.73, and determine the resonant peak magnitude  $M_r$ . Compare that with the approximate value obtained in part (a).
- (d) Use the Nichols chart to determine the resonant-peak frequency  $\omega_r$  and the closed-loop bandwidth.



**6.60.** The Nichols plot of an uncompensated and a compensated system are shown in Fig. 6.106.

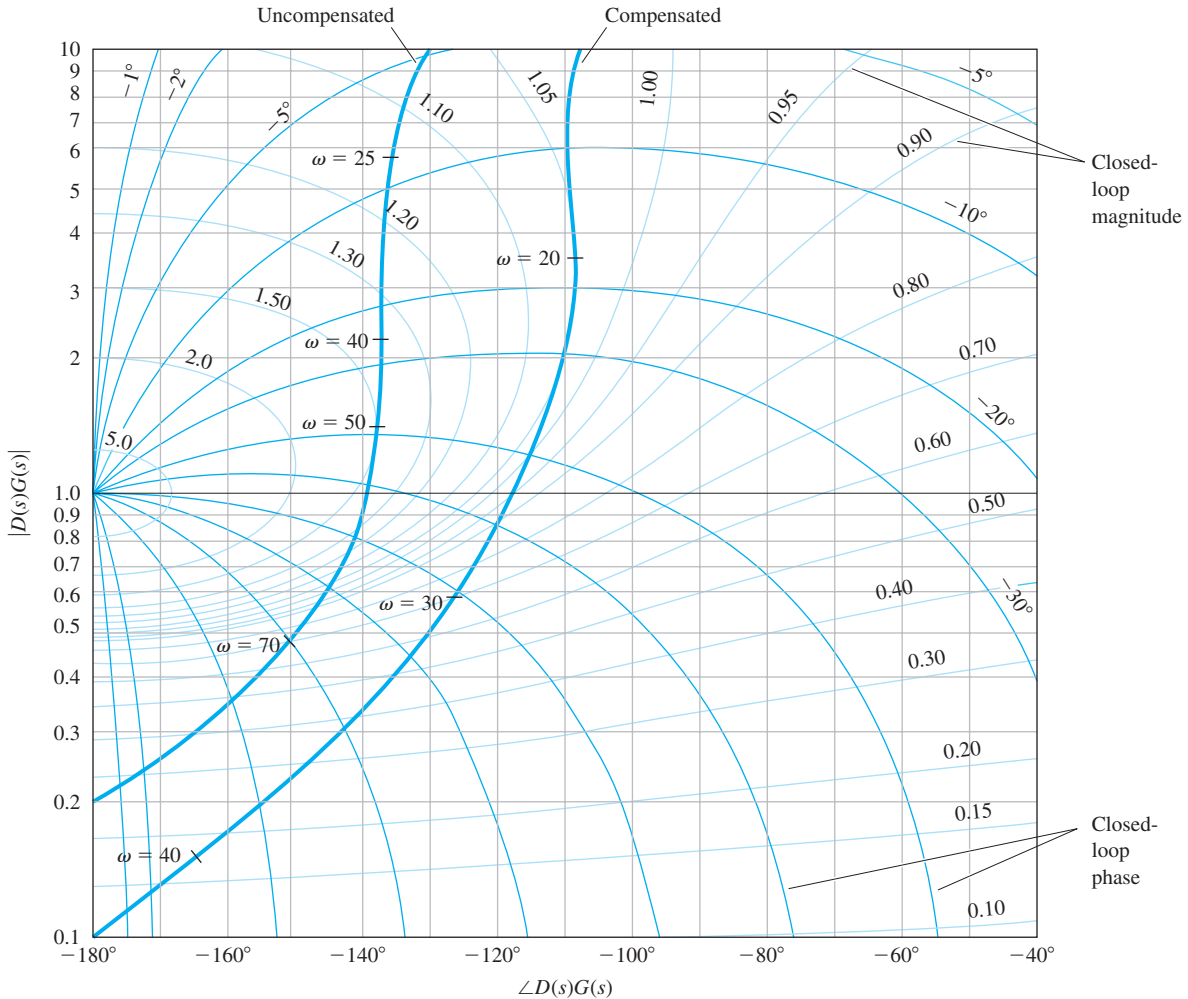


**Figure 6.106** Nichols plot for Problem 6.60

- (a) What are the resonance peaks of each system?
  - (b) What are the PM and GM of each system?
  - (c) What are the bandwidths of each system?
  - (d) What type of compensation is used?
- 6.61.** Consider the system shown in Fig. 6.98.
- (a) Construct an inverse Nyquist plot of  $[Y(j\omega)/E(j\omega)]^{-1}$ .
  - (b) Show how the value of  $K$  for neutral stability can be read directly from the inverse Nyquist plot.

- (c) For  $K = 4, 2,$  and  $1,$  determine the gain and phase margins.
- (d) Construct a root-locus plot for the system, and identify corresponding points in the two plots. To what damping ratios  $\zeta$  do the GM and PM of part (c) correspond?

6.62. An unstable plant has the transfer function

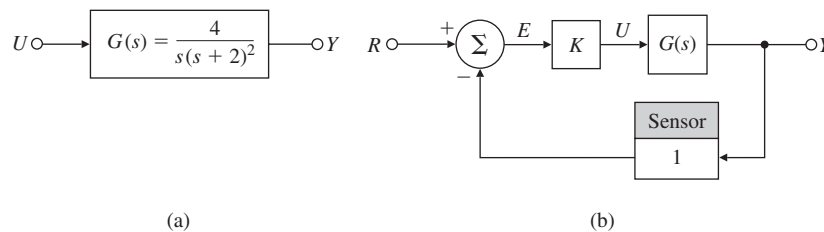
$$\frac{Y(s)}{F(s)} = \frac{s+1}{(s-1)^2}.$$

A simple control loop is to be closed around it, in the same manner as in the block diagram in Fig. 6.98.

- (a) Construct an inverse Nyquist plot of  $Y/F$ .
- (b) Choose a value of  $K$  to provide a PM of  $45^\circ$ . What is the corresponding GM?
- (c) What can you infer from your plot about the stability of the system when  $K < 0$ ?
- (d) Construct a root-locus plot for the system, and identify corresponding points in the two plots. In this case, to what value of  $\zeta$  does  $PM = 45^\circ$  correspond?

6.63. Consider the system shown in Fig. 6.107(a).

**Figure 6.107**  
Control system for  
Problem 6.63



- (a) Construct a Bode plot for the system.
- (b) Use your Bode plot to sketch an inverse Nyquist plot.
- (c) Consider closing a control loop around  $G(s)$ , as shown in Fig. 6.107(b). Using the inverse Nyquist plot as a guide, read from your Bode plot the values of GM and PM when  $K = 0.7, 1.0, 1.4,$  and  $2.$  What value of  $K$  yields  $PM = 30^\circ$ ?
- (d) Construct a root-locus plot, and label the same values of  $K$  on the locus. To what value of  $\zeta$  does each pair of PM/GM values correspond? Compare  $\zeta$  vs. PM with the rough approximation in Fig. 6.36.

▲ **Problems for Section 6.9: Specifications in Terms of the Sensitivity Function**

6.64. Consider a system with the open-loop transfer function (loop gain)

$$G(s) = \frac{1}{s(s+1)(s/10+1)}.$$

- (a) Create the Bode plot for the system, and find GM and PM.
- (b) Compute the sensitivity function and plot its magnitude frequency response.
- (c) Compute the vector margin (VM).

- 6.65. Prove that the sensitivity function  $S(s)$  has magnitude greater than 1 inside a circle with a radius of 1 centered at the  $-1$  point. What does this imply about the shape of the Nyquist plot if closed-loop control is to outperform open-loop control at all frequencies?
- 6.66. Consider the system in Fig. 6.103 with the plant transfer function

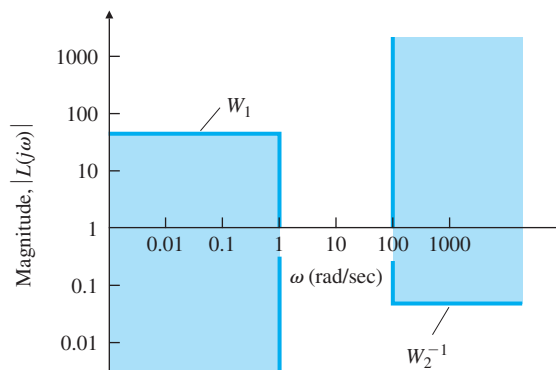
$$G(s) = \frac{10}{s(s/10 + 1)}.$$

- (a) We wish to design a compensator  $D(s)$  that satisfies the following design specifications:
- i.  $K_v = 100$
  - ii.  $PM \geq 45^\circ$
  - iii. Sinusoidal inputs of up to 1 rad/sec to be reproduced with  $\leq 2\%$  error
  - iv. Sinusoidal inputs with a frequency of greater than 100 rad/sec to be attenuated at the output to  $\leq 5\%$  of their input value
- (b) Create the Bode plot of  $G(s)$ , choosing the open-loop gain so that  $K_v = 100$ .
- (c) Show that a *sufficient* condition for meeting the specification on sinusoidal inputs is that the magnitude plot lies outside the shaded regions in Fig. 6.108. Recall that

$$\frac{Y}{R} = \frac{KG}{1 + KG} \quad \text{and} \quad \frac{E}{R} = \frac{1}{1 + KG}.$$

- (d) Explain why introducing a lead network alone cannot meet the design specifications.
- (e) Explain why a lag network alone cannot meet the design specifications.
- (f) Develop a full design using a lead-lag compensator that meets all the design specifications, without altering the previously chosen low-frequency open-loop gain.

**Figure 6.108**  
Control system constraints  
for Problem 6.66





## Problems for Section 6.10: Time Delay

**6.67.** Assume that the system

$$G(s) = \frac{e^{-T_d s}}{s + 10}$$

has a 0.2-sec time delay ( $T_d = 0.2$  sec). While maintaining a phase margin  $\geq 40^\circ$ , find the maximum possible bandwidth by using the following:

(a) One lead-compensator section

$$D(s) = K \frac{s + a}{s + b}$$

where  $b/a = 100$ ;

(b) Two lead-compensator sections

$$D(s) = K \left( \frac{s + a}{s + b} \right)^2,$$

where  $b/a = 10$ .

(c) Comment on the statement in the text about the limitations on the bandwidth imposed by a delay.

**6.68.** Determine the range of  $K$  for which the following systems are stable:

(a)  $G(s) = K \frac{e^{-4s}}{s}$

(b)  $G(s) = K \frac{e^{-s}}{s(s+2)}$

**6.69.** In Chapter 5, we used various approximations for the time delay, one of which is the first order Padé

$$e^{-T_d s} \cong H_1(s) = \frac{1 - T_d s/2}{1 + T_d s/2}.$$

Using frequency response methods, the exact time delay

$$H_2(s) = e^{-T_d s}$$

can be obtained. Plot the phase of  $H_1(s)$  and  $H_2(s)$ , and discuss the implications.

**6.70.** Consider the heat exchanger of Example 2.13 with the open-loop transfer function

$$G(s) = \frac{e^{-5s}}{(10s + 1)(60s + 1)}.$$

(a) Design a lead compensator that yields  $\text{PM} \geq 45^\circ$  and the maximum possible closed-loop bandwidth.

(b) Design a PI compensator that yields  $\text{PM} \geq 45^\circ$  and the maximum possible closed-loop bandwidth.